UNIVERSIDADE
BEIRA INTERIOR

3D CFD Combustion Simulation of a Four-Stroke SI Opposed Piston IC Engine

Maria da Conceição Rodrigues Martins

Dissertação para obtenção do Grau de Mestre em
Engenharia Aeronáutica
(Ciclo de estudos integrado)

Orientador: Prof. Doutor Francisco Miguel Ribeiro Proença Brójo

Setembro de 2020

Dedication

To my father Adelino Rodrigues Martins.

”A good head and good heart are always a formidable combination. But when you add to that a literate tongue or pen, then you have something very special.”

Nelson Mandela

Acknowledgments

I am eternally grateful to my mother for the sacrifices she made for me. To my brothers and sisters, Zé, Rosária, Hirminia and Fernando, for their support and dedication that inspired me to go on.

A big thank you to my supervisor, Professor Francisco Brójo for the pacience and guidence.

I wish to thank all my family, for their kindness and encouragement over the years.

I want to thank my friends for making me feel at home.

A special thanks to Cristiano for being my special friend.

Resumo

O motor alternativo de combustão interna desempenha um papel importante no mundo dos transportes, existindo ainda poucas configurações alternativas com sucesso comercial. Relativamente a aplicações em aeronaves ligeiras, onde as baixas vibrações são de extrema importância, os motores boxer têm predominado o mercado. O aumento do custo do combustível e o aumento da preocupação do público com as emissões de poluentes levaram a um maior interesse em novas alternativas. Nos últimos anos, com o surgimento de novas tecnologias, técnicas de pesquisa e materiais, o motor de pistões opostos surgiu como uma alternativa viável ao motor convencional de combustão interna em algumas aplicações, inclusive na área aeronáutica. Este estudo apresenta uma análise numérica do processo de combustão da mistura de octano-ar num motor de faísca a quatro tempos e de pistão oposto. O modelo utilizado nas simulações representa o volume interno do cilindro do motor UBI / UDI-OPE-BGX286. A simulação foi executada no software Fluent 16.0, dos modelos disponíveis no Fluent o modelo de transporte de espécies foi escolhido para modelar a combustão, e três diferentes velocidades de motor foram simuladas: $2000RPM$,$3200RPM$ e $4000RPM$. Em relação aos resultados obtidos nas três simulações CFD, o comportamento geral e as propriedades do fluxo no cilindro e os gráficos obtidos foram considerados aceitáveis.

Palavras-chave

Combustão; CFD; Emissões; Fluent; Ignição por Faísca; Motor de Combustão Interna; Octano; Motor de Pistões Opostos; Quatro Tempos.

Abstract

The reciprocating IC engine plays an important role in the world transport, with very few alternative configurations having commercial success. In light aircraft applications where low vibrations are crucial, boxer engines have predominated. The rising cost of fuel and the growth of public concern over pollutant emissions has led to an increased interest in alternative designs. In recent years, with the uprising of new technologies, research techniques and materials, the OP engine has emerged as a viable alternative to the conventional IC engine in some applications including in the aeronautical field. This study presents a numerical analysis of the combustion process of octane-air mixture in a four-stroke SI opposed piston engine. The model used in the simulations represents the internal volume of the cylinder of UBI/UDI-OPE-BGX286 engine. The simulation was run in Fluent 16.0 software, the species transport model was chosen to model combustion from the available in Fluent, and three different engines speeds were simulated: $2000RPM$, $3200RPM$ and $4000RPM$. Regarding the results obtained from the three CFD simulations, the overall behavior and properties of the in-cylinder flow and the obtained graphics were considered acceptable.

Keywords

Combustion; CFD; Emissions; Fluent; Four-Stroke; Internal Combustion (IC); Octane; Opposed Piston (OP); Spark Ignition (SI)

Contents

List of Figures

List of Tables

List of Acronyms

BDC	Bottom Dead Centre
CAD	Computer Aided Design
CI	Compression Ignition
CNG	Compressed Natural Gas
CFD	Computational Fluid Dynamics
CLM	Construction Lilloise de Moteurs
DOHC	Double Over Head Camshafts
EDC	Eddy-Dissipation-Concept
EI	Emissions Index
FAME	Fatty-Acid Methyl Esters
HC	Unburned Hydrocarbons
IC	Internal Combustion
IDC	Inner Dead Centre
LNG	Liquefied Natural Gas
LPG	Liquefied Petroleum Gas
MBT	Maximum Brake Torque Timing
OHC	Over Head Camshaft
OHV	Over Head Valve
OP	Opposed-Piston
PDE	Partial Differential Equations
RANS	Reynolds Averaged Navier Stokes
RME	Rapeseed Methyl Esters
RPM	Revolution Per Minute
SE	Specific Emissions
SI	Spark Ignition
TDC	Top Dead Centre
UBI	Universidade da Beira Interior
UAV	Unmanned Aerial Vehicle
URF	Under Relaxation Factors
3D	Three-Dimension

Nomenclature

a	Crank radius	$[m]$
A	Pre-exponential factor	$[s^1]$
A_{ch}	Cylinder head surface area	$[m^2]$
A_p	Piston crown surface area	$[m^2]$
A_θ	Combustion chamber surface area	$[m^2]$
AFR	Air-Fuel Ratio	$[-]$
B	Bore	$[m]$
c_r	Compression ratio	$[-]$
C_8H_{18}	Octane	$[-]$
CO	Carbon-monoxide	$[-]$
CO_2	Carbon-dioxide	$[-]$
E_a	Activation energy	$[kJmol^{-1}]$
F	Force	$[N]$
FAR	Fuel-Air Ratio	$[-]$
H	Atomic-hydrogen	$[-]$
H_2O	Water	$[-]$
k	Arrhenius rate constant	$[m^3mol^{-1}s^{-1}]$
l	Connecting rod length	$[m]$
L	Stroke	$[m]$
m	Mass	$[kg]$
$\dot{m}$	Mass flow rate	$[kgs^{-1}]$
M	Molecular weight	$[kgkmol^{-1}]$
p	Mean effective pressure	$[Pa]$
n_r	Number of crank revolutions per cycle	$[-]$
n_c	Number of cylinders	$[-]$
O	Atomic oxygen	$[-]$
O_2	Oxygen	$[-]$
OH	Hydroxyl	$[-]$
N	Rotational speed	$[RPM]$
N_i	Number of moles	$[kmol]$
$NO2$	Nitrogen-dioxide	$[-]$
NO	Nitrogen-oxide	$[-]$
NO_x	Nitric oxides	$[-]$
N	Atomic-nitrogen	$[-]$
N_2	Nitrogen	$[-]$
p	Pressure	$[Pa]$
P	Power	$[W]$
P_b	Brake power	$[W]$
P_i	Indicated power	$[W]$
Q	Heat transfer	$[W]$
QHV	Heating value	$[kJkg^{-1}]$
R_{bs}	Bore to stroke ratio	$[-]$
R_{la}	Connecting rod length to crank radius ratio	$[-]$
R_{CO}	Carbon monoxide oxidation rate	$[mol\ m^{-3}s^{-1}]$
R	Universal gas constant	$[8315\ Jkmol^{-1}K^{-1}]$

s	Distance between crank and piston pin axis	$[m]$
sfc	Specific fuel consumption	$[gkW^{-1}h^{-1}]$
$\bar{S}_p$	Mean piston speed	$[ms^{-1}]$
SO_x	Sulphur Oxides	$[-]$
T	Temperature	$[K]$
t	Time	$[s]$
v	Velocity	$[ms^{-1}]$
V	Volume	$[m^3]$
V_c	Clearance volume	$[m^3]$
V_d	Displaced volume	$[m^3]$
V_t	Cylinder total volume	$[m^3]$
V_θ	Instantaneous volume	$[m^3]$
W	Work	$[J]$
W_b	Branke work	$[J]$
W_i	Indicated work	$[J]$
Y	Mass fractions	$[-]$

Greek letters

γ	Specific heats ratio	$[-]$
η_m	Mechanical efficiency	$[-]$
η_v	Volumetric efficiency	$[-]$
θ	Crank angle	$[-]$
ρ	Density	$[kgm^{-3}]$
Φ	Equivalence ratio	$[-]$
τ	Torque	$[Nm]$
ω	Angular speed	$[rads^{-1}]$
$\dot{\omega}$	Rection rate	$[s^{-1}]$
Ψ	Mole fraction	$[-]$

Chapter 1

Introduction

Internal Combustion (IC) engines have undergone significant advancements since the introduction of the first commercial engine in the early 19th century.[1] So many different configurations have been produced since then which differ in size, geometry, operating principle, type of ignition, fuel and other technical features that no absolute limit can be stated for any range of engine characteristics. Indeed, nowadays IC engines play an important role in the world, their applications range from common use like tranportation to unusaul military vehicles, invading all fields from the bottom of the ocean to the limits of the heavens. The most important applications of IC engines is in the transport on land, sea and air [15].

Since the purpose of internal combustion engines is the production of mechanical power from the chemical energy contained in the fuel [16], and knowing that regardless of engine configuration, operating principle or fuel type, the combustion process generates by-products, the so called emissions, it is important to understand the nature of the flows and the combustion process in order to improve engine performance and reduce pollutants emissions.

Opposed-Piston engine (OP) is an IC engine characterized by a pair of pistons operating in a single cylinder, opposite to each other, eliminating the need for cylinder heads, therefore differing from the conventional reciprocating IC engine in the arrangement of the cylinder. Since its appearance around 1878 in Germany created by Witting as an alternative to the Otto engine [2], several variants of OP engine were developed because of their ease of manufacture, excellent balance, competitive performance and fuel efficiency; new advantages emerged and some of the current engine performance parameters standards were established. Despite these advantages and their initial diversity of applications its use has greatly decreased mainly due to issues with pollutant and particulates emissions [9].

1.1 Motivation

The last century was marked by an outstanding evolution of the IC engine. Initially this evolution was driven by a quest for performance. This changed with the growth of public concern over pollutant emissions such as CO_2, NO_x and unburned hydrocarbons (UHC) and the limited fossil fuel resources, leading to stringent emissions and fuel economy regulations. Although these concerns represents a real threat to the environment and public health, it is practically impossible to substitute the IC engines since our modern society continues to rely heavily on them and the existent alternatives have not yet reached all the desired requirements and their applications are limited. Therefore, the search of alternative configurations with higher efficiency and that can run

[1] Jean Joseph Étienne Lenoir developed the first marketable and fairly practical IC engine around 1860 and their efficiency was at best about five percent[5].

[2] Nicolaus A. Otto developed and created in 1876 the Otto cycle engine, the first four-stroke spark ignition engine prototype. Only in 1892 Rudolf Diesel introduced the Compression Ignition IC engine[16].

on alternative fuels thrive in an unprecedented scale since the convensional IC engine [3] seems to have reached its maturation limits. In recent years, with the uprising of new technologies, research techniques and materials, the OP engine has emerged as a viable alternative to the conventional IC engine in some applications including in the aeronautical field. However, research is still at a very early stage of development, in that it does not present many variations from its predecessors, and have not expanded yet to include big changes in the operation cycle. Thus, there are not many research on 4-stroke SI engines. Being this one of the main reasons for this study.

Aeronautics [4]has been one of the most recent and most significant of the latter human pursuits, from the 1600s when philosophers and spirited individuals conducted experiments that proved that man could be carried aloft on wings, trough the first wing-borne and controllable powered flight by the Wright brothers[5], into our days where global air travel is a reality, new flying mechanisms emerged with a considerable range of applications improving our quality of life. Regardless of the type of aircraft (and their application) most of them rely on some type of propulsion device to generate power that runs on petroleum-based fuels, therefore, the search for a short-term effective alternative is in the big interest of the aeronautics industry.

Computational fluid dynamics (CFD) has emerged as a valuable tool in providing insight of fluid dynamics and combustion process in IC engines, due to the growth of computational capabilities and software improvement of the past few decades it became a less expensive and timelier research alternative. It enables to solve complex problems involving advanced turbulence modelling, mixing, reaction and multiphase flows on challenging geometries using numerical methods and mathematical models[19]. Since no models are universal, the most difficult part of IC engine simulation is to understand the fluid dynamics interaction with moving parts and determine which models are most appropriate to this particular case in order to judge the potential lack of accuracy. As a fast and complex process, the field of combustion has advanced substantially with the improvements on computational areas by allowing researchers to explore detailed phenomena associated with ignition and combustion processes.

1.2 Main Goals

The main purpose of the present study is to evaluate, through a CFD analysis on the software Fluent, the combustion process of an octane-air mixture in a four-stroke SI opposed piston engine. Taking special interest in the in-cylinder flow behavior, the chemical reactions during combustion and the resulting exhaust pollutants emissions.

1.3 Outline

Apart from the present chapter in which the author introduces his work by manifesting his motivation behind the development of this study, the present dissertation is structured the following way:

[3]Referes to a reciprocating engine that operates on a four-stroke cycle.

[4]Aeronautics is the science of building and flying aircraft.The term covers scientific study, design, and technology, including the manufacture and operation of all types of aircraft[17].

[5]On December 17, 1903, Orville Wright flew the first heavier-than-air aeroplane, travelling about thirty-six meters in twelve seconds[18]

- In Chapter 2 a literature review of the theoretical concepts regarding this study is presented.
- In Chapter 3 all the parameters used in the simulations are setup, such as solver, materials, models, boundary conditions, dynamic mesh, initial conditions, solution methods and controls, and the monitors.
- In Chapter 4 the numerical results obtained from the CFD simulation presented. The results are then explained in detail and discussed throughout this chapter.
- In Chapter 5 presents a summary of the work conducted in this study. Conclusions and recommendations for future work are also included based on the results obtained in the study.

Chapter 2

Literature Review

A brief background knowledge in the field of this research and some basic theory is presented for a better understanding of the present work.

2.1 Internal Combustion Engines

The internal combustion engine (ICE) is a heat engine that derives thermal energy from the chemical energy of a fuel, through combustion, and converts it into mechanical energy. It differs from external combustion engines on how the heat is supplied to the working fluid. Unlike external combustion engines (such as steam power plants), in which heat is supplied to the working fluid from an external source such as a furnace, a geothermal well, a nuclear reactor, or even the sun. In ICE this is done by burning or oxidizing the fuel inside the engine [16] [10]. In these engines, the fuel-air mixture before combustion and the burned products after combustion serve as the engine working fluids. The released thermal energy raises the temperature and pressure of the gases within the engine, and the high-pressure gas then expands against the moving surfaces of the engine, such as the face of a piston in the case of reciprocating and rotary engines, a turbine blade in jet and gas turbine engines and a nozzle in rocket engine, which results in a work transfers directly between the working fluids and the mechanical components of the engine. Therefore, they can be differentiated into continuous-combustion engines and intermittent-combustion engines. The former are characterized by a stable flame and steady flow of fuel and oxidizer into the engine. While the later commonly referred as reciprocating engine is characterized by a periodic ignition of air and fuel. Discrete volumes of air and fuel are processed in a cyclic manner [20][10]. Although continuous-combustion engines, such as jet engines, most rockets and many gas turbines, can be defined as IC engines the term is usually applied to reciprocating and rotary [1] engines.

2.1.1 Reciprocating Engine Operating Principle

Conceived and developed in the late 1800s the first IC engine used the reciprocating piston-cylinder principle and the basic components such as piston, valves, crankshaft and connecting rod have remained unchanged [21], and can be represented by the mechanism shown in Figure 2.1. The name “reciprocating” gives a glimpse of the operating principle as it describes the motion behind the operation. The reciprocating engine, or piston-cylinder engine, can be characterized as a crank-slider mechanism, in which the slider is the piston.

The engine operation can be delineated in terms of a series of events defined by the correlation between pressure, volume, temperature of gases and the moving components. In this type of engines

[1] Rotary engines differ from reciprocating engines in their basic design [16] [5]. Characterized by a rotary motion of the cylinders around a stationary crankshaft, like the Le Rhône rotary engines. In the case of the Wakel engine the piston is the one that rotates, also differs in the nature of the piston, called rotor, and the shape of the cylinder.

the linear back and forth motion of one or more pistons within a cylinder, induced by the working fluids action on the piston, is transformed into rotational motion of the connecting rod and crank mechanism resulting in a cyclic piston motion. The crank mechanism, in turn, is connected to a transmission train, therefore, transmitting the rotating mechanical energy to the desired final use. Figure 2.1 points out the engine components necessary to accomplish the conversion and energy transfer and presents the main terms used to illustrate engine operation.

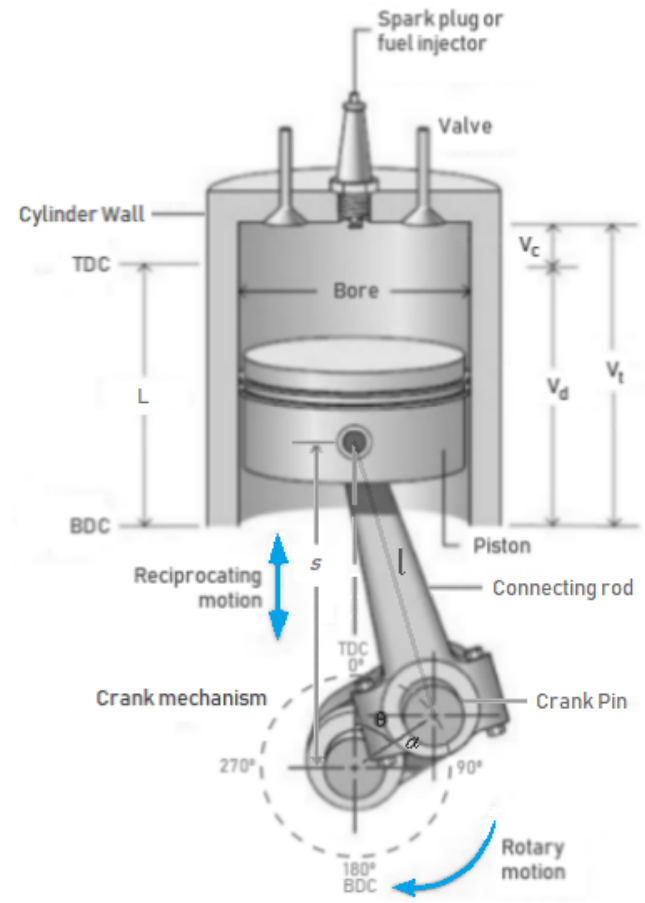

Figure 2.1: Reciprocating IC Engine. Adapted from [1].

The reciprocating motion occurs between two limits of the piston displacement. The top dead centre (TDC) where the piston is at the highest point and the bottom dead centre (BDC) at the lowest point, corresponding to crankshaft being in a position such that the crank angle (θ) is 0º and 180º, and the cylinder volume is minimum and maximum, respectively. The stroke (L) is the distance the piston travels from one limit to the other. The bore (B) is the cylinder inside diameter. The valves at the top represent the induction and exhaust valves responsible for fluid exchange. The clearance volume (V_c) or combustion chamber (during combustion) is the volume occupied between the top of the piston and the upper portion of the cylinder when the piston is at TDC and represents the minimum cylinder volume. The volume swept out by the piston as it moves is called displaced volume (V_d), and represents the difference between the total volume (V_t) of the cylinder and the V_c, Equation 2.5 [16].

To a further comprehension of reciprocating engines a differentiation is made between engine characteristics and operating characteristics. The engine characteristics, such as piston stroke, cylinder bore, connecting rod length (l), crank radius (a), piston displacement and compression ratio (c_r), represent the input parameters and their relationships define the geometric properties of the reciprocating engine. The operating characteristics, such as, power, torque, engine speed, mean pressure, volumetric efficiency, and fuel consumption are the output parameters commonly used to characterize engine operation. These characteristics, which are related, serve as an important aid in designing the engine fundamental dimensions, assessing engine power and consumption and, in the evaluation and comparison of different engines performance [16][8].

2.1.2 Engine Characteristics/Paramenters

With the following engine geometric parameters, piston stroke (L), cylinder bore (B), crank radius (a), connecting rod length (l), some basic relations can be made:

The crank radius is one-half of the piston stroke,

$$L = 2\,a \quad (2.1)$$

Ratio of cylinder bore to piston stroke (R_{bs}):

$$R_{bs} = \frac{B}{L} \quad (2.2)$$

Ratio of connecting rod length to crank radius (R_{la}):

$$R_{la} = \frac{l}{a} \quad (2.3)$$

The compression ratio (c_r), defined as the ratio of the maximum to minimum volume, and can be obtained by Equation (2.4),

$$c_r = \frac{V_{BDC}}{V_{TDC}} = \frac{V_t}{V_c} = \frac{V_d + V_c}{V_c} \quad (2.4)$$

where the piston displacement or swept volume (V_d) can be obtained by Equation (2.5) for a single cylinder with flat-topped pistons, where A_p represents the piston crown surface area. For engines with more than one cylinder, the displacement is the product of the number of cylinders (n_c), and the displacement volume of a cylinder.

$$V_d = V_t - V_c = A_p\,L = \frac{\pi}{4}\,B^2\,L \quad (2.5)$$

Typical values for these parameters are: R_{bs} for small and medium size engines usually presents values from 0.8 to 1.2, which decreases with engine size and speed. R usully has values of 3 to 4 for small and medium size engines, and 5 to 10 for largest engine. V_d values range from 0.001 litres for small model airplanes, to about 8 litres for large automobiles, to much larger numbers for large ship engines[16] [5]

The cylinder volume at any crank position or instantaneous volume (V_θ), and the combustion chamber surface area (A_θ), at any crank angle can be obtained by Equations (2.6) and (2.7) respectively.

$$V_\theta = V_c + \frac{\pi\, B^2}{4}\,(l + a - s) \quad (2.6)$$

$$A_\theta = A_{ch} + A_p + \pi\, B\,(l + a - s) \quad (2.7)$$

where s is the distance between the crank axis and the piston pin axis, Equation (2.8), and A_{ch} is the cylinder head surface area.

$$s = a\,\cos\theta + (l^2 - a^2\sqrt{l^2 - a^2\sin\theta}) \quad (2.8)$$

2.1.3 Operating Characteristics/Parameters

The mean piston speed is an important parameter in engine design since stresses due to the inertia of the moving parts, and flow resistance during intake, scales with piston speed [16][8], which results in a strong inverse correlation between engine size and mean piston speed. Therefore, limiting its values between 8 and 15 m/s is necessary. Since for each crank revolution the piston travels a distance of twice the stroke,

$$\bar{S}_p = 2\,L\,N \quad (2.9)$$

$$N = \frac{n_r}{t} \quad (2.10)$$

where N is the rotational speed of the crankshaft or engine speed, representing the number of crankshaft revolutions (n_r) per time unit, usually expressed in revolutions per minute (rpm). From Equation (2.9), it can be seen that the range of acceptable piston speeds places a range on acceptable engine speeds also [5]. The angular speed (ω) also refers to the rotation rate of the crankshaft but in units of radians per second, Equation (2.11).

$$\omega = 2\,\pi\,N \quad (2.11)$$

Since work is the result of a force acting through a distance, in reciprocating IC engines the work is generated by a force, due to gas pressure inside the cylinder, acting on the piston crown surface area causing its motion throughout the stroke, resulting in a variation in the cylinder volume, Equation (2.12).

$$W = \int F\,dx = \int P\,dV \quad (2.12)$$

The cylinder pressure data and corresponding cylinder volume throughout the engine cycle can be plotted on a p-V diagram and used to calculate the work transfer from the gas to the piston. The work obtained from these diagram is called indicated work (W_i) per cycle and per cylinder,

and will be discussed later. Due to mechanical friction and parasitic loads of the engine the actual work available at the crankshaft is less than W_i, called brake work (W_b), and can be obtained from Equation (2.14), through torque measurements.

In physics, torque, also called moment of a force, is the tendency of a force to rotate the body to which it is applied. In reciprocating engines this can be translated in the tendency of the crankshaft to rotate due to the tangential force applied to the connecting rod, by the piston motion. Therefore, the torque (τ) produced by an engine can be defined as:

$$\tau = F\,d \quad (2.13)$$

where F is the component of the force perpendicular to the rotation axis, and d the shortest distance between the crank axis and the position where the force is applied (crank pin), the crank offset.

Torque can also be defined as the ability of the engine to generate work [5][16], can be related to work by Equation (2.14), therefore, it is a measure of the work done per unit rotation of the crank (crank revolutions) [21].

$$\tau = \frac{W_b}{n_r} \quad (2.14)$$

where n_r is the number of crank revolutions per cycle and per cylinder. Since torque is usually obtained through measurements with a dynamometerand, W_b is applied. [2].

Power can be defined as the rate at which the engine generates work [5][16]. The engine power delivered to the crankshaft and obtained by dynamometer measurements, called brake power (P_b), can be defined as the product of torque and angular speed, equation (2.15). While, the power per cycle (P_i) is related to the indicated work per cycle by Equation (2.16),

$$P_b = \frac{W_b\,N}{n_r} = 2\,\pi\,N\,\tau \quad (2.15)$$

$$P_i = \frac{W_i\,N}{n_r} \quad (2.16)$$

Mean effective pressure (mep) is a more valuable measure parameter to compare engines, since, unlike torque and power, it is independent of engine size or speed. Since throughout the engine cycle, the pressure in the cylinder is continuously changing, the mean effective pressure can be defined as the average pressure that results in the same amount of indicated or brake work produced by the engine [21], and can be obtained by dividing the work per cycle by the cylinder volume displaced per cycle. When the brake work is used, it is called break mean effective pressure (bmep), Equation (2.17), and indicated mean effective pressure (imep), Equation (2.18), when indicated work per cycle is applied,

$$bmep = \frac{W_b\,n_r\,n_c}{V_d} \quad (2.17)$$

[2]Dynamometers are used to measure torque and power over the engine operating ranges of speed and load, by using various methods to absorb the energy output of the engine [5].

$$imep = \frac{W_i \, n_r \, n_c}{V_d} \quad (2.18)$$

The break mean effective pressure can be related to torque and brake power by Equation (2.19) and Equation (2.20), respectively.

$$bmep = \frac{2\,\pi \; n_r \, \tau}{V_d \, N} \quad (2.19)$$

$$bmep = \frac{P_b \, n_r}{V_d \, \frac{N}{60}} \quad (2.20)$$

The fuel consumption characteristics of an engine are generally expressed in terms of specific fuel consumption (sfc), instead of measuring the flow rate or mass flow per unit time it gives the fuel flow rate per unit power output. Therefore, reflecting how good the engine performance is by measuring how efficiently the engine uses the fuel supplied to produce work [16].

$$sfc = \frac{\dot{m}_f}{P} \quad (2.21)$$

Indicated specific fuel consumption ($isfc$) and brake specific fuel consumption ($bsfc$), are the specific consumptions on the basis of P_i and P_b, respectively.

The terms brake and indicated used to describe work, power, mean effective pressure, specific fuel consumption and thermal efficiency are essential/used to determine mechanical efficiency (η_m). The ratio between the parameters defined by these two terms gives the mechanical efficiency, Equation (2.22).

$$\eta_m = \frac{W_b}{W_i} = \frac{P_b}{P_i} = \frac{bmep}{imbp} = \frac{isfc}{bsfc} \quad (2.22)$$

Volumetric efficiency (η_v) indicates the breathing ability of the engine, relating the amount of air introduced into the cylinder with the actual capacity of the cylinder. Defined as the volume flow rate of air into the intake system divided by the rate at which volume is displaced by the piston, this parameter is mainly used to measure the effectiveness of an engine's intake process. This has a great impact in four-stroke engines performance, since they present a distinct induction process [5][16].

$$\eta_v = \frac{m_a}{\rho_a \, V_d} = \frac{n \, \dot{m}_a}{\rho_a \, V_d \, N} \quad (2.23)$$

(ρ_a) is the inlet air density. Getting the relatively small volume of liquid fuel into the cylinder is much easier than getting a large volume of gaseous air. Ideally, the mass of fresh charge admitted in each cycle should be equal to the density of atmospheric air times the displacement volume of the cylinder. However, due to the short cycle time available and the existent flow restrictions, less than the theoretical amount of fresh charge enters the cylinder [5].

2.2 Classification of Reciprocating IC Engines

It is essential to correlate and analyse the choices on engine configuration with its characteristics and performance, therefore, a classification, based on various technical literature, is presented. The large number of components, the complexity of their interaction and the many possible configurations for the reciprocating engine led to a diversity of ways to classify these engines. However, they can be differentiated by several common criteria/features presented in literature of this field, such as: work cycle, method of ignition, fuel type, applications, method of mixture preparation, combustion chamber design, valve or port arrangement, cylinder arrangement, cooling system and the use of super or turbochargers. For a better view on the degree of complexity of IC motors, and better understand the evolution/history of OP engines a summary of these parameters will be presented.

2.2.1 Work Cycle

There are two major work cycles used in reciprocating engines, the two-stroke and four stroke cycle:

Four-stroke Cycle: In this type of cycle, a series of distinct events are necessary to complete the work cycle: the induction of the fresh charge, its compression, ignition and combustion and the expansion and exhaust of the by-products. These events occur while the piston makes four strokes (that are named after four of the events), which requires two revolutions of the crankshaft. The in and out of the fluids is controlled by the camshaft and a set of valves. The four-stroke cycle can be explained with reference to Figure.2.2 and, taking a look at Figure 2.1.

1. First stroke: *Intake or Induction*. The engine cycle begins with the intake stroke. The inlet valve opens shortly before the piston is in TDC. The stroke starts with the piston in this position, the exhaust valve closed, and moving toward the BDC. The downwards motion of the piston creates an increasing volume in the combustion chamber, which in turn creates a vacuum. The resulting pressure differential drawn in the fresh charge into the combustion chamber and cylinder. Shortly after the stroke ends, with the piston in BDC, the inlet valve closes.

2. Second Stroke: *Compression*. Shortly after the BDC, the last position of the previous stroke, the inlet valve closes and the piston travels back to TDC (with all valves closed), therefore, compressing the charge, which reduces the volume and raises the pressure and temperature in the cylinder, making it ready for combustion. Near the end of the compression stroke, ignition occurs and combustion is initiated.

3. Third Stroke: *Expansion or Power*. This stroke starts with the piston at TDC and begins the second revolution of the crankshaft. With all valves closed, combustion propagates throughout the charge, increasing the temperature and the pressure. The pressure created pushes the piston down and forces the crank to rotate, producing the work output of the engine cycle [3] . The cylinder volume increase causes the pressure and temperature to drop. The

[3]About five times as much work is done on the piston during the power stroke as the piston had to do during compression [16].

exhaust valve opens before piston approaches BDC, decreasing the cylinder pressure to near the exhaust pressure, therefore, initiating the exhaust process.

4. Fourth Stroke: *Exhaust*. With the exhaust valve remaining open, the piston travels from BDC to TDC pushing the burned gases out of the cylinder due to the higher pressure inside. Near TDC the inlet valve opens. Just after TDC, the exhaust valve closes, and remains that way when the new intake stroke begins the next cycle, occurring a valve overlap [4]. The purpose of this stroke is to clear the cylinder of the by-products of combustion (preparing for the new cycle) but this is not fully accomplished since some exhaust gas residuals are left and dilute with the next charge.

Most of reciprocating engines operate on this cycle. It is often called the Otto cycle, after its inventor, Nicolaus Otto.

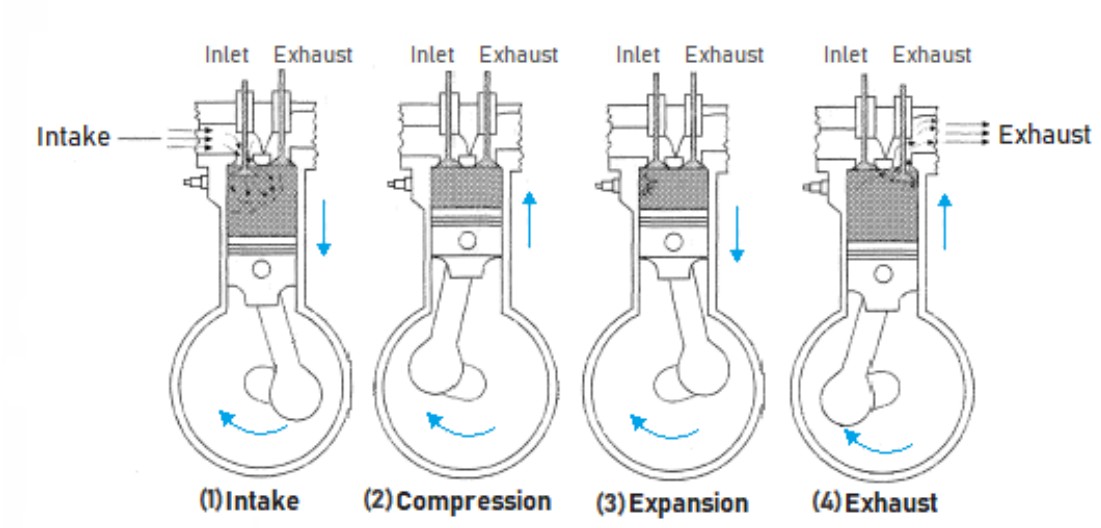

Figure 2.2: The four-stroke engine cycle. Edited from [2].

Two-stroke Cycle: In this type of cycle the above mentioned events occur throughout only one revolution of the crankshaft, therefore only two strokes of the piston are necessary to complete the work cycle. The fluid exchange is made through ports and a valve controlled by the piston motion, instead of a complex valve mechanism. The two-stroke cycle is described with reference to one of the simplest types of design, the crankcase-scavenged design, which can be seen in Figure 2.3.

1. First Stroke: *Compression*. Similarly to four-stroke cycle the piston travels from BDC to TDC. This creates a sub-atmospheric pressure in the underside of the piston, the crankcase, which openens the reed spring inlet valve and draws in the fresh charge. Simultaneously, closing the exhaust and transfer ports and compressing the trapped charge in the top of the cylinder, then the ignition and combustion occurs.

[4] The period when both valves are open is called valve overlap.

2. Second Stroke: *Expansion*. Also similar to the four-stroke cycle, the stroke starts with piston at TDC moving toward BDC. Once the piston reverses direction during combustion and the expansion begins, due to the raise of temperature and pressure, the charge in the crankcase is compressed closing the reed spring inlet valve. Most of the burned charge exit the cylinder when the exhaust port is uncovered as the piston approaches the BDC. At the BDC the port transfer also is uncovered allowing the compressed charge in the crankcase to expand into the cylinder, completing the cycle.

The two-stroke cycle was developed by Dugald Clerk in 1878, to obtain a higher power output from a given engine size, and a simpler valve design. In this cycle the induction and exhaust strokes is eliminated, rising the problem of ensuring that these two events evolve properly, without occur charge dilution. Although the piston and the ports are designed so that the fresh charge doesn't flow directly into the exhaust ports, in order to achieve an efficient scavenging[5], some of it gets mixed with the burned charge, flowing out of the cylinder throughout the process [16] [21].

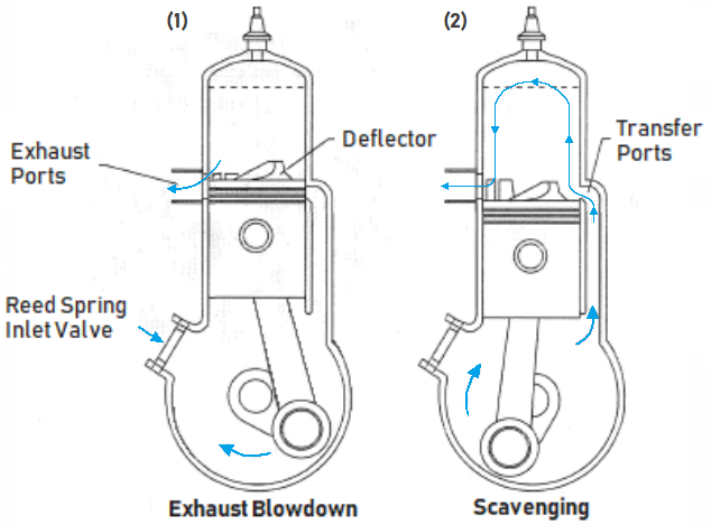

Figure 2.3: The two-stroke engine cycle[2].

In both cycles, the fresh charge drawn into the cylinder can be either naturally aspired when it is done only by the working piston admitting atmospheric air, supercharged or turbocharged when the fresh charge is pre-compressed, by a compressor mechanically driven by the engine or a by compressor powered by the engine's exhaust gases.

Two-stroke Vs Four-stroke Cycle

Both cycles present significant advantages and disadvantages. Looking first at engines operating on two-stroke cycle, it generates more power than the one operating on a four-stroke cycle, since the two-stroke engine has twice as many power stroke per unit time. Since has a simpler design, uses ports instead of a complex valve mechanism, less engine parts are needed, it has a lower weight, resulting in a higher power to weight ratio and low costs of production and maintenance. The problem with charge dilution and subsequent fuel lost affects the efficiency by decreasing it.

[5]Is the process of simultaneously purging burned charge and filling the cylinder with fresh charge for a new cycle.

Oil addition to the fresh charge is required to lubricate the crankshaft, connecting rod and cylinder walls, which normally rule out the need of an oil pump and filter system, allowing it to operate in any position but increasing emissions [7].

Engines that operate on four-stroke cycle present a more complex design, have much more parts, so they often require repairs which leads to greater manufactoring and maintenance expenses. The advantage which led to its widespread is their higher efficiency, since fuel is consumed once every four strokes without losses, and lower emissions.

2.2.2 Ignition Method

The ignition of the charge in reciprocating engines can occur in two distinct ways: Ignited by an external source, such as a spark plug, therefore called Spark Ignition (SI) method, or ignition by compression of the charge, autoignition, called Compression Ignition (CI) method. In the first mentioned type the fresh charge is a mixture of air and fuel, while in the second type the liquid fuel injected ignites the air charge after this has previously been heated by means of compression, to a temperature sufficiently high to initiate ignition. In engines operating with the SI method, a spark plug is located at the top of the cylinder, while in CI it is an fuel injector. Both ignition methods, SI and CI, are applicable to both work cycles, four-stroke and two-stroke cycle.

The concern over the charge dilution and imperfect scavenging is bigger in SI two-stroke engines, since instead of air being in the crankcase, like in the two-stroke CI case, there is a fuel-air mixture with oil added. Therefore, this engines are used where simplicity, lower cost and higher power to weight ratio is more relevant than efficiency, like in motorcycles, chain saws, outboard motors and model airplane engines [21].

The spark ignition engine is also referred to as the petrol, gasoline or gas engine from its typical fuels, and the Otto engine, after the inventor. The compression ignition engine is also referred to as the Diesel or oil engine; the fuel is also named after the inventor.

2.2.3 Method of Cooling

Due to the high temperatures that occur during combustion, the engine needs to be cooled to protect its components and and keep the lubricating oil at operating temperature. The decline of the temperature can be accomplished using air, with or without the assistance of a fan, that flows through the engine (air cooled), or by a cooling system that uses water, with or without adding antifreeze, corrosion inhibitors, or oil (liquid cooling).

2.2.4 Lubrication System

The lubrication system delivers the necessary oil to provide an adequate lubrication of all the moving parts of the engine. They can be differentiated in [6]:

- Mist lubrication system: used in two stroke engines, where the crankcase lubrication is not suitable. The lubricating oil is mixed with fuel, in a usual ratio of 3% to 6%.
- Wet Sump Lubrication System: the bottom of the crankcase contains a sump filled with lubricating oil, which is pumped to the various engine components through a splash system, a splash and pressure system or a pressured feed system.
- Dry Sump Lubrication system: in this case, the lubrication oil is drawn from an external supply, a tank, by an oil pump and circulates it under pressure trough the engine bearings.

2.2.5 Application

The reciprocating engine main applications is in the transport sector. Since, with the exception of portable power system, they are used in automobiles, trucks, locomotives, light aircrafts and marine vehicles [16].

2.2.6 Fuel

The thermal energy required to run reciprocating engines is provided by the chemical energy present in the fuel through combustion. There are many different fuels available for this purpose. They can be gaseous or liquid fuels:

- Gaseous fuels: Methane, propane, butane, natural gas (CNG), biogas (sewage treatment and landfill gas), and hydrogen.
- Liquid fuels:
  - Light liquid fuels: Gasoline, kerosene, benzene, alcohols (methanol, ethanol), acetone, ether, liquefied natural gas (LNG), and liquefied petroleum gas (LPG).
  - Heavy liquid fuels: Diesel, fatty-acid methyl esters (FAME) and rapeseed methyl esters (RME), also referred to as ”biodiesel”, vegetable oils, and heavy fuel oils.
  - Hybrid fuels: Diesel + RME, diesel + water, and gasoline + alcohol.

The different fuel types present different characteristics and availability, which has a considerable influence on design, efficiency and application of the engine.Currently, petroleum based fuels are the most widely produced and used, being the transport sector its biggest consumer [22]. Therefore, these are currently the main source of energy in reciprocating engines. Among the petroleum derived fuels, diesel and gasoline are by far the most used [23].

The two main renewable alternative fuels that are already being used in these engines are ethanol and biodiesel. Although the renewable idea may be attractive, the production of these fuels is limited by the availability of land, water and, in the case of biofuels from the availability of wastes and residues [24].

2.2.7 Method of Mixture Generation

In terms of mixture generation in reciprocating engines, it can be differentiated by the location of the mixture process, the method of fuel input and the type of the mixture generated [8]:

- External mixture generation, when the fuel is pre-mixed with air in the inlet system, or internal mixture generation when the mixture occur in the combustion chamber.

- Carburation. Direct injection, when the fuel is injected into the combustion chamber. Indirect injection when the fuel is injected in a subsidiary chamber, such as pre-chamber or a swirl-chamber, in CI engines, Figure 2.5, and some SI engines with indirect injection; in most of SI engines when fuel is injected into the intake ports, or in the intake manifold (with the injector upstream in intake manifold above the throttle), Figure 2.4.

- Homogeneous mixture generation when the mixture is generated byways of a carburettor, an intake manifold injection or fuel direct injection during the induction stroke in SI engines. Or nonhomogeneous mixture generation when the fuel is injected with extremely short intervals, in CI engines, and in some SI engines with direct injection.

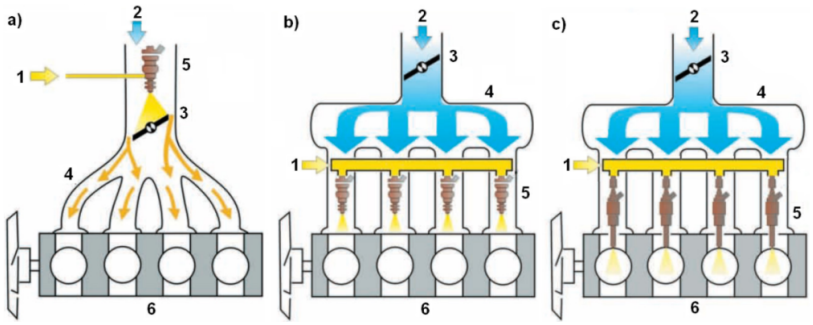

Figure 2.4: Types of fuel Injection in SI engines. Adapted from [3]. (a) Single point injection; (b) Multipoint injection; (c) Direct injection; 1-Fuel supply; 2-Air intake; 3-Throttle; 4-Intake manifold; 5-Fuel injector (or injectors); 6-Engine

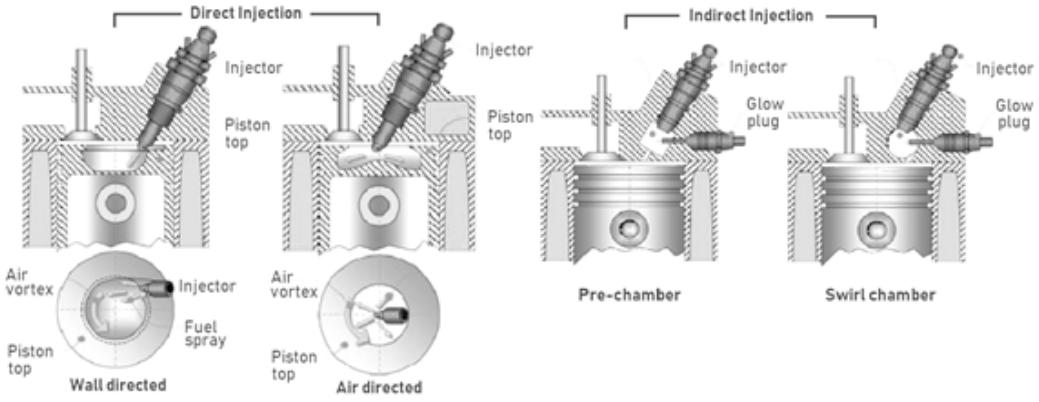

Figure 2.5: Types of fuel Injection of CI engines. Adapted from [4].

2.2.8 Valve or Port Arrangement

The air or air-fuel mixture and the exhaust gases are admitted and expelled from the cylinders by valves that open and close at the proper times, or by ports that are uncovered or covered by the piston. The valve timing is controlled by a camshaft mechanism.

There are many different designs for the intake and exhaust valve and their location. The most common valve type used in in four-stroke reciprocating IC engines is the poppet valve. Regarding their position, they can be located in the engine block, L-head (or *flathead*) and T-head arrangement, in the cylinder head, I-head arrangement, or a much less common configuration, the F-head arrangement, with one valve in the cylinder head (usually intake) and one in cylinder block, Figure 2.6.

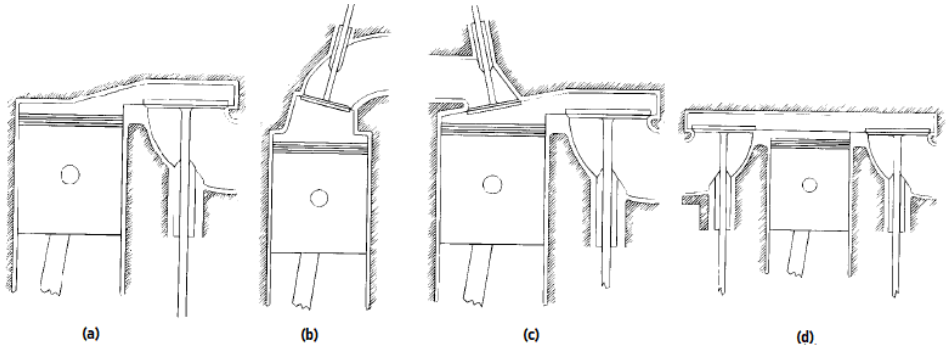

Figure 2.6: Engine Classification by Valve Location. Adapted from [5]. (a) L-head; (b) I-head; (c) F-head; (d) Valves in block on opposite sides of cylinder, T-head.

The position of the camshaft is an important feature in the valve arrangement. Regarding the number of camshaft and their position, the valves positioned in the cylinder block, L-head and T-head, also have the camshaft in this location. The valves located in the cylinder head, I-head arrangement, can be further differentiated in: overhead valve (OHV) arrangement, in which the camshaft is located in the cylinder block, overhead valve with overhead camshaft (OHV/OHC), with the a single camshaft located in the cylinder head, and overhead valve with double overhead camshafts (DOHC), Figure 2.7.

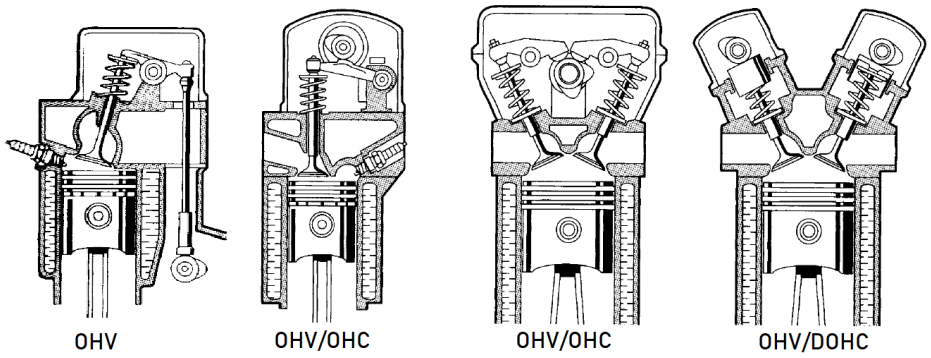

Figure 2.7: Overhead valve and camshaft arrangement.

Regarding the two-stroke ports design they are differentiated by the type of scavenging process in: cross-scavenged porting (inlet and exhaust ports on opposite sides of cylinder at one end),

loop-scavenged porting (inlet and exhaust ports on same side of cylinder at one end), through- or uniflow- scavenged (inlet and exhaust ports or valves at different ends of cylinder)[16].

2.2.9 Combustion Chamber Design

The combustion chamber design involves the shape of the combustion chamber, the type of ignition and mixture generation, and their location. They can be differentiated in [16]:

- *Open chamber*: when the entire volume of combustion chamber is located in the main cylinder and the fuel or mixture is delivered into this volume. Such is the case of the designs for SI engines, Figure 2.8, named after the valve arrangemet, and Figure 2.9, used in OHV arrangements, and the designs for CI direct injection, Figure 2.10. The direct injection CI chambers mainly consist on the space formed between a flat cylinder head and a cavity in the piston crown in different shapes, therefore, they are differenced by the piston head shape in hemispherical, shallow bowl, shallow toroidal and deep toroidal bowl. On the other hand, for SI engines, the combustion chamber is differentiated by the shape of the cavity formed between the cylinder head and a flat upper surface piston, in wedge, hemispherical head, bath-tub head, with exception on the bowls in piston chamber.

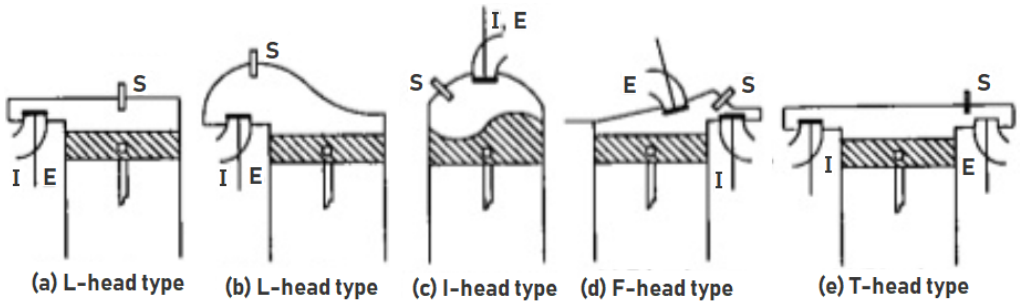

Figure 2.8: Combustion chamber for SI engines. Adapted from[6]. E- Exhaust valve; I- Inlet valve; S- Spatk plug.

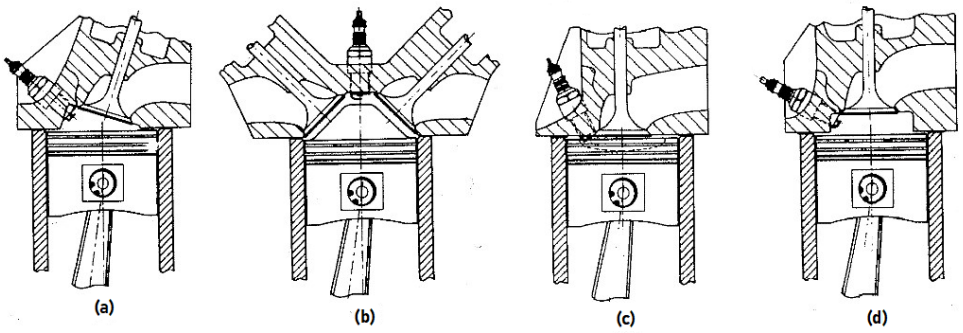

Figure 2.9: Combustion chamber for SI engines. Adapted from [7]. (a) wedge chamber; (b) hemispherical head; (c) bowl in piston chamber; (d) bath-tub head .

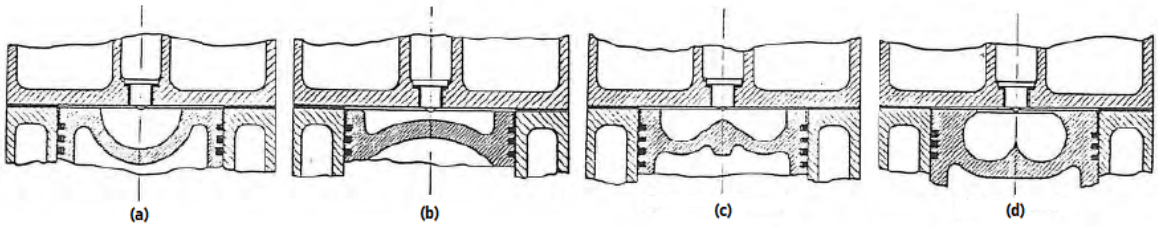

Figure 2.10: Different types of direct injection combustion chambers of CI engines. Adapted from [7]; (a) hemispherical; (b) shallow bowl;(c) shallow toroidal bowl; (d) deep toroidal bowl.

- *Divided chamber*: when the combustion chamber space is divided into two parts, one in the main cylinder and the other in the cylinder head, such is the case of indirect injection CI chambers, Figure 2.5, which can be classified further into: swirl chamber and pre-chamber. This type of chamber can also be encountered in some indirect injection engines with SI, where the fuel injector and spark plug are mounted on a secondary chamber[5].

2.2.10 Cylinder Arrangement

Since the invention of the IC engine many different cylinder arrangements have been experimented with, however, only a few standard configurations have prevail. Figure 2.11 shows a selection of possible combinations for the cylinder arrangement, differing in the cylinders position, orientation, number of cylinders, angle between the cylinder bank [6], number of crankshafts, and number of pistons on each cylinder.

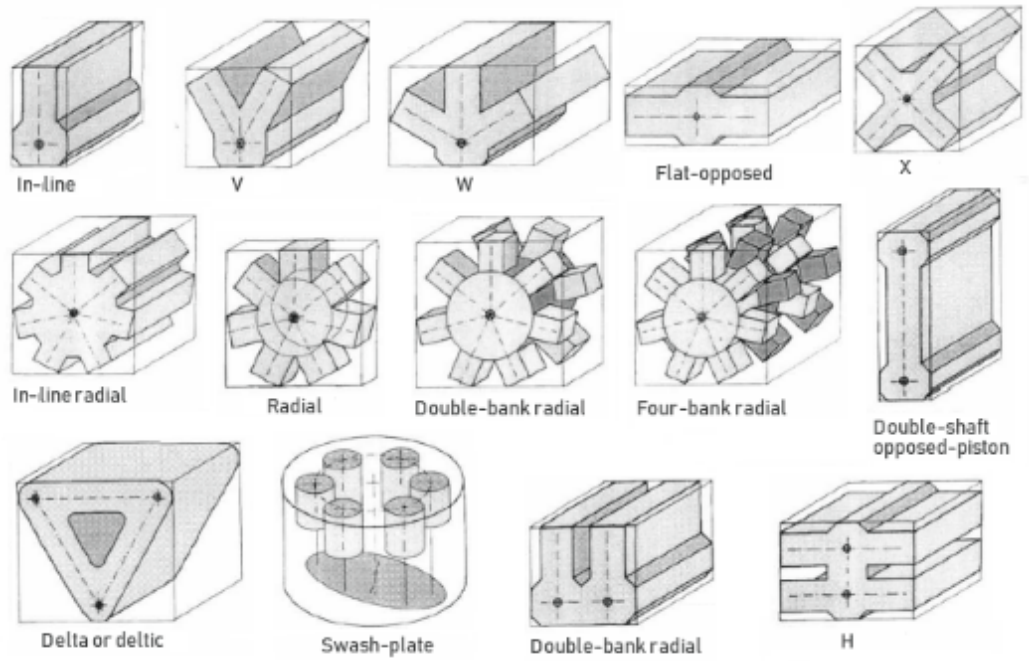

Figure 2.11: Cylinder arrengements in reciprocating engines. Edited from [8].

[6]When engines have a large number of cylinders, they are commonly arranged in two lines, referred to as a *cylinder bank* and the angle between them as *bank angle* or *V-angle*.

The following are presently of significance:

- In the in-line arrangement the cylinders are positioned in a straight line, one behind the other along the length of the crankshaft. Their number of cylinders range from two up to eleven cylinders or possibly more, but the most common is the in-line four-cylinder configuration.

- The V engine is formed from two in-line banks of cylinders, set at an angle with each other, along a single crankshaft, forming the letter V. Two connecting rods are coupled to each crank pin, with exception in the VR arrangement [7]. The angle between the banks range from 15° to 120°, with 45°, 60° and 90° being the most common, and the numbers of cylinder from 2 to 20 or more, being the V6, with six cylinders, three in each bank, and V8, with eight cylinders, four in each bank, the most common ones.

- The W arrangement is similar to the V arrangement, with except of having three in-line banks of cylinders and three connecting rods linked to one crank pin instead of two, forming the letter W. Are usually made with 12 cylinders with about a 60° angle between each bank. A V arrangement consisting of two VR banks is also referred as a W configuration.

- Opposed cylinder, flat opposed or horizontally opposed arrangement also referred as “boxer” is formed by two banks of cylinders opposite each forming a 180° angle (a V engine with a 180°V), connected to a single crankshaft, with each connecting rod connected to a separate crank pin.

- A radial arrangement has all of the cylinders in one plane around the central crankshaft, with equal spacing between cylinder axes. Since the cylinders are in a plane, articulated connecting rods of each pistons are attached to a master rod which, in turn, is connected to the crankshaft. The number of cylinders range from 3 to 13 or more and operates on a four-stroke cycle. They are mainly used in air-cooled, propeller-driven, aircraft applications since each cylinder can be cooled equally. For large aircraft two or more banks of cylinders are mounted together, one behind the other on a single crankshaft.

- In the opposed piston arrangement there are two pistons in each cylinder, with the combustion chamber in the centre between the pistons. Differing from the opposed cylinder in the numebr of pistons per cylinder.

The reciprocating IC engines final configuration depends on/results from a combination on choices of the different criteria. Therefore the engines configuration is characterized by: the work cycle, ignition method, the use or not of super or turbochargers, the method of cooling, type of fuel, fuel delivery system and mixture generation, valves or port arrangement and cylinder arrangement, taking in account its application [21].

Also proven to be a relevant feature in cylinder arrangement, therefore, in engine configuration is the use or not, location and number of camshaft and crankshafts mechanism.

[7] The VR arrangement is characterized by a V-angle of 15° and a crankshaft that have a separate crank pin for each connecting rod [8].

2.3 Opposed Piston Engine

In opposed-piston engines (OP) pistons are arranged in such a way that two pistons are reciprocating opposite to each other, crown to crown, both working in one cylinder. As they approach, the clearance volume or combustion space is formed between them at top dead centre, which in these case called inner dead centre (IDC) [9].

These engine configuration present some inherent advantages compared to a standard crank-slider arrangement with a single piston and a cylinder head regardless of the work cycle, such as, eliminates the need of the cylinder head, when replaced by a second piston that can be maintained at a higher metal temperature, which reduces the thermal losses of that surface of the combustion chamber. Since these engines assemble two pistons inside a single cylinder, a larger cylinder displacement can be attained for a given cylinder bore leading to a reduction in the number of cylinders and engine overall size[25].

Regarding its operation, the engine behave similarly to an typical four-stroke or two-stroke cycle engine, with exception that when combustion takes place the gases act against two pistons instead of one, driving them in opposite directions. Therefore, they not only have opposed piston arrangement, but also the combustion gases, within cylinder, act in opposite directions. Due its inherent configuration the valves or ports have to placed in the middle of the cylinder i.e. near combustion chamber, instead of the convencional OH valve arrangement.

Being a reciprocating IC engine, made up of a large number of components, the OP engine also present variations in their configuration. Of significance is the disposition of the engines components, mainly of crankshaft mechanism. Through time, various arrangements have been used regarding these component, hence, the OP engine can be sorted by the number and arrangement of crankshaft mechanism in mainly six types: Crankless OP engines or ”Free Piston” engines, Single Crankshaft OP engines, Double Crankshafts OP engines, Multi-Crankshaft OP engines, Rotary OP engines and Barrel Cam OP engines [9]. In this study only the Double Crankshafts arrangement will be considered and briefly described.

Double Crankshaft OP Engine

Introduced around 1881 by T. H. Lucas, in this type of arrangement each of the pistons is driving by separate crankshafts, thereby, two crankshafts are used for transmission of power, called “upper and lower” crankshafts in view of the original orientation. One of them is connected to a large flywheel, an inertial energy-storage device [26], which means when it’s spinning at high speed, it tends to want to keep on spinning, storing kinetic energy. During each stroke, reciprocating engines present speed fluctuations, the flywheel absorbs mechanical energy by increasing its angular velocity during expansion stroke, and delivers energy by decreasing it, in the next stroke(s). The other shaft is linked to gearing arrangements, which enables it to move in a prescribed manner relative to the previous crankshaft, thereby controlling the relative piston motion.

2.3.1 Historical Overview of OP Engine

At the start of internal combustion engine development (1850-1900), it was realized that to increase their efficiency it would be necessary to run them much faster than was common in contemporary engines, to do this successfully, it was necessary to improve the design of moving parts so as to reduce weight without sacrificing strength, and also give careful consideration to the matter of balance. Therefore, emphasis was given to single-cylinder engines operating with two- and four-stroke cycles, which offered simplicity and higher efficiency. The opposed piston (OP) concept offered an attractive way of achieving a substantially dynamically balanced single-cylinder engine that eliminated the need for the complex cylinder-head.

The first OP engine, that appeared for public use, was a two-stroke cycle, gas-fuelled engine, created by Wittig in Germany in 1878. Therefore, the "double" stroke presented another significant advantage in these engines, the possibility of large-cylinder displacements with small cylinder bores, reducing the gas loads on the crankshafts. An excellent insight of the opposed-piston engines history can be found in [9], where the development of these engines can be divided into three main periods: pre-1900, 1900-1945, and post 1945. Thus, in this work only a brief summary is presented.

- **Pre-1900**

  The pre-1900 period defines the beginning OP engine concept, characterized by the mention and introduction of many key features of the OP engine.The earliest example of an OP engine is the one constructed by Gilles of Cologne in 1874. An OP single-cylinder engine with one piston linked to a crankshaft and the other being a free piston. Although a considerable number of these engines were manufactured, they were not really commercially successful, since the engine was neither economical nor a match for the Otto four-stroke engine of 1876. Hence these title went to the Witting gas engine Figure 2.12, the first successful OP engine, developed around 1878 by Wittig of the Hannoversche Maschinenbau- Aktiengesellschaft. Probably the first OP engine where both pistons were crank driven, this engine used a single three-throw crankshaft, introducing the single-crank arrangement.

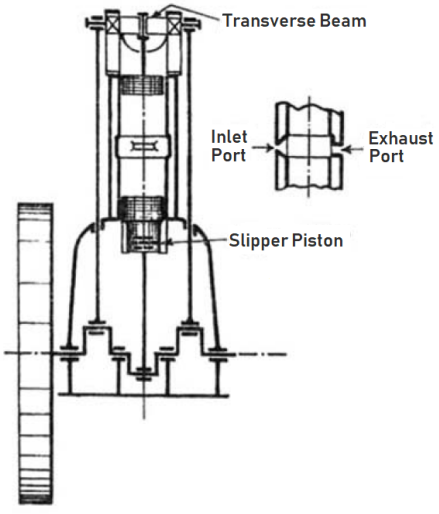

Figure 2.12: Wittig Gas Engine. Adapted from [9].

A significant advantage of the Wittig concept was the cancellation of forces acting on the main bearings, since two-piston systems produce essentially equal and opposite net gas and inertia forces, which enabled the use of relatively narrow main bearings. However, resulting in a longer crank than other equivalent-displacement single-cylinder OP engine arrangements. This arranegement also allowed the use of relatively lightweight or lightly stressed engine crankcases, which were a major benefit in the early days of engine casings and during the period when engines operated with exposed moving parts.

The use of two crankshafts for an OP engine was introduced around 1881 by T. H. Lucas. Regarding its arrangement, brought a significant advantage by enabling substantially more compact inline arrangements than the single-crankshaft configurations.

In 1890, Robson of Sunderland suggested a variant of the Wittig engine in which the cranks were arranged to avoid both pistons reaching their dead centres simultaneously, an alternative that facilitated engine starting.

The most remarkleble engine of this development period was the two-stroke OP engine, created by Hugo Junkers and Oechelhaeuser in 1892, Figure 2.13. This engine used the three-throw, Wittig-type crank with side rods to crossheads that were connected via a pair of side connecting rods to the outer air piston and the pair of rods acted on the piston via a rocking beam. The $31\,l$ engine, presented an output power of $84.3\,kW$ at $160\,rpm$, $bmep$ of $10\,bar$ and $imep$ of approximately $13\,bar$ therefore, with an astounding mechanical efficiency of 77 %, which was, and still is an extraordinary performance. In 1896 Oechelhaeuser derived a variant of these engine that was manufactured in different sizes, with power ranging from $225\,kW$ to $1100\,kW$ according to the number of cylinders. Oechelhaeuser and Junkers parted company in 1893.

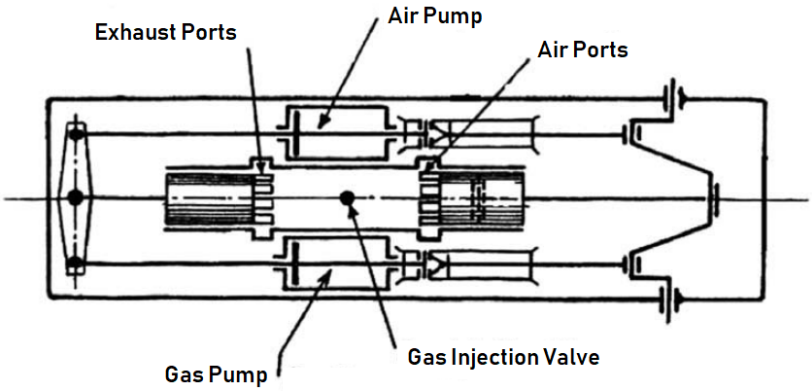

Figure 2.13: Oechelhaeuser and Junkers Gas Engine. Adapted from [9].

At the end of the century, also the end of these successful exploratory phase, the key advantages of the OP engines over their competitors were: simplicity, balance, no need of the then-problematic cylinder head joint, relatively light mechanical loading of the crankshafts due to the possibility of large engine capacities with low bore-to-stroke ratios, the “two directions” gas expansion, which was a benefit in terms of mixing the air with the fuel and turbulence generation, and the substantial improvement of the efficiency of two-strokes operating cycle.

- **1900-1945**

From the beginning of the 20th century until World War II, many stationary, marine and later aviation applications were developed, with varying degrees of success, despite the break during World War I. At least four major OP engine creators are noteworthy mentioning of the achievements of these period.

R.Lucas introduced many conceptual aspects that made its engine, a precurson of Fairbanks Morse railway, stationary, and marine engines manufactured in the United States from the 1940s until the present. One relevant aspect that he tacked in account was the importance of the crankcase compression pressure, since the crankcase volume was minimized. The Fairbanks Morse CI engine, inspired on Lucas OP engine was originally intended for locomotive application, but the first commercial sales were for submarine propulsion in WWII. Thousands of these engines were manufactured, with small changes from the original 1940s design, and are still being manufactured nowadays with emissions compliance.

William Beardmore introduced several important features to the traditional Oechelhaeuser design, from 1904 to1910, that made possible an overall height reduction to 35% lower than the original Oechelhaeuser engine, resulting in a more compact arrangement, which enabled significant reductions in inertia load, and therefore enabled higher engine speeds. However, these engines did suffer side connecting rod fractures.

Using its acquired knowledge from gas turbines to IC engines, Hugh Francis Fullagar introduced several significant improvements in OP packaging and weight reduction with its OP gas engine, with paired cylinders and diagonal cross-rods arrangement. Although the engine behaved reliably its performance at certain speeds was not satisfactory. The responsible deficiency were then rectified but due to relatively high cost of the gas fuel used in this engine, it was rendered economically unfeasible and the project was dismantled. The Fullagar concept was latter applied to the Q and R engines. These engines where noted for their, simplicity, robustness, efficiency, and longevity. About 115 engine of these engines were built and remained in service with high break thermal efficiency for 15 years without serious faults.

A considerable amount of research work on opposed piston engines for different applications was carried out in Germany by Hugo Junkers. Through the years he operated commercially under several company names including Junkers Co. which produced in 1901 the tandem OP engine. From then, he produced a variety of designs having different mechanical arrangements.

The first oil engines, which were derived from the Junkers and Oechelhaeuser gas engine, that entered production in 1908. Although these engines were horizontal, a three-cylinder vertical marine version was built, but due to difficulties regarding its height, length and serious vibration issues they were replaced by steam machinery, which led Junkers back to the single-cylinder per three crank throw engine configuration. These engines were more practical than the tandem arrangements, but they also experienced difficulties that led to their replacement by steam power. Therefore, Junkers experience in marine field was unsuccessful, in contrast to Doxford engines which were being built and successfully operating, known

for its endurance, reliability, and higher achieved BTEs than the Jumo.

Junkers engine development in the field of aeronautics began in the 1910. He started by chose adopting the two-crankshaft arrangement instead of the single-crankshaft three-throw Wittig system to achieve OP operation, over the concern with the speed capability of the side connecting rods at high piston speeds of this configuration and the greater flexibility of drives of the former. Also because the Wittig arrangement results in a relatively long crankshaft and a comparatively large empty crank case, which wasn't an issue for stationary engines, but at the time seemed to be unacceptable for high power-to-weight ratio applications. The first aero engine with this configuration was the horizontally arranged, six-cylinder, two-stroke, spark-ignited, gasoline fuelled Fo2 engine, which delivered $280\,kW$ at $1800\,rpm$, from $17.1\,l$. The Mo3, a four-cylinder, two-strokes, diesel engine, with a power output of $76.8\,kW$ at $1288\,rpm$ from $19.12\,l$ came after. These engines saw aerial service toward the end of WWI. Despite their success, with the official ending of the war, all existing engines were destroyed and the projects in development were cancelled under the rules of the Treaty of Versailles in 1918.

In the years after, the Fo4 was created derived from the Fo2 but with a vertical arrangement. The six-cylinder Fo4 engine powered the first diesel engine airplane flights in 1929. Although other engines were already been used for airships in which weight was a lesser issue, the Fo4 pioneered the power density capability (kW/kg) of an engine for airplane use. The series of development changes that followed led to the creation of Jumo 4 [8] engine witch was later renamed as Jumo 204. Despite its weight reduction, durability improvement and performance enhancement, Junkers considered the power-to-weight ratio and power density of the Jumo 204 to be too low for military applications and began to design a reduced-stroke engine that would enable higher rotational speeds, and therefore more power.

In the early 1930s Hugo Junkers decided to focus only in the aero engine business, which led to an evolutionary aviation period from 1932 to 1939, in which the Jumo engine family evolved, of which the 205 and 207 entered production. The jumo 205 become well renowned for being the first engine for commercial applications, the only diesel engine used in regular aircraft service in significant quantities worldwide, setting many long distance records, and historically remains the most efficient piston aero engine in aviation. The turbocharged jumo 207 was notable for its use in high-altitude applications. Different version followed, some were later built under license by Construction Lilloise de Moteurs (CLM) in France and D.Napier in the United Kingdom.

D. Napier also had a significant impact in the field of aeronautics with the spark–ignited W12 Napier Lion[9] engine, which powered aircrafts during WWI, and after applied in various commercial aircraft, flying boats, and military aircraft. By the early 1930s, Napier shown interest in diesel engines but since gasoline engines were needed to meet the high power-to-weight targets of fighter aircraft, this led to the creation of the Napier Sabre, an H24 sleeve-valve,

[8]The name "Jumo" came from Junkers Motorenwerke AG, the original name of Hugo Junkers engine manufacturing division.

[9]The Napier Lion engine powered the Gloster VI Seaplane that established a world speed record in 1929 with a top speed of 565.36 km/h.

four-stroke, spark-ignition engine which was widely used in WWII Mustang and Typhoon fighter aircraft.

William Doxford followed the Gilles and Wittig-type configuration of three-throw crankshafts per cylinder, but eventually was forced to adopt a more compact crankshaft arrangement in order to mitigate packaging and torsional vibration issues. Although these engines, which remained substantially unchanged from 1930 to 1965, were a big success in the marine field, the Doxford reluctance to adopt key technologies such as turbocharging, and in refusing licenses to other engine manufacturers led to the its downfall.

In the late 1930s the Sulzar brothers started to explore the application of turbocharging and high-pressure charging to two-stroke diesels OP engines, for stationary and marine applications, however, they were unsuccessful due the large engine height required to operate at very low marine speeds.

- **Post 1945**

  While the first half of the twentieth century was certainly the formative period for OP engines, the second half of the century was the most prolific time regarding OP engine production, although mainly in land and marine applications. Post WWII research into OP arrangements and prototypes began in 1946 in the United Soviet Socialist Republic (USSR), United States, in France, with probably the most diverse and in-depth work being done in the United Kingdom, as witnessed by the number of subsequent production applications. Dismissed and in production OP engines were used to investigate various aspects of engine behaviour. The main motivations for this work were the desire for multifuel capability and easier cold starting, since these aspects were important to military engineers of the time. The Napier Deltic engine was the first post war application of OP principles, introducing the equilateral triangle arrangement. Others engines fallowed, for military applications the Rolls Royce K60 and K60T, the Leyland L60 battle tank engine, the Coventry Climax H30 engine and the Kharkiv Morozov 6TD battle tank engine were created. More recently, the Bonner Engineering produced the Africar engine a 2l, three-cylinder, two-strokes, SI, prototype for the Africar project in 1987 and in 1995 the Air airship Industries commissioned the Diesel Air Engine, a 2l two-strokes diesel engine which has been used to power light aircraft.

  Although in the last decade OP units are still being used in a few countries, such as the United States, United Kingdom, Russia, India, Iran, and some Arabian Gulf states, their use has greatly decreased due to issues with emissions and particulates. In spite of these decline in potential buyers and emission challenges, some of the older engines continue in service and the design and development of new OP engines are currently being pursued commercially by the Achates Power Inc., Diesel Air Limited, Fairbanks Morse, Golle Motor AG, Kharkiv Morozov Machine Building, Monolith Engine, Pattakon, Pinnacle Engines and Superior Air Parts.

2.3.2 Challenges Facing OP Engines

OP engines initially evolved because of their excellent balance, fuel efficiency, competitive performance and manufacturing simplicity. Regardless the field of application, other significant advantages emerged with the progressive development of the OP engine, such as outstanding specific output and power-to-weight ratio, high specific torque, very high power density and power-to-bulk ratio. Other OP two-stroke advantages, compared to the four-stroke engine, were relatively low heat-to-coolant ratios witch enabled smaller radiators, high reliability and low maintenance, relative ease of servicing, excellent multifuel tolerance, low injection pressures, and simple fuel injection nozzles. Therefore, although both two and four-stroke work cycles can be applied to the OP engine concept, trough time, most OP engines developed operated on CI, two-stroke cycles, for simplicity, to achieve high thermal efficiency as well as high power density. A noteworthy mention of a four-stroke OP engine is the famous Gobron Brillié racing engine, built around 1900.

The OP configuration with the two-stroke cycle has many of the traditional two-stroke challenges witch caused its demise. The main issues for the OP engine with this operating cycle was, and probably remains, oil consumption, hydrocarbons and particulate emissions, low efficiency at high boost and relatively lower power-to-weight ratio comparing with an equivalent SI engine. Besides the operation and maintenance costs of oil consumption, the emission implications of oil carryover into the exhaust and the oxygen-rich exhaust, there were frequent examples of gross oil deposits onto houses, gardens, and clotheslines from the exhaust of OP engines used for locomotives and airborne OP engines.

In spite of these issues and challenges, the OP engine are currently still used in certain applications that have unconstrained emission levels. The advancement of the technology available today, enable the appearance of new solutions to overcome some of the problems regarding the two-stroke CI OP engine, such as, catalyst technology, the possibility of very low ash lubricants and special additives, therefore, extending the use of these engines to a wider field of applications and enhancing the reasons for considering OP engine as a favourable solution to challenges facing the IC engine in certain applications.

2.3.3 Aeronautical Applications

Aeronautical applications are inevitably very demanding functionally, as well as challenging from product liability and customer confidence standpoints, since any aircraft incident is likely to be fatal for the engine manufacturing company, even if the cause of the accident is not directly related to engine failure. In consequence, there are very few successful commercial piston engine in this field of application, because of the high risk and liability of these power units, and even less OP engines. It is only since 2000 that some companies carry forward with the design and development of OP engines for aeronautical purpose. British company Diesel Air Limited and Superior Air Parts, a wholly owned subsidiary of Superior Aviation Beijing headquartered in the Unites states, are the ones currently pursuing this very sensitive field of application.

Diesel Air Limited, developed and presented in 1999 the DAIR-100 engine a modern horizontal version of the OP engine concept configured for installation in most light aircraft on the market. This 1.8 litre opposed-piston flat twin CI engine has two half-length crankshafts linked by a gear train driving a centrally mounted propeller, produces $75\,kW$ at a propeller speed of $2500\,rpm$

and operates with jet A1 or diesel fuels. Several Aircraft and airship installations are now flying successfully, including the AT-10 airship form the Airship Technologies witch first flight with the DAIR-100 engine was in March of 2002 [27].

Formerly in development by the British company Powerplant Developments, in collaboration with Weslake Air Services and Jade Air, also British companies, for more than a decade, the Gemini 100, is a CI two-stroke three-cylinder $75\,kW$ engine, that runs on Jet A, diesel or bio-diesel fuels and was based on Junkers Jumo 205 engine. In 2015, Superior Air Parts acquired the engine concept and begun active development to improve the basic design and create a new Gemini series diesel engines, aspiring to achieve up to 400 kW in future variants. The company intend to create smaller engines in comparison with contemporary ones, providing a significant power-to-weight ratio advantage, and making it especially attractive to the experimental and light sports aircrafts markets. To be in keeping with these applications, the current engine version is horizontally opposed to minimize frontal area, and displaces a much more modest volume. Comparing with the DAIR-100, this engine has one cylinder and two more pistons but the propeller is driven through a reduction drive where both of the crankshafts runs at 4000rpm and the propeller at 2500 rpm, which increases power to almost the same weight [28] [29].

OP engines are well suited for fixed-wing light aircraft and helicopter engines applications, where power-to-weight ratio, power-to-bulk ratio, fuel efficiency, simplicity, and safety are compelling advantages. However, a lower risk route would be to address the increasingly important niche market of unmanned aerial vehicles (UAVs) with 1-100 kW power range, which applications are changing from purely military to civilian such as aerial surveillance, and the growing market of powered gliders, and the segment of aircrafts between the larger microlights[10] and light aircraft.

[10] Called ultralight aicrafts in some countries.

2.4 Thermodynamic Cycle

Thermodynamics can be defined as the science of energy. The name thermodynamics stems from the Greek words heat and power, which is most descriptive of the early efforts to convert heat into power. The same name is broadly interpreted to include all aspects of energy transformations, from one form to another, and the interaction of energy with matter, with particular regard to the relationships of heat, work, and properties of systems [10]. From the beginning of ICE development, some simple thermodynamics was used for evaluation. For many years, the major tool for analysis of the processes that occur inside the engine was the *ideal gas standard cycle*[30]. In recent years, particularly since the advent of modern computers, much more detailed information about engine processes, emissions etc. can be obtained from modern analysis. Nevertheless, a study of the air standard cycle as models of ICE is still useful for illustrating some of the important parameters influencing engine performance. In addition, it provides the structure from which more complex engine cycle analysis can be later understood.

In thermodynamics a system can be defined as a quantity of matter or a region in space chosen for study. Any characteristic of a system is called a property, such as, pressure, temperature, volume and mass. These variables are related to one another, and can be measured or calculated throughout the entire system, which gives a set of properties that describes the condition, or the state of the system. A system is said to have undergone a cycle if it returns to its initial state. Therefore, a thermodynamic cycle can be defined as a series of thermodynamic processes being repeated continuously implying that the same thermodynamic states are reached repetitively [10]. Most power producing devices operate on cycles, the IC engine being one of them, is no exception. The mechanical or real cycle experienced in the cylinder of an IC engine can be described as an open system with changing composition. The working fluid follows a cycle, in which a range of chemical, thermodynamic and flow processes are rapidly occurring, then at some point of the cycle is thrown out of the engine as exhaust gases instead of being returned to the initial state. These cycles like others encountered in actual devices are difficult systems to analyse. To make the analysis much more manageable, the real cycle is stripped of all the internal irreversibilities and complexities, resulting in a cycle that resembles the actual cycle, but is made up of idealised processes. Each easily described by simple mathematical equations, and represented on a state diagram as approximations for the very complex, real processes which occur in practice. Such a cycle is called an ideal cycle, when combined with the ideal gas model or air-standard assumptions, results in the so-colled ideal air standard cycle. The idealizations and simplifications commonly employed can be summarized as follows [10][5]:

- The working fluid is treated as air, which continuously circulates in a closed loop and always behaves as an ideal gas. This can be justified by arguing that the main constituent of the gas mixture, nitrogen, hardly undergoes any chemical reactions, thus, the working fluid closely resembles air at all times.
- The combustion process is replaced by a heat-addition process from an external source. By modelling the combustion process as a heat release process, the analysis is simplified since the details of the physics and chemistry of combustion are not required.
- The exhaust process is replaced by a heat-rejection process that restores the working fluid to its initial state.
- Friction and heat losses can be neglected.

- All the processes that make up the cycle are considered internally reversible.

There are several thermodynamic cycles on which an engine can operate, usually designated by the names of some of the most significant inventors from the early period of engine development. In the case of reciprocating engines analysis, the main difference between the two best-known and most applied, consists in how the combustion process is modelled. Thus, they can be differentiated according to the type of heat supply in constant volume heat addition and constant pressure heat addition [8][21]. However, in line with the purposes of this study only the constant volume cycle will be considered.

2.4.1 Constant Volume Cycle

This cycle considers the special case of an IC engine whose combustion is so rapid that the piston does not move during the combustion process, and thus combustion is assumed to take place at constant volume. Often referred to as Otto cycle, named after one of the early developers of this type of engine, it is the ideal air-standard cycle most representative of four-stroke SI reciprocating engine operation. The cycle consists of four idealized processes:

(1) → (2) : Isentropic compression.
(2) → (3) : Constant volume heat addition.
(3) → (4) : Isentropic expansion.
(4) → (1) : Constant volume heat rejection.

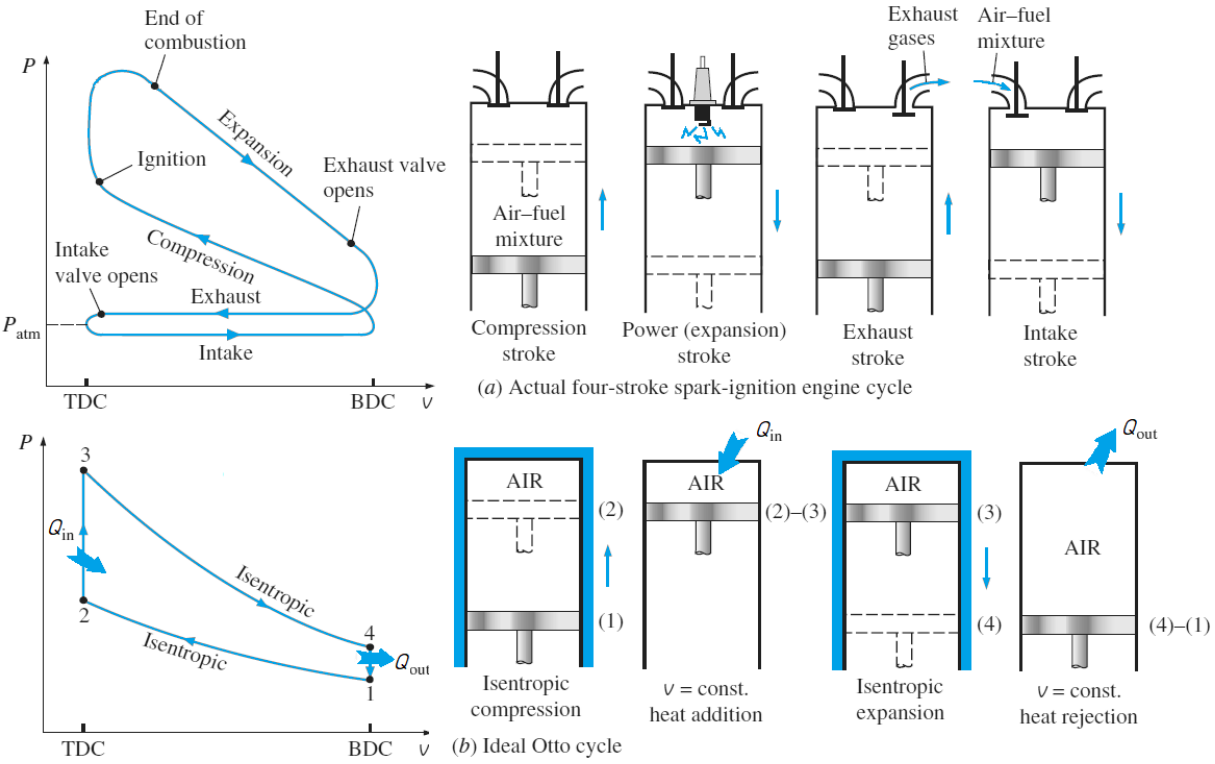

Figure 2.14: Actual and ideal cycles in spark-ignition engines and their P-v diagrams. Adapted from [10].

The sequence of processes which make up a typical four-stroke engine operating cycle has been described in Section 2.2. The particular case of a SI is illustrated in Figure 2.14, with their corresponding indicator diagram and state diagram. Pressure-volume diagrams are very useful, as the enclosed area equates to the work in the cycle.

The intake and exhaust processes, which can sometimes be found represented in the p-V diagram of the ideal cycle, do not appear in Figure 2.14. The reasoning to justify this is that these two processes cancel each other thermodynamically [5].

2.4.2 Thermodynamic Analysis of Air-Standard Otto Cycle

Any equation that relates the pressure, temperature, and specific volume of a substance is called an equation of state. There are several equations of state, some simple and others very complex. The simplest and best-known is the ideal-gas equation of state, Equation 2.24, where R is the universal gas constant. A gas that obeys this relation is called an ideal gas [10]. Since the working fluid in ideal cycles is assumed to be an ideal gas, these equation can be used to predict the behaviour of the gas throughout the engine cycle. By writing twice to a fixed mass and simplifying, it is possible to obtain the properties of an ideal gas in two different states.

$$p\,V = m\,R\,T \quad (2.24)$$

The ideal gas equation of state can be written in several different ways. For the special case of an isentropic process i.e, a process in which no heat exchange occurs between the system and its surroundings, the ideal-gas equation can be written as Equation (2.25) and Equation (2.26), [5]:

$$p\,V^{\gamma} = constant \quad (2.25)$$

$$T\,V^{\gamma-1} = constant \quad (2.26)$$

where the exponent (γ) is the ratio between heat capacity at constant pressure (c_p) and heat capacity at constant volume (c_v), Equation (2.27). For thermodynamic analysis the specific heat (γ) can be treated as constant, which simplifies calculations at a slight loss of accuracy. Its typical value for an Otto air cycle calculation is 1.4, which corresponds to the specific heat ratio of air at room temperature.

$$\gamma = \frac{c_p}{c_v} \quad (2.27)$$

Taking into consideration that the Otto cycle is executed in a closed system and applying the first law of thermodynamics, the energy balance for any of the processes can be expressed as:

$$(Q_{in} - Q_{out}) + (W_{in} - W_{out}) = \Delta U \quad (2.28)$$

Taking in account the above mentioned equations the Otto cycle processes can now be mathematically described.

- $(1) \rightarrow (2)$ **: Isentropic compression.**

  At the start of the cycle, with the piston in BDC position indicated by point 1 in Figure 2.14 (*b*), the cylinder contains a mass (m), of air at atmospheric pressure (p_1), ambient temperature (T_1), and volume (V_1) equivalent to the cylinder total volume (V_t). The mass can be determined resorting to Equation (2.29) and remains the same for the entire cycle [5].

$$m = \frac{p_1 V_1}{R T_1} \quad (2.29)$$

  When the piston moves from point 1 to point 2 (TDC), compresses adiabatically the gas in the cylinder. Therefore, the pressure (p_2) and temperature (T_2) at the end of the process is given by:

$$p_2 = p_1 \left(\frac{V_1}{V_2}\right)^{\gamma} = p_1 \, (c_r)^{\gamma} \quad (2.30)$$

$$T_2 = T_1 \left(\frac{V_1}{V_2}\right)^{\gamma - 1} = T_1 \, (c_r)^{\gamma - 1} \quad (2.31)$$

  The work absorbed and the variation of internal energy during the isentropic compression process can be related and determined by:

$$W_{1-2} = U_1 - U_2 = m \, c_v (T_1 - T_2) \quad (2.32)$$

- $(2) \rightarrow (3)$ **: Constant volume heat addition.**

  The piston remains at TDC without moving. Heat added to the gas causes an exponential increase in temperature and pressure, which can be related to the heating value of the fuel[11] (Q_{HV}). by Equation (2.33). Assuming that the heat addition occur instantaneously, there is no change in the gas volume, hence no work is involved during the process. Therefore, heat transfer to the working fluid can also be expressed by Equation (2.34).

$$Q_{in} = Q_{2-3} = m_f \, Q_{HV} \, \eta_c \quad (2.33)$$

$$Q_{in} = Q_{2-3} = U_3 - U_2 = m \, c_v \, (T_3 - T_2) \quad (2.34)$$

  Relating these two equations, with combustion efficiency (η_c) as unity and solving to (T_3), the maximum temperature of the cycle can be obteined from Equation (2.35).

$$T_3 = T_2 + \frac{m_f \, Q_{HV}}{m \, c_v} \quad (2.35)$$

  The maximum pressure can be determined from the state equation applied at points 2 and 3, for constant volume and solving for ($p3$):

$$p_3 = p_2 \, \frac{T_3}{T_2} \quad (2.36)$$

[11] Typical heating values for the commercial hydrocarbon fuels used in engines, such as gasoline, are in the range of 42 to 44 MJ/Kg[16].

- $(3) \rightarrow (4)$ **: Isentropic expansion.**

  The gas expands while pushing the piston to the original volume (V_1) at point 4 (BDC). The expansion process is also assumed to be reversible and adiabatic. Analogous to the first process, the pressure (p_4) and temperature (T_4) is given by:

$$p_4 = p_3 \left(\frac{V_3}{V_4}\right)^{\gamma} = p_3 \left(\frac{1}{c_r}\right)^{\gamma} \quad (2.37)$$

$$T_4 = T_3 \left(\frac{V_3}{V_4}\right)^{\gamma-1} = T_3 \left(\frac{1}{c_r}\right)^{\gamma-1} \quad (2.38)$$

  The work produced and the variation of internal energy during in isentropic exhaust process can be related and determined by:

$$W_{3-4} = U_3 - U_4 = m\, c_v (T_3 - T_4) \quad (2.39)$$

- $(4) \rightarrow (1)$ **: Constant volume heat rejection.**

  The piston remains at BDC. Heat is removed from the gas at constant volume, returning to its original state. From the first law of thermodynamics:

$$Q_{out} = Q_{4-1} = m\, c_v\, (T_1 - T_4) \quad (2.40)$$

IC engines are designed for the purpose of converting thermal energy to work. Hence, one engine operating parameter of greate interest which can be determined from thermodynamic analysis of the engine ideal cycle is the indicated thermal efficiency (η_t), which may be defined as the ratio of the work produced per cycle to the heat input during the process which corresponds to combustion in the actual cycle. Therefore, for a thermodynamic cycle the thermal efficiency can be expressed through Equation (2.41), where the indicated work per cycle (W_i) is the sum of the compression work W_{1-2} Equation (2.32) and the expansion work W_{3-4} Equation (2.39) [16].

$$\eta_t = \frac{W_i}{Q_{in}} = \frac{W_{1-2} + W_{3-4}}{Q_{2-3}} = \frac{(T_3 - T_4) - (T_2 - T_1)}{T_3 - T_2} = 1 - \frac{T_4 - T_1}{T_3 - T_2} \quad (2.41)$$

This can be further simplified by applying ideal gas relationships for isentropic compression and expansion and recognizing that $V_1 = V_4$ and $V_2 = V_3$. Thus, the thermal efficiency relation can be rearranged to:

$$\eta_t = 1 - \frac{1}{c_r^{\gamma-1}} \quad (2.42)$$

It can be observed from Equation (2.42) that the thermal efficiency of an ideal Otto cycle depends on the compression ratio of the engine and the specific heat ratio of the working fluid, and increases with both. Which is also true for actual SI engines. However, for a given compression ratio, the thermal efficiency of an actual SI engine is lower due to irreversibilities, such as friction, and other factors such as incomplete combustion, the specific heat ratio decrease with an increase in temperature and change according to the working fluid composition. Thus, thermal efficiencies of actual SI engines range from about 25 to 30 percent, while the ideal cycle can easily present twice these values [10].

2.5 Combustion / Combustion Considerations

Combustion is the oldest and most important energy conversion method known to mankind. Although combustion in the form of simple fires was known to the earliest man, and its applications evolved hand in hand with the evolution of human civilization, with many experimental, theoretical, and practical progress, due to its inherent complexity, research on these phenomenon, is far from being completely understood. Of course, the elements of combustion, such as flame and explosion are, known for a long time, but somehow their first analytical description has been obtained not such a long time ago. Only in recent times a more coherent picture has begun to emerge. More precisely, since the mid-1970s, there has been a really significant advancement in combustion science, driven by society concerns over energy sufficiency and environmental quality, and made possible by the rapid increase in the sophistication of mathematical analysis and computational simulation [31].

The importance of combustion can be more clarified by realizing that the vast majority of the energy currently consumed worldwide is obtained through combustion processes. In 2015 approximately 91% of the world energy supply came from oil, coal, gas biomass and waste [22]. Hence, it is fair to say that a very substantial part, of the energy used today in transportation, power production, space heating, even domestic cooking is generated directly, or indirectly, by combustion of solid, liquid and gaseous fuels. Energy sources like nuclear, hydro, solar or wind energy still play a minor role. Thus, combustion and the devices that rely on it to generate power will remain a key technology in the foreseeable future.

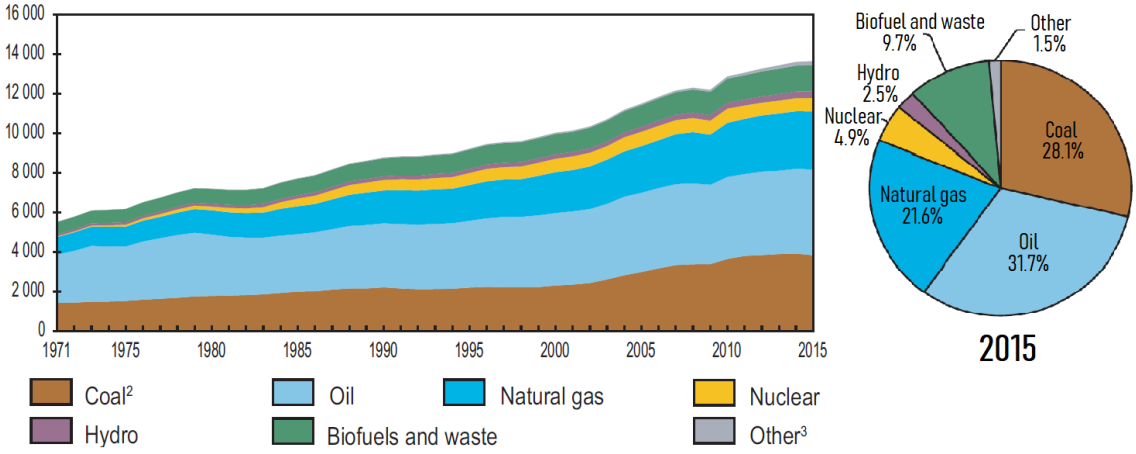

Figure 2.15: World total primary energy supply (TPES) by fuel. Adapted from [10]. Other: Includes geothermal, solar, wind, tide/wave/ocean, heat and other.

The concept of Combustion is not easy to define. In general terms combustion can be described as a phenomenon that involves the change in the chemical state of a substance or substances, from a fuel state to a product state via fast exothermic chemical reactions, accompanied by mass and heat transfer[31][32]. Combustion of the fuel-air mixture inside the engine cylinder is one of the processes that controls engine power, efficiency, and emissions [16]. Therefore, some background in relevant combustion phenomena is necessary in order to understand engine operation and to predict combustion numerically.

2.5.1 Classifications of Fundamental Combustion Phenomena

A combustion reaction which can propagate sub-sonically through space is denominated flame. In combustion system, such as IC engines, self-sustaining chemical reaction occurs within a narrow zone which is small in thickness, compared to its boundaries. These intense chemical reaction zone is commonly refer to as flame or flame front [16] [33]. The flame propagation results from the strong coupling of the chemical reaction with the molecular transport process. This interaction leads to the classification of the combustion phenomena in the following modes of combustion or flames[34][35]:

- **Premixed or Nonpremixed Combustion**: Probably the most important characterization of combustion phenomena, since combustion systems behave quite differently depending on whether the reactants are mixed or not as they enter the reaction zone. If the reactants are essentially uniformly mixed together, the flame is designated as premixed. If the reactants are mixed only in the region where reaction takes place, the flame is called nonpremixed flame or diffusion flame[12].

- **Laminar or Turbulent Combustion**: Characterization of the flame, regarding the nature of the gas flow through the reaction zone, whether it is laminar or turbulent. In a laminar flow, there are distinct streamlines for the convective bulk motion, mixing and transport are done by molecular processes and they only occur at low Reynolds number[13] i.e. viscous forces are dominant compared to inertial forces. Whereas, in a turbulent flow the streamlines do not exist, such that at any point in space the flow quantities randomly fluctuate in time, and they only occur at high Reynolds number i.e. inertial forces are dominant over viscous forces.

- **Steady or Unsteady Combustion**: Another classification of the flame regarding the nature of the flow if it is steady or unsteady. The distinguishing feature is whether the flame structure and motion change with time. A flow in which the fluid properties at a point in the system do not change over time is called steady flow. Time dependent flows are known as unsteady or transient. As is the case of some cyclic devices, such as reciprocating engines (an obvious consequence of their operating cycle), in which the fluid properties vary with time in a periodic manner. However, the flow through these devices can still be analyzed as a steady-flow process by using time-averaged values for the properties [10].

- **Homogeneous or Heterogeneous Combustion**: This is among the most confusing terminology in combustion literature. Conventionally /Traditionally, these feature is related to the initial phase of the reactants—gas, liquid, or solid. The flame is called homogeneous if both reactants initially exist in the same phase and heterogeneous if the two reactants initially exist in different phases. On the other hand, the chemists define it by the reactants phase at the location where reaction takes place. Sometimes, this terminology is also used to describe the uniformity of the mixture i.e. whether there is a temperature or concentration gradient in the mixture. In order to avoid confusion it will be considered the first way of characterization, which is believed to be simpler and more comprehensive.

[12] In reference to the mixing process that reactants goes through before reaction is initiated.

[13] The Reynolds number is a dimensionless number used to characterize different flow regimes, defined as the ratio of inertial $\rho u^2 L^2$ and viscous forces $\mu u L$ [33]

2.5.2 Combustion in Four-Stroke SI Engines

In a reciprocating SI engine, combustion can be expressed as a premixed unsteady turbulent flame progressing through a homogeneous air-fuel mixture in the gaseous state [5] [8][16]. Combustion can either occurs normally or abnormally. Under normal operating conditions, the combustion process can be divided in two main stages, see Figure 2.16(a): $(A \rightarrow B)$ ignition and flame development[5] or delay period[7] and flame propagation $(B \rightarrow C)$. In the first stage of combustion, ignition occurs and the combustion process starts. The flame front is initiated by a spark discharge that releases the amount of energy necessary to ignite a self-sustaining combustion (about 0.2mJ) in around 0.001s, anywhere from 10°to 30° before TDC. Generally, the flame can only be detected at about 6° of after spark plug firing. At first, the small spherical flame propagates outward into the combustion chamber at a very low rate , consuming only about 5% of the air-fuel mixture, which in turn affects the cylinder pressure so that little pressure rise is noticeable and little or no useful work is produced. Until the flame is of the same order of size as the turbulence scale, the propagation cannot be enhanced by the turbulence, which causes the "delay period" from which these stage is also named after.

During the second stage of combustion, the flame front moves very quickly through the combustion chamber, due to the continuous increase in the rate at which the fuel-air mixture is consumed, which causes a significant chemical energy release, hence pressure and temperature rise. The spread of the flame front is also substantially increased by the induced turbulence, swirl, and squish within the cylinder, and greatly distorted and spread by these motions[14]. As the fuel-air mixture burns, the density of the burned gases decreases and they expand, in turn compressing the unburned mixture ahead of the flame, displacing it toward the combustion chamber walls and piston head, thus supplying the force necessary in the expansion stroke to provide useful work. Throughout this phase about 80-90% of the air-fuel mixture is consumed and just about all useful engine work is generated. Ideally, at TDC the flame diameter should be about two-thirds of the cylinder bore, likewise, the air-fuel mixture should be about two-thirds burned. The end of this phase occurs shortly after the maximum temperature and maximum pressure of the cycle, which usually occurs around 5° to 15° after TDC.

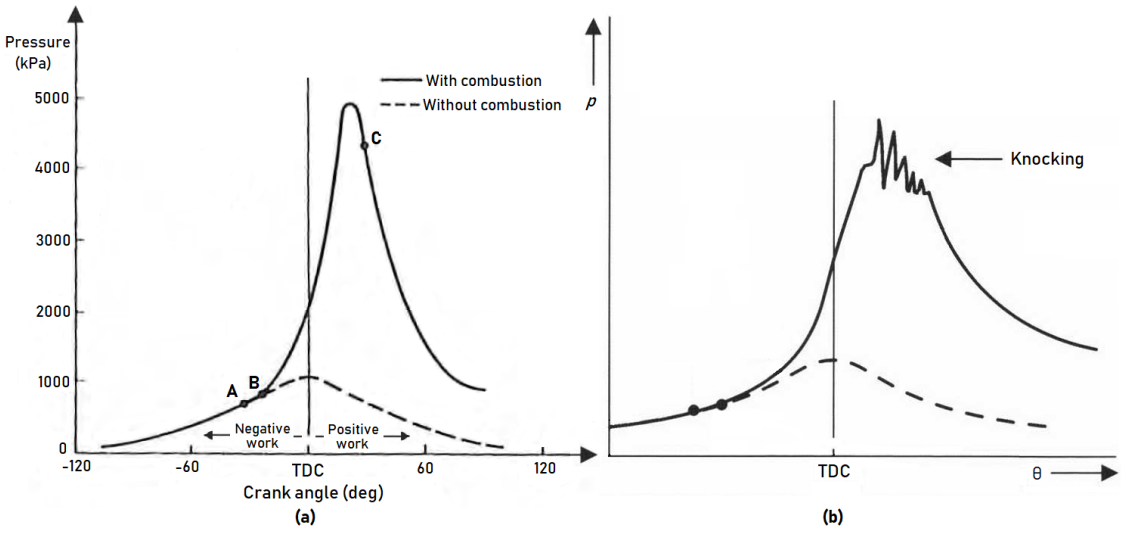

Figure 2.16: (a) Hypothetical pressure diagram for a four-stroke SI engine. (b) Sharp pressure fluctuations in the pressure curve during knocking combustion. Adapted from [7] and [8].

[14]For more details about this motions and their influence in IC engines combustion phenomena, see[5].

The air-fuel mixture should be almost completely burned at about 15° after TDC, when the flame reaches the extreme corners of the combustion chamber. This is commonly considered as the end of combustion process. However, combustion continues around the corners of the combustion chamber and along the chamber walls for another 10° at a much reduced rate of reaction and flame speed, which is a desirable occurrence, in order to achieve a smooth engine operation. Obviously, this is only a rough approximation and there is some variation from engine to engine.

So far, normal combustion has been described, in which the flame moves steadily through the combustion chamber until the fuel-air mixture is fully consumed. However, when the flame starts at a different time and/or location from the one initially defined, and causes to some part or all of the air-fuel mixture to be consumed at extremely high rates, it is referred to as abnormal combustion. Abnormal combustion can take several forms, which can be summarized in two main ones: *surface ignition* and *self-ignition*. Surface-ignition or pre-ignition, is caused by the mixture igniting as a result of contact with a hot surface, such as an overheated valve or spark plug, combustion-chamber deposits, or any other hot spot in the engine combustion chamber i.e., by any source other than the normal spark ignition. Since it can occur before the spark discharge (pre-ignition) or after (post-ignition), the former terminology seems more appropriate. After ignition of the surface, a turbulent flame develops at each surface ignition location and begins to propagate through the chamber in a manner analogous to that of normal ignition, thus making it difficult to notice, with except that the ignition source is at a different time and probably location.

As mentioned before, when the flame front moves across the combustion chamber the unburned mixture ahead of the flame is compressed rising in temperature as well as pressure. Self-ignition occurs when the pressure and temperature of the last portion of the unburnt mixture, called the end-gas, becomes so high such as to cause spontaneous ignition. When this abnormal combustion process takes place, there is an extremely rapid release of chemical energy, causing very high local pressures and the propagation of pressure waves of substantial amplitude across the combustion chamber. Which can be identified by a noise that is transmitted through the engine structure, generally termed ”knock”; or by observing sharp pressure fluctuations whose amplitude decay with time in the engine pressure curve, see Figure 2.16(b). The cause of the end-gas reaching auto-ignition conditions is either too high a compression ratio, too long a flame front travel or poor cooling in the region of the end gas.

2.5.3 Ignition Timing

The optimum spark setting depends on the rate of flame development and propagation, the length of the flame travel path across the combustion chamber, and the details of end of combustion process. Which in turn, depend on engine design, operating conditions, and the properties of the fuel, air and burned gas mixture. Therefore, the actual moment of ignition is an optimization parameter. It is adapted to the engine operation so that an optimum combustion process is obtained. The spark plug is usually located near the intake valves to assure a richer mixture, which ignites more easily, gives a higher flame speed, and a better start to the overall combustion process. In addition, the combustion phenomena must be properly located relative to TDC. The key feature is to position the peak pressure relative to the spark ignition timing, so that it’s not too early or too late.

Since combustion takes a limit time, and for that the mixture is ignited before TDC. There is an increase in pressure before the end of the compression stroke, thus, in the compression stroke work transfer from the piston to the cylinder gases (negative work). Advancing the ignition timing causes a progressive increase in this negative work. On the other hand, if higher pressure at TDC leads to higher pressures during the expansion stroke, retarding the spark timing so as the maximum cylinder pressure occurs later in the expansion stroke, reduces the expansion (positive) work, see Figure 2.17. Therefore, there is a trade-off between these two effects, and this leads to an optimum ignition timing, referred to as minimum (ignition) advance for best torque (MBT) [7]or maximum brake torque timing (MBT)[16], which occurs when the magnitudes of these two opposing trends offset each other. By using the MBT, the peak pressures and temperatures in the cylinder are reduced, which helps to restrict heat transfer, engine noise, emissions, and susceptibility to abnormal combustion.

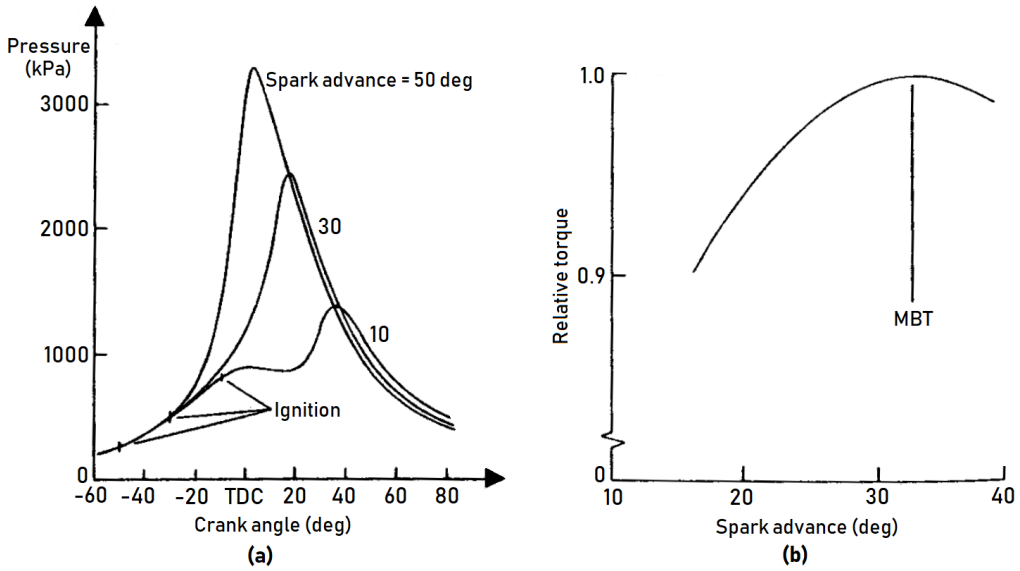

Figure 2.17: (a) Hypothetical pressure diagram for a four-stroke SI engine. (b) Sharp pressure fluctuations in the pressure curve during knocking combustion. Adapted from [7] and [8].

2.6 Combustion Analysis-Thermodynamic and Kinetic

Because combustion occurs through a flame propagation process, changes in the state and motion of the unburned and burned gas are much more complex than the ideal cycle analysis in Section 2.4.2 suggests. Even so, thermodynamics still important in the reacting systems analysis, as it provides information of the beginning and end states of the system. However, it has no concern for the process path between them, that is, the rate at which species are consumed and produced. This is the subject of chemical kinetics. Thus, chemical kinetics, when describing the transient states of the system, has a key role in products composition prediction, hence in pollutants control.

In this chapter, thermodynamic topics related specifically to systems whose chemical composition changes with time, and some chemical kinetics concepts will be presented. Although, pollutants are present in small amounts in the products, yet their impact on the environment and human health can be significant, so another area also important to combustion analysis is emissions, which will be overviewed at the end of the chapter.

2.6.1 Mixture Composition

Combustion systems, such as the working fluids in engines consist of many different gases. They are not inert because under the right conditions of temperature and pressure, they can react chemically. Hence, they are called reacting mixtures [31]. The thermodynamic properties of a gas mixture, result from a combination of the properties of all of the individual gas species, so it depends on the composition of the mixture, as well as on the amount of each component in the mixture. There are two important and useful concepts used to characterize the composition of a mixture, which are: species mole fraction (Ψ_i) and species mass fractions (Y_i). As in the current study the gaseous mixture will be expressed in mass fractions, only these will be described. However, they can be easily related through the species molar mass M_i Equation (2.43), where (N_i) is the number of moles of species (i).

$$m_i = N_i M_i \quad (2.43)$$

Considering a gas mixture composed by a finite number of (n) different especies. The total mass of the mixture (m_{mix}) is clearly the sum of the masses of the individual species, i.e.,

$$m_{mix} = \sum_{i=1}^{n} m_i \quad (2.44)$$

The mass fraction describe the relative amount of a given species (i) compared whit the total mixture, and it can be defined by,

$$Y_i = \frac{m_i}{\sum\limits_i m_i} = \frac{m_i}{m_{mix}} \quad (2.45)$$

By definition, the sum of all the species mass fractions must be unity, as shown in Equation (2.46).

$$\sum_i Y_i = \sum_i \frac{m_i}{m_{mix}} = 1 \quad (2.46)$$

2.6.2 Combustion Stoichiometry

In a combustion process the chemical species in the beginning of the process, the reactants, give rise to different chemical species, the products, through the chemical reaction. The reactants are usually a hydrocarbon fuel with the general composition ($C_x H_y$), and an oxidizer. Although hydrocarbon fuels are mixtures of many different hydrocarbons, for convenience, they are usually considered to be a single hydrocarbon, for example, gasoline is treated as octane, ($C_8 H_{18}$). The oxidizer most often used in combustion processes is simply air, since it would be extremely expensive to use pure oxygen, so the atmosphere used as a rich source of oxygen. To simplify calculation in the analysis of combustion processes air can be modelled as being made up of approximately 21% oxygen (O_2) and 79% nitrogen (N_2).

During combustion, the chemical composition of the reactive mixture varies over time. The main problem in combustion analysis is to discover the exact composition of the products from a known composition of reactants. This can be achieved through idealization of the reaction. Thus, the representative chemical equation is balanced on the basis of the conservation of mass principle, which means that the total mass of each element is conserved in the course of the reaction.

The simplest reaction model is that of a stoichiometric reaction. When the fuel and an oxidizer concentrations is chemically correct, and all the carbon in the fuel are converted to CO2, and all hydrogen to H2O, i.e. a complete combustion in which all the reactants are totally consumed and form an ideal set of products, then the combustion intensity is close to the highest and this mode of burning is called stoichiometric combustion. This ideal mixture approximately yields the maximum flame temperature, called *adiabatica flame temperature*, as all the energy released from combustion is used to heat the products. The balanced stoichiometric combustion of a given hydrocarbon fuel reacting with oxygen can be generally expressed by Equation (2.47), and if octane is the fuel component by Equation (2.48).

$$C_xH_y + \left(x + \frac{y}{4}\right) O_2 \rightarrow x\, CO_2 + \frac{y}{2} H_2O \quad (2.47)$$

$$C_8H_{18} + 12.5\, O_2 \rightarrow 8\, CO_2 + 9H_2O \quad (2.48)$$

For every mole of oxygen entering a combustion chamber there is also 0.79/0.21 = 3.76 moles of nitrogen. Stoichiometric combustion of octane with air is then:

$$C_8H_{18} + 12.5\, O_2 + 12.5\, (3.76)\, N_2 \rightarrow 8\, CO_2 + 9H_2O + 12.5\, (3.76)\, N_2 \quad (2.49)$$

In this reactions, the species on the left-hand side are reactants, and the ones on the right-hand side are products. The number of atoms of elements are exactly the same on both sides and must not change. Considering the atomic weights of the atoms of Carbon(12), Oxygen(16), Hydrogen(1), and Nitrogen(14), by multiplying with the number of moles of each of them, it can be determined the concentration of the reagents in mass units Equation (2.43): $C8H18 = 114Kg$, $O2 = 400Kg$, and $N2 = 1316Kg$. Furthermore, the reactants mass fraction, which will be later used in this study, can be obtained by dividing each of the reactants mass with their total mass (1830.6). Which results in approximately: $C8H18 = 0.062$,$O2 = 0.219$ and $N2 = 0.719$.

2.6.3 Mixture Ratios

The relative proportions of fuel and air is one of the most important parameters of a IC engine system, since it affects the mixture flammability, and the engine performance, efficiency and emissions. The minimum amount of air required for combusting a stoichiometric mixture is called stoichiometric or theoretical air. However, in practice fuels are often combusted with an amount of air different from the stoichiometric ratio. For this reason, it is convenient to quantify the combustible mixture. Various terminology is used to evaluate the air used in combustion applications. The ratio of the mass of air to the mass of fuel in the mixture (AFR) Equation (2.50), similarly the fuel-air ratio (FAR), Equation (2.51), are two of commonly used methods to express the mixture ratio, the former being generally applied to IC engines. For octane the stoichiometric AFR is approximately 15, which can be calculated from the above determined masses.

$$AFR = \frac{m_a}{m_f} \quad (2.50)$$

$$FAR = \frac{m_f}{m_a} \quad (2.51)$$

The amount of air used in combustion processes can also be expressed in terms of equivalence ratio (ϕ), to indicate the deviation of the mixture concentration from stoichiometry. When less air than the stoichiometric amount is used, the mixture is described as fuel rich, and if excess air is used as fuel lean. Defined as the ratio of the actual fuel–air ratio (FAR_{act}) to the stoichiometric fuel–air ratio (FAR_{stoic}), from Equation (2.52) we see that for stoichiometric mixtures ($\phi = 1$), for fuel-rich mixtures ($\phi > 1$) and for lean mixtures ($\phi < 1$). An alternative variable based on AFR, the air-fuel equivalence ratio or lambda (λ) can also be used, which is simply the reciprocal of ϕ ($\lambda = 1/\ \phi$). SI engines normally operate with an equivalent ratio close to stoichiometric, in the range of 0.9 to 1.2, and have combustion efficiency in the range of 95% to 98% for lean mixtures and lower values for rich mixtures, where there is not enough air to react all the fuel [5].

$$\phi = \frac{(FAR)_{act}}{(FAR)_{stoic}} \quad (2.52)$$

2.6.4 Reaction Rates/Kinetics

A chemical reaction such as the one represented by the stoichiometric relation in Equation (2.47), only names the observed reactants and final products and their relative molar amounts. The actual reaction path in combustion systems hardly proceed in such a simple manner. In reality, many sequential processes can occur involving many intermediate species. Thus, is generally described as a chain reaction, in which the products of one reaction serve as reactants of other reactions, i.e, the molecular bonds holding atoms are broken and new bonds are formed between radicals, ions, excited atoms and molecules, which results in new molecules appear. Each reaction occurring during the global reaction Equation (2.47) is referred to as an elementary reaction and the whole set of elementary reactions, which describe the global reaction as combustion mechanism.

Most elementary reactions of interest in combustion are binary reactions, that is, two molecules with the capability of reacting together collide and react to form two different molecules [33]. Thus, the chemical expression of a elementary forward reaction can be described by the following general form:

$$aA + bB \rightarrow cC + dD \quad (2.53)$$

where a, b, c, d are the respective stoichiometric coefficients[15]. In order to know how fast the elementary reaction proceeds, a reaction rate or consumption rate ($\dot{\omega}$) is defined as the derivative of the concentration of a species with respect to time due to the reaction involved. For example, the rate of change in the molar concentration of species (A) can be expressed as:

$$\dot{\omega}_A = -\frac{d[A]}{dt} \quad (2.54)$$

where the notation $[A]$ is used to denote the molar concentration in ($kmol/m^3$). Since the rate of reaction is directly proportional to the concentrations of each of the reactant molecules, a *mass action rate law* connects the reaction rate to the reactant concentrations [37]. Thus, for Equation (2.53), the rate at which the reaction proceeds can be expressed by the following empirical form:

$$\frac{d[A]}{dt} = -k\,[A]\,[B] \quad (2.55)$$

[15]Usually the values of a, b, c, d are one or two as not more than two molecules are likely involved in elementary reactions [36].

where the proportionality constant, referred to as Arrhenius rate constant (k) gives the functional dependence of the reaction rate on temperature and is usually modeled using the empirical Arrhenius law Equation (2.56).

$$k = A \exp\Big(- \frac{E_a}{RT}\Big) \quad (2.56)$$

where (R) is the universal gas constant, and (A) is the pre-exponential factor, which expresses the frequency of the reactants molecules colliding with each other. The activation energy (E_a), can be viewed as the minimum energy required for breaking the chemical bonds of the molecules during a collision in order to reaction to occur. And the Boltzmann factor[16] $exp(E_a/RT)$, can be interpreted as the probability of a successful collision leading to products. The constants are determined experimentally. Some authors use Equation (2.57) a modified Arrhenius equation to achieve better reproduction of experimental results, in which (β) is called the temperature exponent.

$$k = A\,T^{\beta} \exp\Big(- \frac{E_a}{RT}\Big) \quad (2.57)$$

2.7 Emissions

In real combustion applications, such as IC engines, the release of combustion products into the atmosphere is unavoidable. Thus, for environmental and health reasons, predicting the composition and concentration of these products is a very important part of engine analysis. As previous mentioned, ideally the combustion of a hydrocarbon yields only (CO_2) and (H_2O). However, in actual engine operation, even when the fuel and air entering an engine are at the ideal stoichiometric mixture, perfect combustion does not occur. Thus besides these two, the combustion products can contain certain amounts of carbon monoxide (CO), nitrogen oxides (NO_x)[17], unburned hydrocarbons (HC), and particulate matter. This are the main pollutants of concern in the case of combustion process in SI engines, with exception of particulate matter, which formation is very important in CI engines, but negligible in SI engines [5]. These emissions pollute the environment and contribute to global warming, acid rain, smog, odors, and respiratory and other health problems.

When dealing with actual combustion processes, it is almost impossible to predict the composition of the exhaust mixture on the basis of the mass balance, as they present a large variety of components and incomplete combustion. Then the only alternative is to measure the amount of each component in the products directly or through computational simulations of the combustion process. Two common methods of expressing the pollutants emissions are specific emissions (SE), mass flow rate of pollutant per unit power output, and the emissions index (EI) mass flow rate of pollutant per fuel flow rate [16][5]. Since, there is no data available of this parameters which can be related to the engine characteristics of this study, the pollutants emissions will be presented in their respective mass fractions.

[16] According to a Maxwell-Boltzmann energy distribution, only a very small fraction of the reactive molecules that belong to the high energy "tail" of the distribution can react, i.e. the ones that have an energy greater than E_a[32].

[17] Nitric oxide (NO), and nitrogen dioxide (NO_2), are usually grouped together as NO_x.

2.7.1 Carbon Monoxide (CO)

The fuel conversion process can be general described as a chain reaction from the primary fuel, followed by smaller intermediate hydrocarbons, ending up as (CO), which is then oxidized to (CO_2). If a fuel-rich mixture is used, there is insufficient oxygen to convert all carbon in the fuel to (CO_2), and some fuel stays as (CO),thus CO emissions increases with ϕ Figure 2.18. Insufficient oxygen is an obvious reason for CO formation, but it is not the only one. Another cause is that, oxygen has a much greater tendency to combine with hydrogen than it does with carbon, i.e. to form (H_2O) instead of (CO_2). Insufficient mixing in the combustion chamber, consequent fuel-rich regions creation, as well as fast expansion, which quench the final oxidation reaction can also contribute to CO formation. Therefore, even with fuel-lean mixtures, some CO will be generated in the engine. Conversion of CO to CO2 is governed primarily by reaction[11]:

$$CO + OH \rightarrow CO_2 + H \quad (2.58)$$

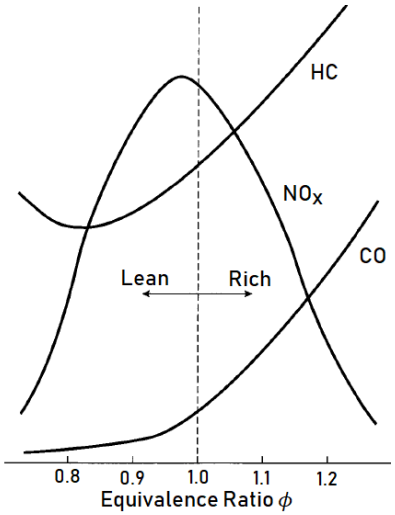

Figure 2.18: Emissions from an SI engine as a function of equivalence ratio (ϕ). Adapted from [5]

2.7.2 Nitric Oxides (NO_x)

Nitric oxide (NO_x) is formed through chemical reactions involving nitrogen and oxygen atoms and molecules, which do not attain chemical equilibrium, and recombine into NO_x. The series of reactions that lead to its formation, occur mainly throughout the burned gases behind the flame, where these elements can be found and due to the high temperatures in this zone. Thus, higher combustion temperatures lead to high rate of NO formation. Unlike in CI engines in which nitric dioxide (NO_2) is present in substantial amounts, the levels of nitrogen dioxide (NO_2) formed in SI engines is negligible small [11]. Thus, the NO_x of relevance in SI engines is only NO. There are a number of possible reactions that form NO in a combustion system, these include but are not limited to:

$$N_2 + O \rightarrow NO + N \quad (2.59)$$

$$N + O_2 \rightarrow NO + O \quad (2.60)$$

$$N + OH \rightarrow NO + H \quad (2.61)$$

Equations (2.59),(2.60) and (2.61) express the main reactions governing NO formation, and are refered to as thermal route or the Zeldovich-Keck[18]mechanism[16]. Since the NO formation is directly related to changes in temperature and oxygen concentrations in the unburned gas during combustion process. Any operating parameter that leads to alterations in these variables has a pronounced effect on NO formation. Therefore, in the case of SI engines the main factors that affect NO emissions are: ϕ, spark timing and burned gas fraction[19]:

- **Equivalence ratio**: It affects both the gas temperature and the oxygen concentration in the burned gas. From Figure 2.18, it can be observed that NO formation is greater near stoichiometric conditions, when temperatures are the highest, and NO peak emissions occur at slightly lean conditions i.e. when there is an excess of oxygen to react with the nitrogen.
- **Spark timing**: Significantly affects NO emissions levels. Advancing the timing so that combustion occurs earlier in the cycle increases the peak cylinder pressure, which result in higher peak cylinder temperatures Section 2.5.3, hence in higher NO formation rates. In turn, retarding it the opposite occurs.

2.7.3 Unburned Hydrocarbon (HC)

Unburned hydrocarbons or organic emissions, result from different mechanisms, usually called sources, in which fuel escapes the main combustion event during flame propagation. A detailed description of this mechanisms can be found in [5][11]. They are generally influenced by the combustion chamber geometry and some engine operating parameters.

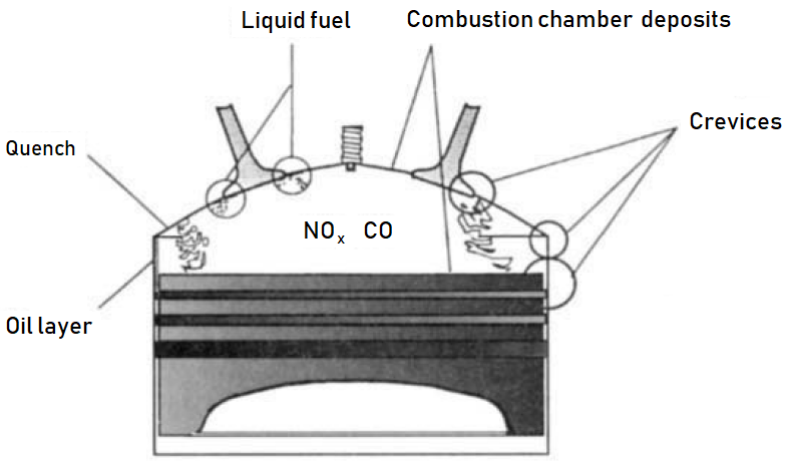

Figure 2.19: Main sources of HC emissions. Adapted from [11].

[18]Zeldovich was the first to suggest the importance of reactions (2.59) and (2.60). G.A.Lavoie added reaction (2.61) to the mechanism [16]

[19]As in this study only one complete combustion cycle will be performed, the burned gas fraction dilution on the unberned mixture will not be considered.

Figure 2.19 presents the main sources of hydrocarbon emissions in SI engines. One relevant source of HC emissions, related to the engine operation, that is not illustrated is the valve overlap time. During valve overlap, both the exhaust and intake valves are open, creating a path where air-fuel intake can flow directly into the exhaust.

A fraction of the hydrocarbons that escapes combustion through one of these processes emerge from the sources, especially during expansion, and is partially oxidized in the burned gas mixture. Thus, the so-called hydrocarbon emissions are composed by the original fuel compounds, as well as a considerably variety of hydrocarbon compounds, which complicates the prediction of their composition and amount in the exhaust mixture.

2.8 Computational Fluid Dynamics (CFD)

Computational fluid dynamics (CFD) can be described as the science of predicting fluid flow behaviour and how it influences processes such as heat transfer, mass transfer, chemical reactions, and related phenomena, by means of computer-based simulations. In which, the three-dimensional (3D) simulation represents the most sophisticated approach for detailed numerical investigations on any thermo-fluid dynamical problem.

Combustion, even without accunt for turbulence, is an intrinsically complex process involving a large range of chemical time and length scales. Since the chemical precess occur in short times over thin layersi and are associated with very large mass fractions, temperature and density gradients. Turbulence itself is probably the most complex phenomenon in non-reacting fluid mechanics. So, when the flame front interact whith the in cylineder turbulent flows, and the laminar flame mode is replaced by a turbulent one. The phenomena become more difficult to model and analyse, and impossible without numerical simulations. Thus, the goal of this chapter is to provide a brief overview on the set of equations which, when implemented in CFD softwares can predict the fluid motion of reacting systems. As wells as a general view of the numerical algorithm [20] from which the softwares are based on, such as the one used in Chapter[3]. A complete description of these equations is outside the scope of this thesis, but can be found in [19][32][39], and others.

2.8.1 Governing Transport Equations

The physical property of the fluid motion can usually be described through fundamental mathematical equations, called governing equations. These equations speak physics. They represent the mathematical statements of the conservation laws of physics upon which all of fluid dynamics is based [13]:

- Conservation of mass.
- Conservation of momentum.
- Conservation of energy.

Table 2.1 summarize the possible flow models from which the governing equations can be derived. From this application results the mathematical equations which embody such physical principles, namely, the continuity, momentum, and energy equation, also known as Navier-Stokes equations

[20] A systematic procedure that produces, in a finite number of steps, the answer to a question or the solution of a problem [38].

[21][40][39]. The set of equations become complete with the addition of the equation of state, and the terms to account for the effects of the chemical reactions.

Table 2.1: Models of a flow. Adapted from [13]

Flow model	Flow type	Directly leads to:
Finit control volume	Fixed in space with the fluid moving through it. (Eulerian approach)	Integral equations in conservation form.
	Moving with the fluid. (Lagrangian approach)	Integral equations in nonconservation form.
Infinitesimally small volume	Fixed in space with the fluid moving through it. (Eulerian approach)	Partial differential equations (PDE) in conservation form.
	Moving with the fluid. (Lagrangian approach)	Partial differential equations (PDE) in nonconservation form.

These equations are not fundamentally different equations; rather, they are four different forms of the same equation that can be derived by suitable manipulation from any of the others.

Fluid dynamics of reacting flows can be described with aditional equation based on the conservation of molecular species or conservation of atomic species, and additional terms that account for reaction kinetics and transport processes of thermal conduction, fuel diffusion and viscosity in the Navier-Stokes equations. Therefore, the governing equations for an unsteady, three-dimentional, reacting flow can be written in the following general form [13][41][32]:

- **Continuity equation**: The low of mass conservation states that matter may neither be created nor destroyed, hence, the corresponding continuity equation governs the conservation of mass, which means that the rate of change of mass within an arbitrary control volume must be equal to the total mass flow over its boundaries. Because combustion does not create or destroy mass, the equation of conservation of mass is the same for reacting and non reacting flows. In cartesian coordinates:

$$\frac{\partial \rho}{\partial t} + \left[\frac{\partial(\rho u)}{\partial x} + \frac{\partial(\rho v)}{\partial y} + \frac{\partial(\rho w)}{\partial z} \right] = 0 \quad (2.62)$$

  Furthermore, considering the vector operator (or gradient) $\bigtriangledown$ defined by Equation ((2.64)), and the velocity vector ($\vec{v}$) in cartesian space, given by Equation (2.65). In Equation (2.62), the term in brackets is simply $\bigtriangledown(\rho\vec{v})$. Thus, a simplified continuity equation can be expressed by Equation(2.63). The first term on the left hand side is the rate of change in time of the density (mass per unit volume). The second term describes the net flow of mass out of the control volume across its boundaries and is called the convective flux.

$$\frac{\partial \rho}{\partial t} + \bigtriangledown . (\rho\, \vec{v}) = 0 \quad (2.63)$$

$$\bigtriangledown \equiv i\, \frac{\partial}{\partial x} + j\, \frac{\partial}{\partial y} + k\, \frac{\partial}{\partial z} \quad (2.64)$$

[21] In modern CFD literature, the Navier-Stokes equations, usually applied to identify the momentum equations for a viscous flow, include the entire system of flow equations for the solution of a viscous flow [13].

$$\vec{v} = u\,i + v\,j + w\,k \quad (2.65)$$

- **Continuity equation of mixtures**: Also based on the conservation of mass principle, in this case the total mass of each element is conserved in the course of the reaction. And, also becouse combustion process does not produce or destroy mass. This equation is used to predicts the local mass fraction of each species (Y_i), through the solution of a convection-diffusion equation for the N species (i). This conservation equation takes the following general form:

$$\frac{\partial \rho Y_i}{\partial t} + \bigtriangledown\Big[\rho\vec{v}Y_i(+V_i)\Big] = -\bigtriangledown \vec{J_i} + \dot{\omega}_i + S_i \quad (2.66)$$

where, ($\vec{J_i}$) is the diffusion flux of species , which arises due to gradients of concentration and temperature and (S_i) a reaction rate source therm. From Ficks law [22], it can be expressed as Equation (2.67), where is ($D_{i,m}$) the mass diffusion coefficient, and is ($D_{T,i}$) the thermal diffusion coefficient.

$$\vec{J_i} = -\rho_i D_{i,m} \bigtriangledown Y_i - D_{T,i}\frac{\bigtriangledown T}{T} \quad (2.67)$$

Equation (2.67) will be solved for $N-1$ species where N is the total number of fluid phase chemical species present in the system. Since the mass fraction of the species must sum to unity, the N^{th} mass fraction is determined as one minus the sum of the $N-1$ solved mass fractions. To minimize numerical error, the N^{th} species should be selected as that species with the overall largest mass fraction, such as N_2 when the oxidizer is air [43].

- **Momentum equation**: governs the conservation of linear and angular momentum. According to Newton's second law, the rate of change of momentum on a fluid particle equals the sum of forces acting on that particle. These forces can be distinguish in two types: *body forces*, which "act at a distance" on the volumetric mass of the fluid element, such as gravitational, centrifugal, Coriolis and electromagnetic forces. *Surface forces*, which act directly on the surface of the fluid element, due to the pressure distribution imposed by the outside fluid surrounding the fluid element, and the shear and normal stress distributions acting on the surface by means of friction (viscous forces).

$$\frac{\partial \rho u}{\partial t} + \bigtriangledown(\rho u V) = -\frac{\partial p}{\partial x} + \frac{\partial \tau_{xx}}{\partial x} + \frac{\partial \tau_{yx}}{\partial y} + \frac{\partial \tau_{zx}}{\partial z} + \rho f_x \quad (2.68a)$$

$$\frac{\partial \rho v}{\partial t} + \bigtriangledown(\rho v V) = -\frac{\partial p}{\partial y} + \frac{\partial \tau_{xy}}{\partial x} + \frac{\partial \tau_{yy}}{\partial y} + \frac{\partial \tau_{zy}}{\partial z} + \rho f_y \quad (2.68b)$$

$$\frac{\partial \rho w}{\partial t} + \bigtriangledown(\rho w V) = -\frac{\partial p}{\partial z} + \frac{\partial \tau_{xz}}{\partial x} + \frac{\partial \tau_{yz}}{\partial y} + \frac{\partial \tau_{zz}}{\partial z} + \rho f_z \quad (2.68c)$$

Equations (2.68a), (2.68b) and (2.68c) are x, y, and z components, respectively, of the momentum equation, obtained by adding up all of the mentioned contributions. The terms on the left-hand side of the equations represents the rates of increase of x, y and z momentum.

[22] Fick´s law of diffusion states: Species always diffuse in the direction from high concentration to low concentration of the same species[42]

In the right-hand side we have a normal stress due to the pressure, denoted by (p), the viscous stresses are denoted by τ_{ij}, and the effects of the body forces are expressed as the source terms (ρf). These equation is the same in reacting and non reacting flows.

- **Energy equation**: governs the conservation of energy. This equation is based on the first law of thermodynamics which states that any changes in time of the total energy inside the fluid element are caused by the net heat flux into the element and by the rate of work of forces acting on it. Thus, in Equation (2.69) we have, the rate of change in terms of total energy i.e., the sum of internal energy and kinetic energy ($e + \frac{V^2}{2}$) per unit mass; equals to the net heat flux: due to volumetric heat addition ($\dot{q}$), and due to thermal conduction ($\dot{q}_j$) in x, y, z direction, which according to Fourier's law is proportional to the local temperature gradient Equation (2.70), where (k) is the thermal conductivity; and in last, the rate of work done on the element due to surface forces and body forces ($\rho f.V$).

$$\begin{aligned}\frac{\partial \rho}{\partial t}\Big[\rho\Big(e+\frac{V^2}{2}\Big)\Big] + \bigtriangledown\Big[\rho\Big(e+\frac{V^2}{2}\Big)V\Big] &= \rho\dot{q} + \frac{\partial}{\partial x}\Big(k\,\frac{\partial T}{\partial x}\Big) + \frac{\partial}{\partial y}\Big(k\,\frac{\partial T}{\partial y}\Big) + \frac{\partial}{\partial z}\Big(k\,\frac{\partial T}{\partial z}\Big) \\ &- \frac{\partial (up)}{\partial x} - \frac{\partial (vp)}{\partial y} - \frac{\partial (wp)}{\partial z} + \frac{\partial (u\tau_{xx})}{\partial x} + \frac{\partial (u\tau_{yx})}{\partial y} \\ &+ \frac{\partial (u\tau_{zx})}{\partial z} + \frac{\partial (v\tau_{xy})}{\partial x} + \frac{\partial (v\tau_{yy})}{\partial y} + \frac{\partial (v\tau_{zy})}{\partial z} \\ &+ \frac{\partial (w\tau_{xz})}{\partial x} + \frac{\partial (w\tau_{yz})}{\partial y} + \frac{\partial (w\tau_{zz})}{\partial z} + \rho f.V\end{aligned} \tag{2.69}$$

$$\dot{q}_j = -k\frac{\partial T}{\partial j} \tag{2.70}$$

These equations are used together with the transport equations and the equation of state to solve flow property distributions, including temperature, density, pressure, velocity, and concentrations of chemical species.[42]. In which, the relationships between the thermodynamic variables can be obtained through the assumption of thermodynamic equilibrium [40][23].

2.8.2 Solution of Governing Equations

An analytical solution of the set of governing equations is only possible for some simplified flow problems. Thus, these equations have to be solved numerically. There are many different numerical solution techniques available, being the finite volume (or control volume) method, currently the most popular one in CFD applications. The corresponding algorithm will be described below.

In order to solve the equations numerically with the finite volume method, the entire continuum fluid must be represented by a finite number of discrete elements. Thus, the domain is divided into

[23]The fluid velocities may be large, but they are usually small enough that, even though properties of a fluid particle change rapidly from place to place, the fluid can thermodynamically adjust itself to new conditions so quickly that the changes are effectively instantaneous. Thus the fluid always remains in thermodynamic equilibrium [40]

a number of small sub-volumes or cells (finite volume approximation), through a process known as grid generation or mesh build-up to form the mesh. So that, the computational mesh will serve as a framework for the local numerical solution of the discretized governing equations. The time variable is similarly discretized into a sequence of small time intervals called time-steps, and, in case of unsteady flow, the transient solution is carried out in time: the solution at time t_{n+1} is calculated from the known solution at time t_n. After domain discretization, fallows the integration of the governing equations on each individual control volumes, to construct algebraic equations for the discrete unknown dependent variables. At last, is the linearization of the discretized equations and solution of the resulting system of linear equations, to yield update values of the dependent variables, by an iterative method[44][14].

2.8.3 Turbulent Racting Flows/Combustion-Numerical Approach

In order to understand and model turbulent reacting flows, some knowledge of turbulent flows is required. Turbulence is a propriety of a flow that presents irregular, random and chaotic nature. It can be described as a state of continuous instability in the flow, where at any point of time and space, the field variables, such as velocity, show fluctuation (i.e., differences from a local mean value). More detail about the characteristics of turbulent flows can be found in [42].

Due to, turbulent flows large number of degrees of freedom and the extreme sensitivity to perturbations, the field variables are difficult to reproduced exactly at any point of space and time. Yet the flow can be defined by the Navier-Stokes fundamental conservation equations, and the flow variable determined in a statistically manner i.e., in terms of mean values and probability density distributions. To do so, the major physical variables are decomposed into fluctuating and average components, and an averaging procedure is performed to the Navier-Stokes equations. Which, leads to new equations in terms of statistical field variables (e.g., mean velocity components). Thus, generating several unknown variables, which in turn require closure models in order to solve the system of equations. In this case, a turbulence model to deal with the flow dynamics in combination with a turbulent combustion model to describe chemical species conversion and heat release.

The Reynolds Averaged Navier Stokes(RANS)[24] approach is the most used one, regarding turbulent combustion simulations. Two different averaging procedures are commonly used in these approach: conventional time averaging also known as Reynolds averaging and mass-weighted time averaging, also known as Favre averaging. While the former is more popular for constant density flows, Favre averaging is used for flows with varying density, such as turbulent flames. However, both techniques have been used in the combustion field. The detailed averaging procedures and the relationships between the quantities averaged, can be found in [45].

2.8.4 Combustion Modeling

Depending on the amount of detail, a combustion mechanism can consist of only a couple of steps, or thousands of elementary reactions. For instance, in the case of hydrocarbon fuels, the number of species and reaction steps grows nearly exponentially with the number of carbon atoms in the fuel.

[24] RANS equations are the most widely used approach, although there are other approaches that can simulate with higher precision, as Large Eddy Simulation (LES) or Direct Numerical Simulation (DNS) [45].

A recent detailed mechanism for isooctane contains 860 species and 3,606 steps [36]. Generally, they can be differented in the following levels of complexity [42]:

- **Complete mechanism (or detailed reaction mechanism)**: when all chemical and kinetic processes are taken into account.
- **Reduced mechanism**: the combustion mechanism is reduced to the main reaction pathways corresponding to the specific operation conditions. Tipically these mechanisms consider 5 to 20 species.
- **Semiglobal mechanism**: Usually considers less than 5 reactions involving 5 to 10 species and neglects most chemical pathways.
- **Single-step or one-step global mechanism**: None of the intermediate reactions is considered.

Ideally a transport equation should be solved for each of the species of the reacting system in order to accurately describe the physical and chemical processes occurring during combustion. Computing a complete reaction mechanism in turbulent flows, would require a significant amount of computer resources even for one-dimensional flames and is almost impossible to do in multidimentional simulations. Thus, a simplified description is extremely useful for practical applications of combustion problems. For single component fuels, a one-step global reaction is often used in practical simulations due to its simplicity [36][42].

Numerous models have been designed to characterize the combustion processes. The following are the combustion models for premixed-combustion, available in the software used in this study:

- **Species Transport and Finite-Rate Chemistry**: With a wide range of applications including laminar or turbulent reaction systems, and combustion systems with premixed, non-premixed, or partially-premixed flames. It models the mixing and transport of chemical species by solving conservation equations describing convection, diffusion, and reaction sources for each component species.
- **Premixed Combustion**: The most suiteble for turbulent premixed combustion.
- **Composition PDF Transport**: Computationally expensive, so it is recommended for modeling with small meshes and preferably in 2D.

Regardless of the model, several input parameters are required for the chemically reacting system. Which include the chemical reactions, the kinetic parameters of these reactions, and the thermochemical properties of chemical species. In addition, good initial conditions and boundary conditions influnece the solution accuracy.

Chapter 3

Case Study-Combustion Simulation

The engine used as reference in this study is the UBI/UDI-OPE-BGX286, a four-stroke SI OP engine designed and built by Jorge Gregório [12] with the purpose of developing a low-cost OP engine from two existent ones (two Robin-EY15 engines). Thus, reducing manufacture and development costs. Some of the engine requirements consisted in being able to work with more than one type of fuel, be adaptable to different exhaust emissions treatment systems, be light and compact and with high power to weight ratio in order to be suitable for aeronautical applications. In addition, with low fuel consumption and emissions.

Inspired by the Gobron-Brillié engine, one of the few succeful examples of SI four-stroke OP engines and the renowned Jumo 205 engine. [1].The new engine, which will serve as model in this work, is composed by four side valves on the block in a (L-head or *flathead* arrangement) ,two admissions and two exhausts, in which each admission is facing an exhaust valve, and double crank-arrangement. The engine operates horizontally with a set of gears connecting the two crankshafts and the method of mixture generation is through two Mikuni carburettors from the original engines. Figure 3.1 presents the final configuration of these engine.

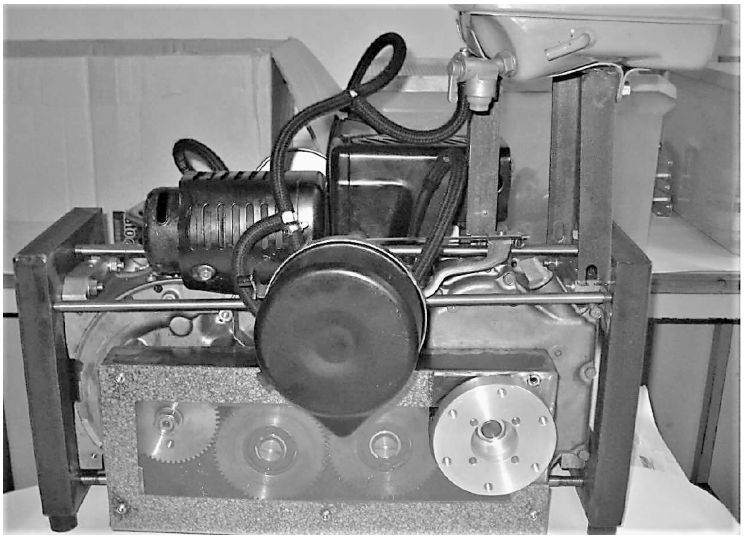

Figure 3.1: UBI/UDI-OPE-BGX286 final configuration. Adapted from [12].

As mentioned in Section 2.3.2, when taking a look in OP engines history , there is not much OP with SI ignition, even less operating in a four-stroke cycle. Which seemed to be an opportunity to revitalize OP engines and innovate IC engines in general.

[1]The former influenced in the arrangement of some of the mechanical components such as the engine valves and spark plug. The second in the engine overall architecture and in the synchronization and power transmission between the two crankshafts that integrate the new engine.

With the engine built and ready to work, Jorge Gregório carried on an experimental study in which the following operating characteristics were measured or determined from the collected data: rotational speed, torque, fuel consumption, power, specific consumption and overall efficiency. Although emissions tests also have been made, due to technical difficulties the data gathered could only be used in a subjective manner in evaluating this parameter.

3.1 Model Generation and Meshing Process

There are several stages that have to be fulfilled to assemble the numerical simulation. Of which include the model construction, decomposition and meshing process. The simulation assemble starts by creating the engine geometry which in this case include the model construction and decomposition. The following steps were performed and presented in[12].

3.1.1 Geometry

The model represents the internal volume of the cylinder of UBI/UDI-OPE-BGX286 engine, which is the zone of interest of this study. The design of the model was created resorting to CAD software CATIA V5. Figure 3.2 presents the domain of the model engine and valve bodies, in which we can see the displaced volume, the intake and exhaust ducts and the lateral combustion chamber. The lateral combustion chamber configuration brings the advantage of more freedom regarding valve timing and lift. However, the lack of piston direct contact with the combustion chamber could lead to a nonuniform combustion since the flame may not spread throughout the entire interior of the cylinder bore [46].

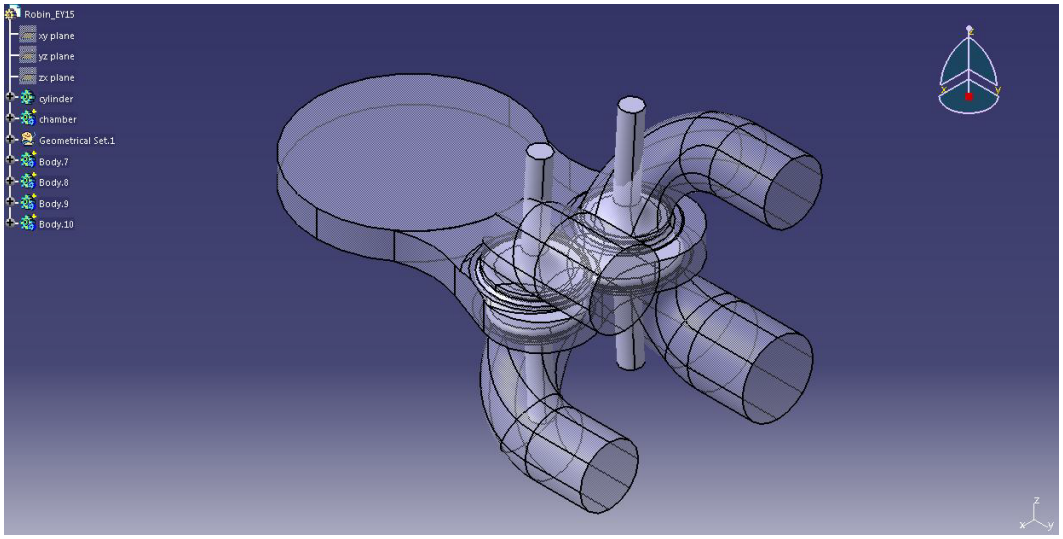

Figure 3.2: Domain of the model engine and valve bodies.

In order to simulate the movement of the engine pistons and valves, certain zones were created and modified. This corresponded to the decomposition step, in which the model is divided into different zones, so that different mesh motion strategies can be applied to the different regions during meshing step.

After importing the model into Ansys Design Modeler in an IGES file format, all valve bodies were removed, leaving an empty space with the same shape of the valves, in which two bodies were created:

- *Inboard*- A cylindrical body that surrounds the zone above the head of the valve, next to the valve stem. This allowed the mesher to create a structured mesh in this zone and use the *Layering* function, which is much more economical regarding computational cost, when compared to the *Remeshing* function (see Figure A.1 in App.A).
- *Vlayer*- A layer has been created between the valve head and valve seat for the same reason as the *Inboard*, also to prevent direct contact and to serve as a starting point for valve movement, taking into account that a mesh cannot be created out of nothing (see Figure A.2 in App.A).

Also in this stage all zones that could cause some mesh problems and divergence issues where properly treated. In the combustion chamber, the two ”corners” adjacent to the cylinder were cut off in order to define certain methods in these areas (see Figure A.3 in App.A), but remained as the same body of the chamber to retain the same parameters as the rest of the chamber. In all ports, the zone closer to the valve head, and above the *vlayer*, were separated from the rest of the port in order to later improve the mesh in these bodies (see Figure A.4 in App.A). For meshing reasons, the bodies created in both exhaust ports were not defined as the same body as the rest of the port, which led to the creation of an *interface* between both of them.

The last step of the decomposition was naming all the 88 faces and zones that compose the model domain, in order to ease the next stages of the simulation.

3.1.2 Mesh

The next step was the mesh generation or grid generation of the 3D model. The aim of the mesh is to divide the domain into a number of smaller, non-overlapping sub-domains, that is, in a grid or mesh of cells where the solution will be calculated. This is one of the most important stages in a CFD simulation, since the quality of the mesh is directly related to the accuracy, convergence and speed of the solution. The meshing process had a special attention in this case, since the parts of the engines such as the piston and valves were later provided with a dynamic mesh.

This step was carried on in Ansys ICEM CFD. When working with this software it is common practice to begin the meshing process by defining the global settings and, only after, locally. This allows the user to have a general idea of the areas or zones that need more attention and where to refine the mesh. A reference size obtained by using the exhaust valve diameter was used to calculate the mesh parameters for each zone. The mesh parameters and the global mesh settings can be seen in Table B.1 and Table B.2, respectively, in App.B.

Locally, mesh modifications were performed on each body in order to improve the quality of the mesh. This was accomplished by taking in account the type of mesh required and zone format, and by using different construction methods of the software. In the case of the *vlayers*, *inboards* and cylinders the Sweep Method, which creates a high quality structured mesh, was applied. Tables B.3, B.4, B.5, B.6, B.7 of App.B present more detailed information of the local mesh modifications.

The resulting mesh presents a total of 1622412 cells and 518640 nodes. However, due to the pistons motion during simulation the number of elements will increase. Figure 3.3 and 3.4 present the final mesh configuration of the domain and a detailed view of the mesh in the *Vlayer* and *Inboard* zones.

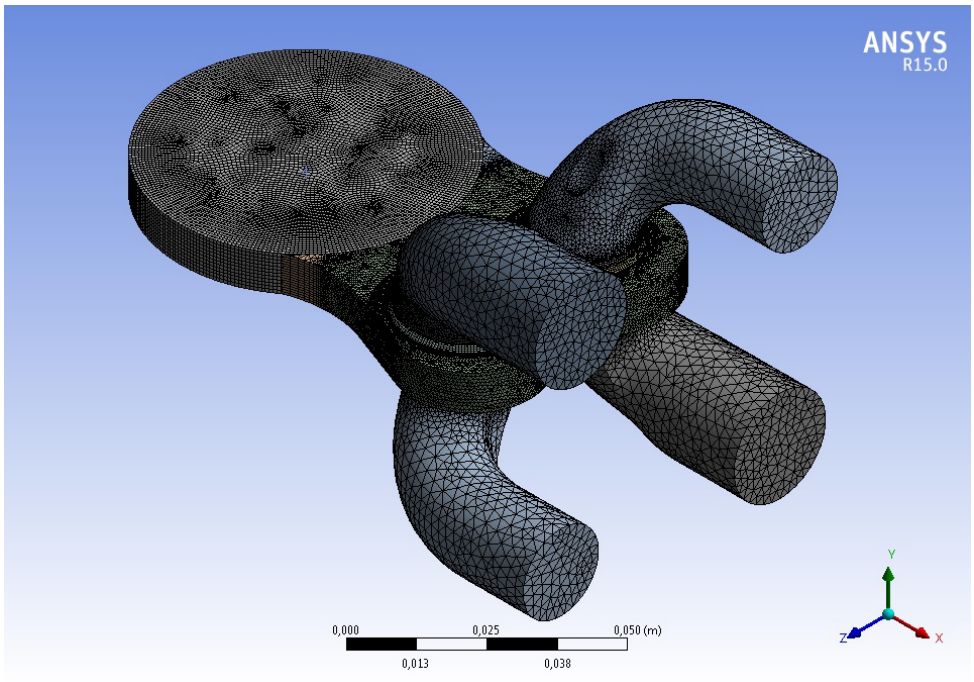

Figure 3.3: Global mesh view of the domain [12].

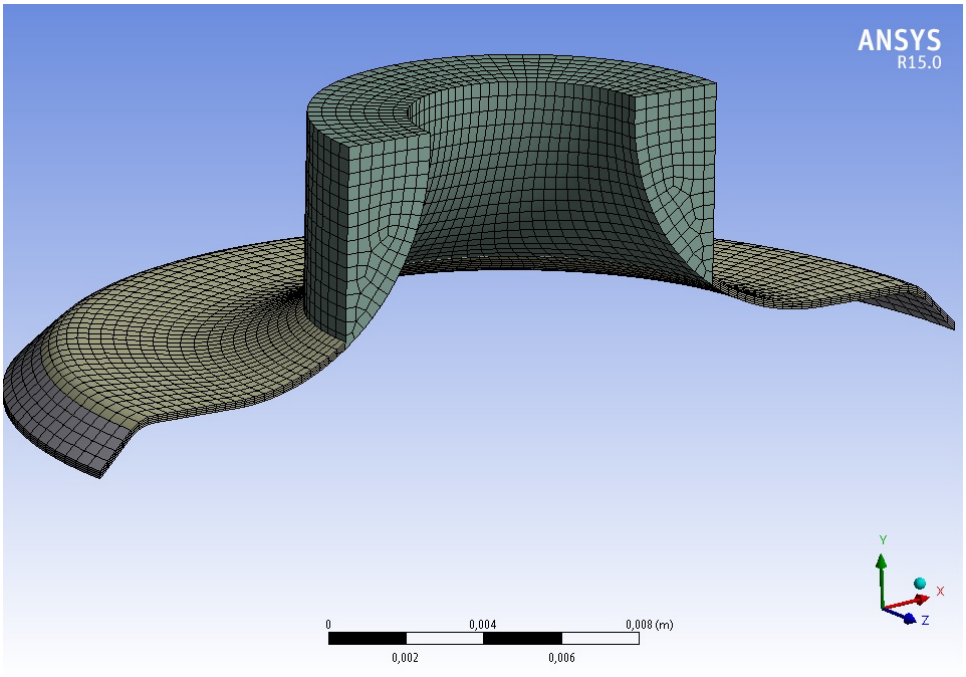

Figure 3.4: Structured meshing in both *Vlayer* and *Inboard* [12].

3.2 Physical Model Setup

The present study was performed using the CFD software Ansys Fluent 16.2, due to its simplicity, user friendly interface, and availability at the UBI cluster where this computational demanding simulation was performed.

Once Fluent is launched, it is essential to verify the quality of the mesh, which can be done by "report the quality" in the General-setup Mesh box. Among the available mesh quality parameters, orthogonal quality and mesh skewness are of great importance. Table 3.1 and 3.2 serve as guide in their evaluation. The model initially present maximum values of skewness of 0.767571, and a minimum orthogonal quality of 0.152236, respectively. Thus, is found in the range of good and acceptable quality. However, due to the movement of the pistons during the simulation the number of elementes will increase, which can lead to issues regarding the mesh quality, hence, solution convergence and results.

Table 3.1: Mesh skewness metrics spectrum [14].

Excellent	**Very Good**	**Good**	**Acceptable**	**Bad**	**Unacceptable**
$0 - 0.25$	$0.25 - 0.50$	$0.50 - 0.80$	$0.80 - 0.94$	$0.95 - 0.97$	$0.98 - 1.00$

Table 3.2: Orthogonal quality mesh metrics spectrum [14].

Unacceptable	**Bad**	**Acceptable**	**Good**	**Very Good**	**Excellent**
$0 - 0.001$	$0.001 - 0.14$	$0.15 - 0.20$	$0.20 - 0.69$	$0.70 - 0.95$	$0.95 - 1.00$

3.2.1 Solver

To achieve the numerical solution for each step, we can either use a pressure- or density-based solver. Although pressure-based solvers were typically used for low velocity incompressible flows and density-based are typically used for high-velocity compressible flows, recent adaptations to both methods allows for their use in a variety of flow conditions while presenting similar results [43]. However, various combustion models in Fluent present a limitation of only being avaliable for pressure-based solver. Hence, due to the nature of this study the pressure-based solver will be used, the velocity formulation kept as absolute [2] and transient is enabled for the time solver. [47][46].

3.2.2 Models

A variety of models can be activated for a given simulation. Each model provides outputs for different variables of interest. Since the combustion process can be studied as a turbulent reacting flow, thus, the following three models will be utilized:

- **Energy model** - The energy model must be activated as this regards the energy related to the temperature change within the combustion process.

[2]The absolute velocity formulation is preferred in applications where the flow in most of the domain is not moving. On the other hand, the relative velocity formulation is appropriate when most of the fluid in the domain is moving. However in a situation in between either of the formulations may be used[43].

- **Viscous Model** -Through this model, laminar and turbulent flows can be studied. The chosen model is the $k - \varepsilon$ model, with its constants maintained at the default values. This is the most used turbulence model in engineering applications [40]. It is known for being robust, economic and with a satisfactory accuracy for turbulent flows. This is a two-equation model, which allows to calculate the turbulent length and time scale by solving two transport equations. One for the turbulence kinetic energy (k) and the other for dissipation rate (ε).
- **Species model** - This model allows Fluent to model the mixing, transport and combustion of chemical species. Due to the importance of this model for this work, the inputs will be described below.

3.2.2.1 Species Transport and Finite-Rate Chemistry

Due to the already computation demanding geometry and respective dynamic mesh, the species transport model was chosen from the three available in Fluent to model premixed reacting flows, Section 2.8.4.

The problem setup for species transport and volumetric reactions begins in the panel *Species Model*. First-off, in the species model dialog box the species transport model was enabled alongside the volumetric reaction. From the additional options available the diffusion energy source which adds the effect of enthalpy transport in the energy equation was selected.

When the species transport model is selected, Fluent predict the mass fraction of each input species by solving the conservation Equation (2.66), for each inputted chemical species. To do so, the reaction rates that appear as source terms in this equation are computed by one of the first tree models below. For that, one of the four Turbulence-Chemistry Interaction models is used:

- **Laminar finite-rate model**: The effect of turbulent fluctuations are neglected, and reaction rates are determined by Arrhenius kinetic expressions.
- **Eddy-dissipation model**: Reaction rates are assumed to be controlled by the turbulence, so Arrhenius chemical kinetic calculations are avoided. The model is computationally cheap, but for realistic results only one or two step heat-release mechanisms should be used.
- **Eddy-dissipation-concept (EDC) model**: Detailed Arrhenius chemical kinetics can be incorporated in turbulent flames. However, at a high computating cost.
- **Finite-Rate/ Eddy-Dissipation**: Computes both the Arrhenius rate and the mixing rate and uses the smaller of the two.

The determination of which model to apply was only possible through an extensive trial and error approach through simulations. Since the most suitable models Eddy-dissipation-concept (EDC) and Finite-Rate/ Eddy-Dissipation presented major convergence problems and with Eddy-Dissipation model combustion did not occur, the Laminar finite-rate model was chosen to advance with the simulations.

The next step in the species model was specifying the mixture material and defining the properties of the mixture. A mixture material[3]may be thought of as a set of species and a list of rules governing their interaction. Mixture properties include the following:

- Species in the mixture

[3]This concept was implemented in Fluent to facilitate the setup of species transport and reacting flow [43].

- Reactions
- Other physical properties (e.g., viscosity, specific heat)

There were three options for specifyng the mixture: import a chemical mechanism in CHEMKIN format, use Fluent materials database or create the mixture from scratch. Since it was not possible to find the first one and octane-air was available, resorting to Fluent materials database was the chosen option. In it one/two-step reaction mechanisms and many physical properties of the mixture and its constituent species are ready to use. Thus, the mixture customization was performed in the *Materials* panel by copying the n-octane-air mixture from fluent database. Also in this section, the Species dialog box shows the *Selected Species* list with all the species in the mixture and the *Available Materials* list with materials that are available but not in the mixture. Regarding this study seven species from the available material were added to the selected species resulting in twelve species: gasoline (C_8H_{18}), oxygen (O_2), water (H_2O), carbon-monoxide (CO), carbon-dioxide (CO_2), atomic-oxygen (O), nitrogen-dioxide (NO_2), nitrogen-oxide (NO), atomic-nitrogen (N), hydroxyl (OH), atomic-hydrogen (H) and nitrogen (N_2), in this order. The order of the species in the *Selected Species* list is very important Equation (2.67) Section 2.8.1. Therefore, the most abundant specie (by mass) is retained as the last specie, in this case N_2.

Returning to the *Species Model* panel in *Mixture Material* drop-down list under *Mixture Properties* the n-octane-air mixture generated is selected and the respective species in mixture, reactions and other properties are loaded into the solver. Which can be verified by the *Number of Volumetric Species* in the mixture (12) displayed in the dialog box and by clicking in the edit which displays the same information as the *Materials* panel.

3.2.2.2 Spark Model

Spontaneous ignition of fuel and oxidant does not occur unless the temperature of the mixture exceeds the activation energy limit required to maintain combustion. This physical issue manifests itself in a simulation as well. Initiation of combustion at a desired time and location in a combustion chamber is required and can be accomplished by creating a spark. The spark event in typical engines happens very quickly relative to the main combustion in the engine. The physical description of this simple event is very complex, making it difficult to accurately model the spark in the context of a multidimensional engine simulation. However, taking in account that the energy from the spark event is several orders of magnitude less than the chemical energy release from the fuel, and that the ignition of a mixture at a point in the domain is more dependent on the local composition than on the spark energy, in Fluent engine modeling the spark event does not need to be modeled in great detail, but simply as the initiation of combustion over a duration [16][43]. Thus, a spark ignition was selected and defined with the quantities mentioned in Section 2.5.2 see Table 3.3.

Table 3.3: Spark Ignition Setup

Spark Location		**Spark Parameters**	
X-Center (m)	0.035	Start Crank Angle (deg)	700
Y-Center (m)	-0.002	Duration (s)	0.001
Z-Center (m)	-0.02	Enery (j)	0
Initial Radius (m)	0.002	Flame Speed Model	Turbulet Curvature

3.2.3 Boundary Conditions

One of the most important steps of this entire work is correctly defining the boundary conditions as this greatly affects convergence and results. Depending on the type of case, different boundary conditions should be applied. Regarding this case four types of boundary conditions are used in this model, which are listed below:

- ***Walls*** - All boundary faces were considered walls, such as cylinder, chamber and piston walls, as well as ports and valves. Table C.1 in App.C presents the conditions applied to each wall. Regarding to Species Boundary Conditions in Species dialog box, for all walls the condition of Zero-gradient (zero-flux) was kept for all species, since no surface reactions were defined.
- ***Interfaces*** - As explained in Section 3.1.1, several zones were created in order to allow continuity of the fluid through every zone. Thus, the interface boundaries are applied where two faces of different zones are in contact.
- ***Pressure-inlet*** - Taking into account the limited information available in relation to the cylinder inlet, i.e. parameters such as velocity or flow rate are unknown, thus, for the present case the pressure-inlet was chosen for the inlet boundary condition. Even so, this type of boundary condition is known to be suitable for incompressible and compressible flows, which is a greater value and pressure can be assumed as atmospheric pressure, since this is a naturally aspirated engine. See Table 3.4 for details of the conditions applied.
- ***Pressure-outlet*** - It is often to give better rate of convergence when backflow occurs, rather than out flow condition. See Table 3.5 for more details of the conditions applied.

Table 3.4: Inlet boundary conditon parameters for both admission ports.

Pressure Inlet		
Momentum	Reference Frame	Absolute
	Gauge Total Pressure	101325 Pa (Constant)
	Supersonic/Initial Gauge Pressure	101325 Pa (Constant)
	Direction Specication Method	Normal to Boundary
	Specication Method	Intensity and Hydraulic Diameter
	Turbulent Intensity	2 %
	Hydraulic Diameter	0.023 m
Thermal	Total Temperature	350 K (Constant)
Species - Species Mass Fraction	C_8H_{18}	0.062
	O_2	0.219

Table 3.5: Outlet boundary conditon parameters for both exhaust ports.

Pressure Outlet		
Momentum	Gauge Pressure	101325 Pa (Constant)
	Backflow Direction Specication Method	Normal to Boundary
	Specication Method	Intensity and Hydraulic Diameter
	Backflow Turbulent Intensity	2 %
	Backflow Hydraulic Diameter	0.019 m
Thermal	Total Temperature	550 K (Constant)

3.2.4 Mesh Interfaces-Dynamic Mesh

During the work cycle of an IC engine the fluid domain is constantly changing due to the existence of moving parts in their geometry i.e. due to the motion of the piston and the valves. Therefore, for the fluid domain, a dynamic mesh which can adapt to the changes in the geometry of the domain is required. First, mesh interfaces are created, to allow faces of different zones to interact, Table C.2. Then, to achieve this the software uses three different methods simultaneously (Table C.3 presents the settings used for all three):

- ***Smoothing*** - For relatively small changes in the domain the smoothing method expands or contracts the mesh but will not add or remove cells and nodes nor will it change their respective connections.
- ***Layering*** - When larger changes occur to the domain it may be necessary to increase/decrease the overall number of cells. This method allows for the split, in case the domain is expanding, or collapse, if it is shrinking, of a given layer in the mesh.
- ***Remeshing*** - When the smoothing method is used, and large changes occur in the domain, the quality of the mesh may deteriorate to the point that the mesh may become invalid, which can lead to convergence problems when the solution is updated to the next time step. To prevent this to occur, the remeshing process attempts to correct/improve the cells that do not comply with previously defined skewness and size settings. If the method is not successful, the mesh is discarded and the mesh from the previous step is used.

Table 3.6: In-cylinder parameters.

Parameters	
Crankshaft Speed	2000/3200/4000 rpm
Starting Crank Angle	0
Crank Period	720°
Crank Angle Step Size	0.25
Crank Radius	0.023 m
Connecting Rod Length	0.083 m
Piston Pin Offset	0 m
Piston Stroke Cutoff	0 m
Minimum Valve Lift	0.0002 m

The In-Cylinder option is also enabled, which allows the model to behave as a reciprocating engine. In this section, engine speed, crank radius and connecting rod length are some of the settings that are defined here, see Table 3.6. Also, the minimum valve lift is assigned to prevent a complete closure of the valves, thus avoiding any deformation of the mesh layer between the valve and the valve seat by automatically stopping the valve movement. In addition, flow motion, such as swirl, tumble and cross tumble, are also configured to be recorded here as an output control information [46].

In transient flows, such as the case in study, the Events option can be used to control the timing of specific events during the simulation, thus simplify the simulation process. These events go from create and delete sliding interfaces, activate and deactivate cell zones to changing the time-step or

URF's. Certain steps of the work cycle are more complex than others, therefore the time-step and URF's can be optimized for given events, for example, during valve operations the time-step and URF's were decreased to better model the variations that occur to the domain during this process. Table C.5 of Annex C presents a list of all events defined for the purpose of this thesis. [43].

The last step is do define the motion of the dynamic zones. This is done by attributing one of three types of dynamic mesh zones:

- ***Rigid Body*** - This type of mesh is defined for bodies that are assumed to behave similarly to rigid-bodies such as the piston-head or the valves. For the valves, a valve profile file is uploaded to the software, which contains the information concerning the valve movement. As for the pistons Fluent provides a built-in function that can define the location of the piston as a function of crank angle, named ***piston-full***, and is selected from the *Motion/UDF Profile* drop-down list in the *Dynamic Mesh Zones* dialog box.
- ***Deforming*** - For those zones or faces that will deform due to the movement of other bodies, the deforming setting is used. Limits of maximum cell skewness and minimum and maximum cell length are chosen to maintain the quality of the mesh on these zones/faces (see Table C.7 in App. C.
- ***Stationary*** - Assigned to a face or cell zone that is considered to be motionless (moving or deforming). They are usually defined only when a face adjacent to a moving zone is stationary. See Table C.4 on App.C for the stationary zones created.

3.3 Solution

This chapter discusses the main tasks related to solving the numerical calculations required to achieve a valid solution for the CFD simulation. First the solution algorithm is presented, then the spacial discretization schemes for the variables are presented as well as the methods used for solution control and monitoring. Finally, brief discussions regarding solver initialization and solution analysis are presented.

3.3.1 Solution Methods

For the pressure-based solver, Fluent provides four distinct algorithms to solve the pressure-velocity coupling method. These are the SIMPLE, SIMPLEC, PISO and Coupled algorithms.

- ***SIMPLE*** - Default option. Hight rate of convergence means that it provides solutions fast, but it is not recommended for complex flows.
- ***SIMPLEC*** - SAn adaptation of the SIMPLE algorithm. Due to high URF factors this algorithm is recommended for more complex turbulent flows.
- ***PISO*** - The recommended algorithm for transient flows. It provided very robust results for both large and small time-steps and even for URF.
- ***Coupled*** - Typically used for steady state flows where pressure and velocity are calculated simultaneously. It provides stable and efficient solutions.

Since the PISO algorithm is recommended for transient flows, this algorithm is chosen for the following simulations. Furthermore, when PISO algorithm is used, FLUENT recommends the skewness correction options which will be enabled.

The next step is to choose the spatial discretization schemes and gradients for each variable. On inrregular skewed and distorted unstructured meshes, the accuracy of the Green-Gaus Node-Based Cell Based gradient method is comparable to that of the Least-Squares Cell Based gradient, and both are much more superior then the Green-Gaus Cell-Based gradient. Therefore, the Green-Gauss Node Based gradient method was selected. For the Pressure the PRESTO! scheme was chosen because it is recommended in cases where high-speed rotating flows and strongly curved domains are present. For the density, momentum, turbulent kinetic energy, energy and the chemical species variables the scheme that was chosen is the Second Order Upwind since it is particularly advantageous for complex flows. However if convergence difficulties arise, the First Order is advisable. Finally, for the turbulent dissipation rate a First Order scheme is used.

The last step is specifying the desired Transient Formulation. The First Order Implicit formulation is sufficient for most problems. However, Second Order Implicit should be selected, if improved accuracy is required.

3.3.2 Solution Controls

In this section Under Relaxation Factors (URF's) and solution limits are defined in other to control the solution. URF's controls the influence of the previous variable result on the new one in each iteration. Its values range from 0.0 to 1.0, where 0.0 has no influence in the next iteration and 1.0 has maximum influence in the next iteration. While many simulations may require no modifications to the URF default values in the solution controls, changing these values can help to accelerate the convergence or improve the stability of more complex simulations, especially when modeling transient combusting flows. If the solution of a variable manifest unstable behaviors or divergence, the problem can be solved by reducing their respective URF values. In this study the default values had to be changed multiple times using a "trial and error" approach which was very time consuming. See Table 3.7 for detailed information of the under-relaxation factors used. Table 3.7 shows the values adopted for the different parameter available for the solution control.

Table 3.7: Under-Relaxation Factors (URF) values.

URF	
Pressure	0.3
Density	1
Body Forces	1
Momentum	0.5
Turbulent Kinetic Energy	0.4
Turbulent Dissipation Rate	0.4
Turbulent Viscosity	0.8
Species	0.5
Energy	0.6

URF-reduced	
Pressure	0.2
Density	0.8
Body Forces	1
Momentum	0.4
Turbulent Kinetic Energy	0.2
Turbulent Dissipation Rate	0.2
Turbulent Viscosity	0.8
Species	0.5
Energy	0.4

Another way to improve the solution stability is to define the limits of the solution to keep it within an acceptable range at any point during calculations. A minimum and/or maximum values of limited variables are presented in Table C.8 in App. C.

3.3.3 Monitors

The purpose of the monitors is to evaluate the solution convergence for each variable during the simulation process. The various convergence criteria can be selected in the Residual Monitors dialog box from the Monitors panel. On a computer with infinite precision the residuals should go to zero as the solution converges. However, in an actual computer, the residuals decay to a small value ("round-off") and then stop changing ("level out"). For most computers the residuals can drop as many as six orders of magnitude before hitting round-off and for most problems, the default convergence criterion in Fluent is sufficient [43]. Therefore, as a convergence criterion, all variables, including species, were set to converge when the residuals reach 1.0e-04, except for energy, which converges when the value of 1.0e-06 is reached.

3.3.4 Solution Initialization

Since the pressure-based solver is based on averages, an initial guess is required for each variable. In practice, the user must define initial values of how the flow is behaving. These initial values can be determined from the ideal Otto cycle when applied to this engine. The initial values used for each variable can be found in Table C.9 in App. C. *Standard initialization* was used with a reference frame *Relative to Cell Zone* is used.

3.3.5 Calculation Activities

In order to later see and analyze what is happening in the engine, in the *Calculation Activities* panel, an *Autosave* task for each time step and an *Automatic Export* task for every 20 time-steps were setup to be performed during the calculation. Next, the solution can then started, the case and data file were imported to the cluster and, for this study, the calculation was configured perform 5960 time-steps (resulting in $1440°$, taking into account when the time step is reduced) and a maximum of 50 iterations per time-step.

The simulated solutions may be presented in a numerical, graphical or visual form. For the numerical solution, since the computation workload is performed in a cluster, the results are imported from the cluster and analyzed and, in the interest of a more intuitive exposition, presented in graphical form. For the visual form, animated solutions are created. To better visualize what is happening inside the engine, three planes: a symmetry, a transverse and profile through the valves planes are created. These animated solutions can be created for any given variable of interest.

Chapter 4

Results

In the course of this study countless simulations were performed, most of which were not completed due to various obstacles and problemsobstacles and problems - from cluster errors to fluent bugs. By far the greatest challenge was to find a capable and suitable model for the combustion phenomena, as mentioned in Section 3.2.2. Initially, many attempts were made, which required long hours of computation, so the final results are a round off of many months of simulation.

The results presented in this chapter are considered to be the best among the simulations performed. Two cycles were simulated for three different engines (crankshaft) rotations, 2000 RPM, 3200 RPM and 4000 RPM. Which corresponds to the maximum torque, continuum power and maximum power, respectively, of the present engine[12]. Thus, the overall simulation resulted in 17880 time steps, 894000 iterations and countless hours of simulation. Two complete cycles (cold flow and reactive flow) would take almost a month to simulate if everything went well.

Obtaining a converged solution in a reacting flow can be difficult for a number of reasons. One of the main ones is the strong impact of the chemical reaction on the basic flow pattern, leading to a model in which there is strong connection between the mass/momentum balances and the species transport equations. Which is particularly true in combustion, where the reactions lead to a large heat release and subsequent density changes and large accelerations in the flow. These coupling issues can be best addressed by the use of a two-step solution process, and by the use of under-relaxation factors. Thus, solving a reacting flow as a two-step process can be a additional method for reaching a stable converged solution in combustion problems [43]. In this process, we start by solving the flow, energy, and species equations with reactions disabled (the ”cold-flow” or ”unreacting flow”), i.e. by turning off *Volumetric Reactions* in the *Species Model* panel. When the basic flow pattern has been established, the reactions are re-enabled and the calculation continues.

The cold-flow solution provides a good starting solution for the calculation of the combusting system as wells as saves time. Thus, the two-step approach was applied to this study. The engine cycle was pre-defined to start at TDC right after combustion, with the first cycle as a cold flow simulation until 700^o crank angle, where the combustion simulation begins. In the following sections, the diagrams will exhibit only the second cycle (or right before it) i.e. the combustion simulation itself.

4.0.1 In Cylinder Variables

Several in cylinder variables are presented and analyzed in order to verify a proper engine operation as well as combustion process. Although there are no relevant data to compare with this type of engine, it is legitimate to assume that its behavior is similar to those of a conventional four-stroke spark ignition internal combustion engine.

Figure 4.1 shows the pressure variation inside the combustion chamber. Right after spark ignition and combustion start a quick rise in the pressure is observed before TDC, reaching its pick little after TDC. The maximum pressure values got close to the initial guess, however, since the initial guess was based on the ideal cycle lower values were expected. During expansion stroke, with all valves closed, a gradual decrease in pressure is visible, which can be read as the engine work-energy transfer, similar to real engine operation. Around $135°$ there is a less accentuate decline in the pressure due to the exhaust valve opening and related pressure difference, followed by a slight increase around $345°$ due to intake vale opening. Finally, at the of the cycle (and beginning of a new one) with both valve closed, there is a quick rise during compression stroke an following spark ignition and combustion.

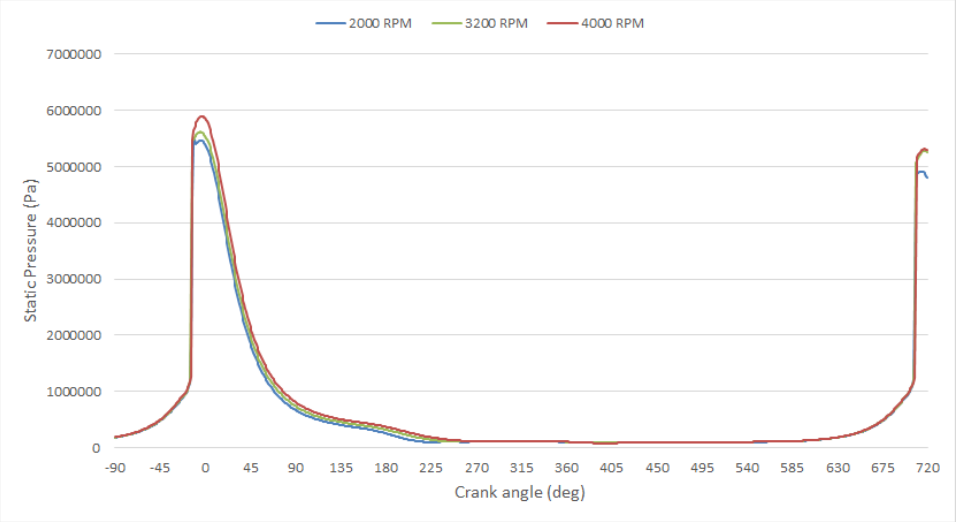

Figure 4.1: In-cylinder static pressure.

Comparing the pressure diagram with the one in Section 2.5.2 the combustion process seems to occur without abnormal phenomena. However, the overall process presents some unconformities. The pressure rises to fast with the peak pressure occurring too early. This can be corroborated by the temperature diagram Figure 4.2. In these diagrams can also be noticed a slight increase in the pressure and temperature with RPMs.

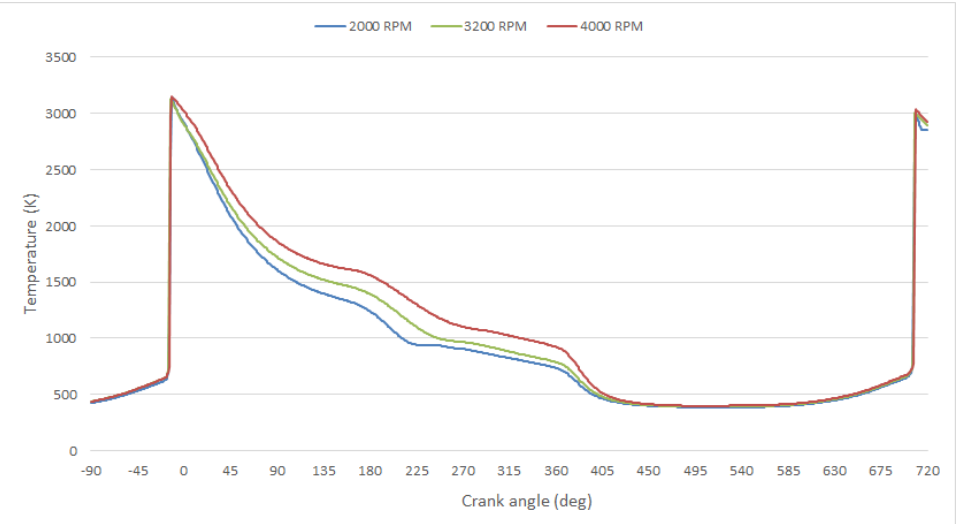

Figure 4.2: In-cylinder static temperature.

The temperature variation inside the cylinder, shown in Figure 4.2, presents a behavior similar to that of pressure. Initially, there is a quick rise near TDC followed by a progressive decline, and it is also influenced by the opening and closing of the exhaust and intake valves. However, it is possible to observe a significant temperature difference between the different rotation speeds. In addition, the maximum temperature is much higher than the initial guess.

In order to evaluate the combustion process, the chemical composition of the reactive mixture was analyzed. The following diagrams present the most relevant species concentrations within combustion chamber throughout the cycle. From Figure 4.3 trough Figure 4.8 it can be observed that the reagents C_8H_{18} and O_2 were almost completely consumed slight after spark ignition, giving place to the main products H_2O and CO_2 and small fractions of CO and NO. However, unlike H_2O and CO_2 which concentrations shows slight variations until intake valve opening, CO and NO start to decrease during exhaust. It can also be observed an increase of reactants with when the intake valves open. Due to the nature of the combustion process as a fast exothermic rection Section 2.5, a almost instantaneous change from fuel state to product state was expected.

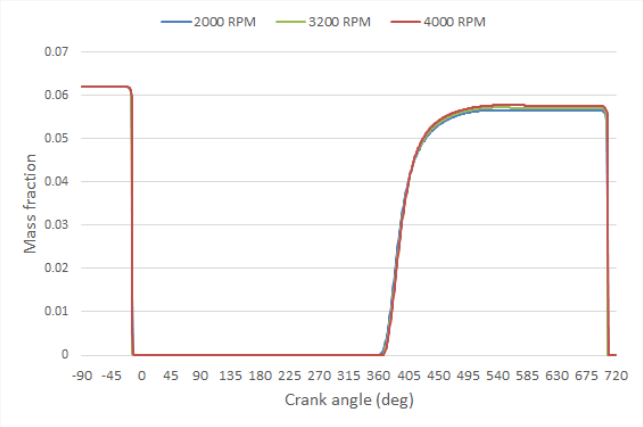

Figure 4.3: Octane (C_8H_{18}) in cylinder mass fraction.

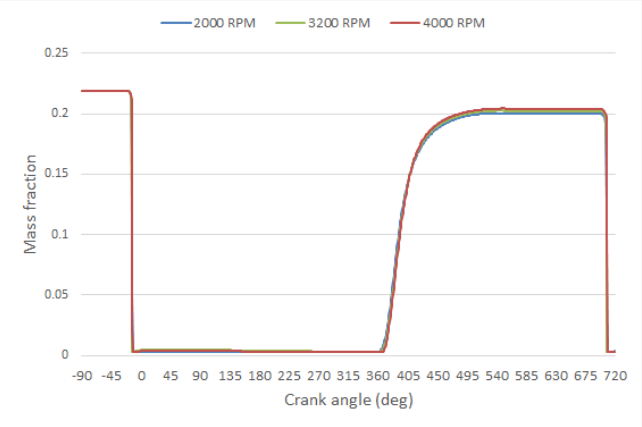

Figure 4.4: Oxigen (O_2) in cylinder mass fraction.

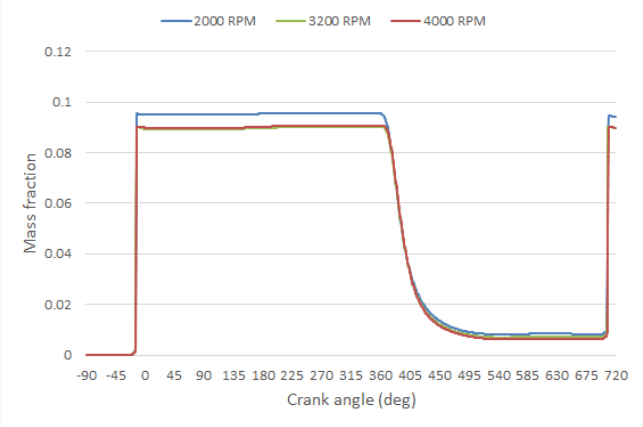

Figure 4.5: Water vapor (H_2O) in cylinder mass fraction.

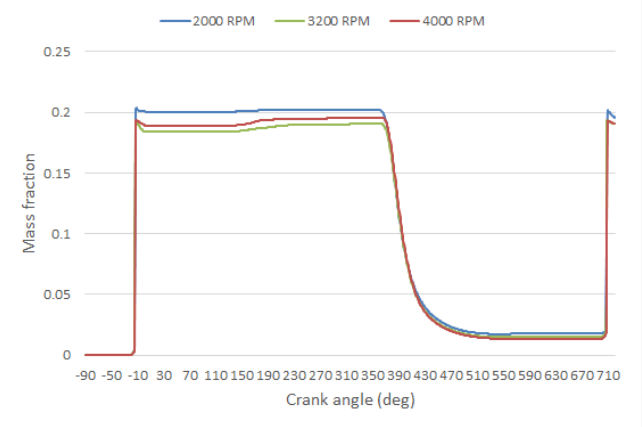

Figure 4.6: Carbon dioxide (CO_2) in cylinder mass fraction.

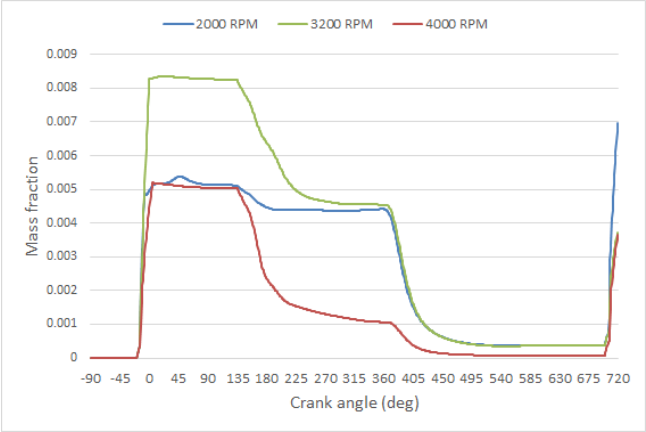

Figure 4.7: Carbon monoxide (CO) in cylinder mass fraction.

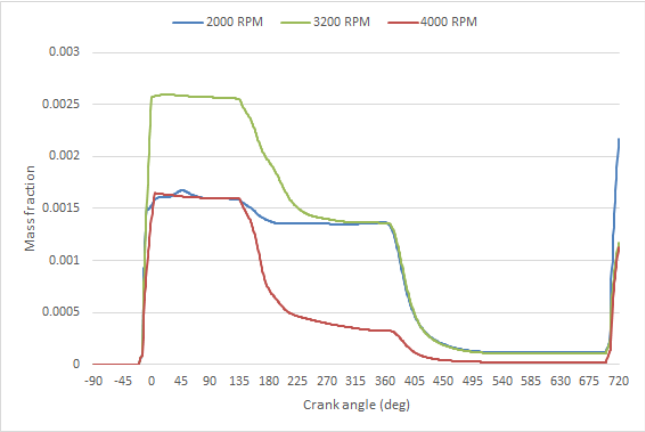

Figure 4.8: Nitric oxide (NO) in cylinder mass fraction.

4.0.2 Flame Propagation

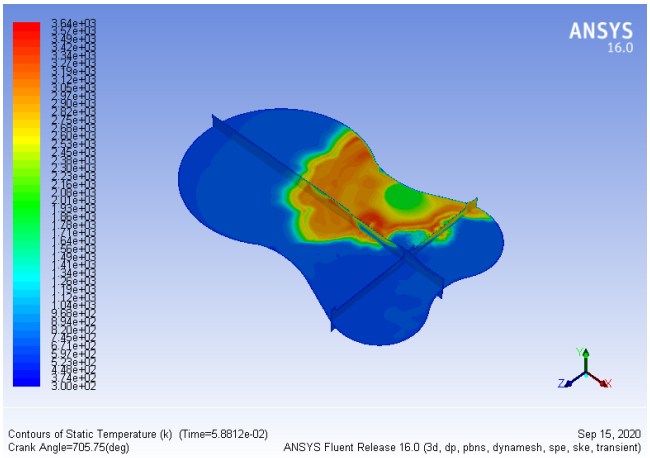

Figure 4.9: Contours of static temperature at $705.75°$ crank angle and $2000RPM$.

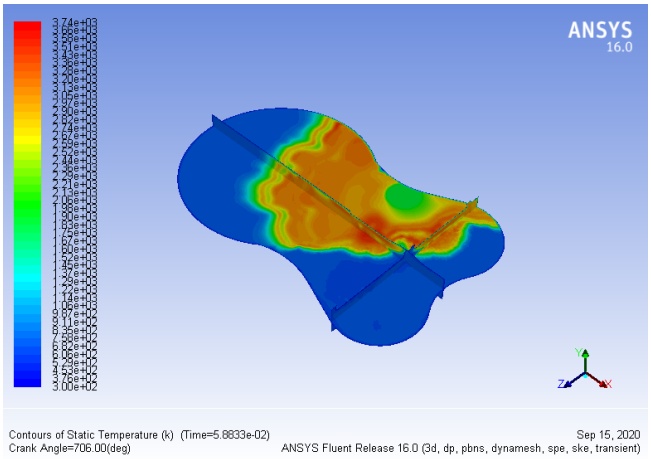

Figure 4.10: Contours of static temperature at $706°$ crank angle and $2000RPM$.

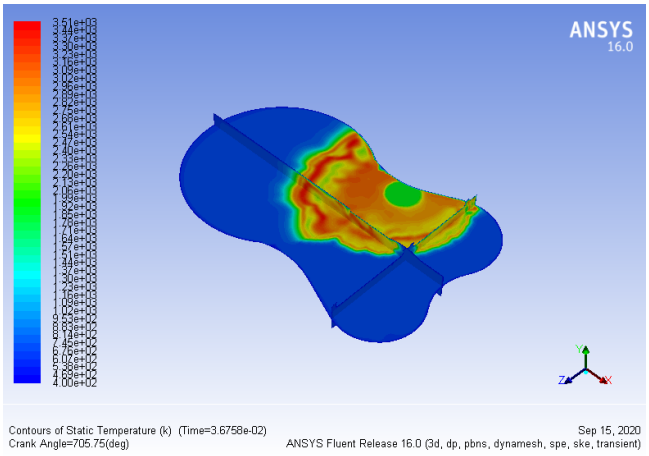

Figure 4.11: Contours of static temperature at $705.75°$ crank angle and $3200RPM$.

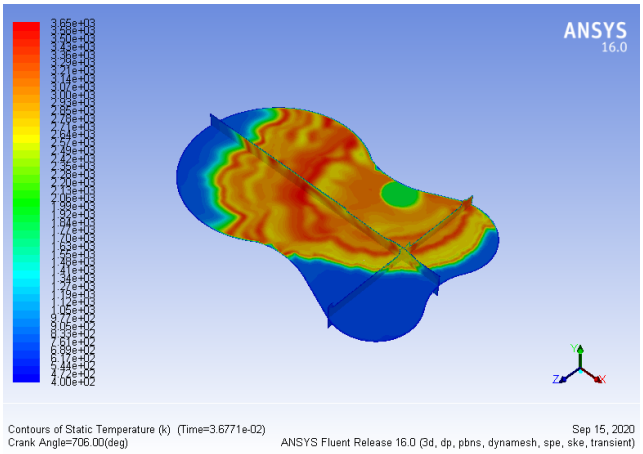

Figure 4.12: Contours of static temperature at $706°$ crank angle and $3200RPM$.

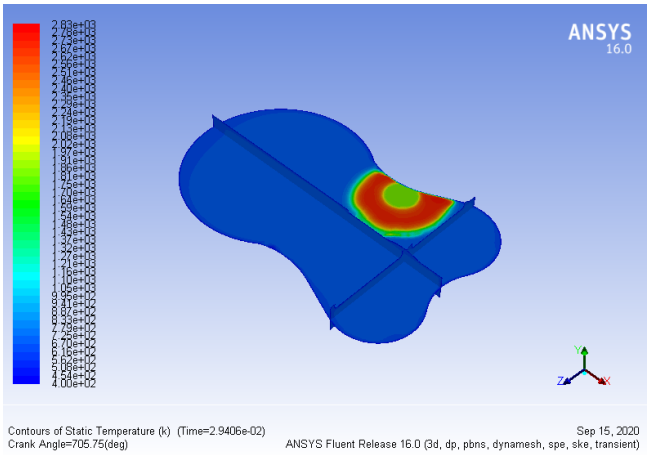

Figure 4.13: Contours of static temperature at 706° crank angle and $4000RPM$.

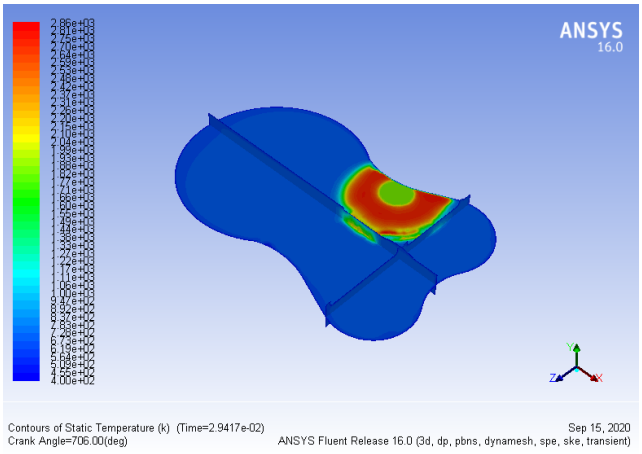

Figure 4.14: Contours of static temperature at 707° crank angle and $4000RPM$.

Under normal operating conditions, the combustion process can be divided in two main stages, flame development and flame propagation Section 2.5.2. The flame development also refered to as delay period in this simulation takes place in the first 5°crank angle after spark ignition (700° crank angle). In the second stage of combustion the flame front moves very quickly through the combustion chamber, which can be observed in Figure 4.9 through Figure 4.14. It can also be noticed the flame front greatly distorted due to the in-cylinder flow motions. During this phase it can also be observed the chemical rection taking place. C_8H_{18} and O_2 being consumed and originating CO_2 and H_2O.

The overall flame propagation presents some divergences from what ideally should happen. The flame diameter should be about two-thirds of the cylinder bore at TDC, likewise, the air-fuel mixture should be about two-thirds burned. However, in this case the rection rate is so high that the flame reaches the cylinder walls and the fuel-air mixture burns almost completely before TDC. Which can be reinforced with the in cylinder static temperature grah 4.2. In addition, apart from the slightly slower advance of the flame at 4000RPM, there is no clear pattern regarding the flame temperature variations, mixture reaction rates and related reactants consumption and products generated with the different crank rotations.

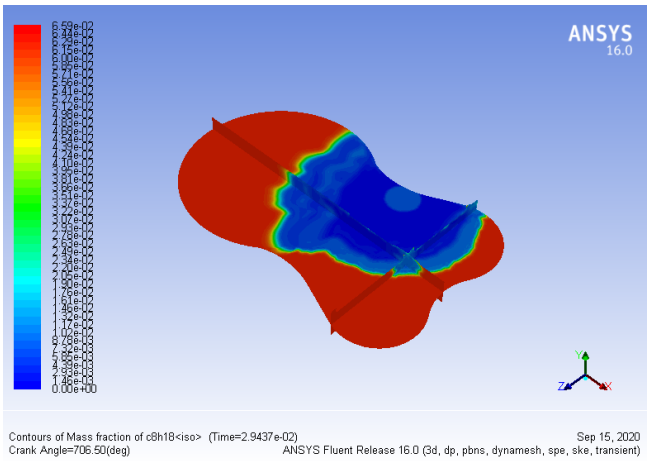

Figure 4.15: Octane (C_8H_{18}) mass fraction at 706.5° crank angle and $4000RPM$.

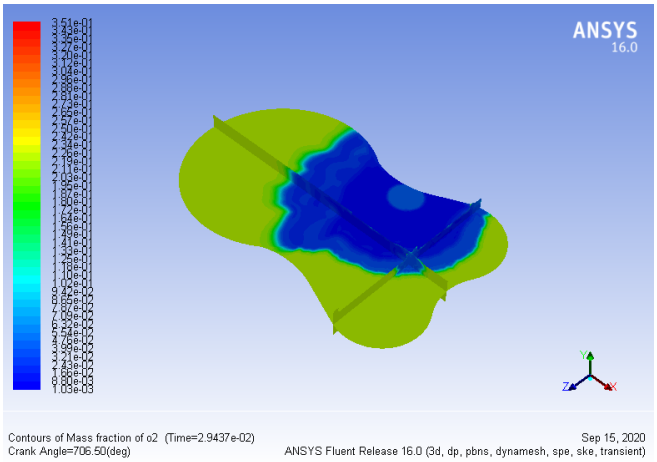

Figure 4.16: Oxigen (O_2) mass fraction at 706.5° crank angle and $4000RPM$.

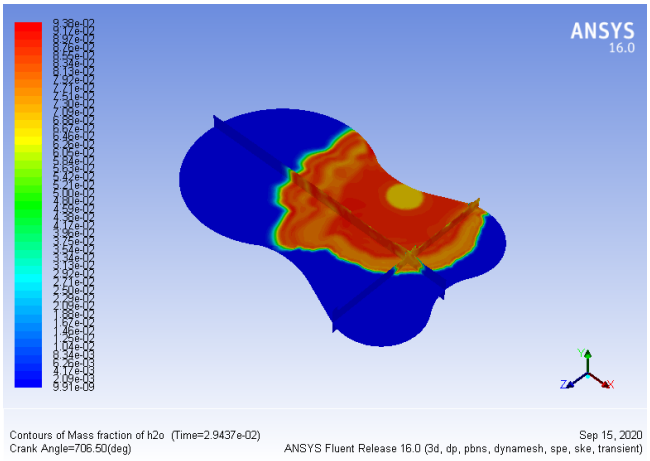

Figure 4.17: Water vapor (H_2O) mass fraction at 706.5° crank angle and $4000RPM$.

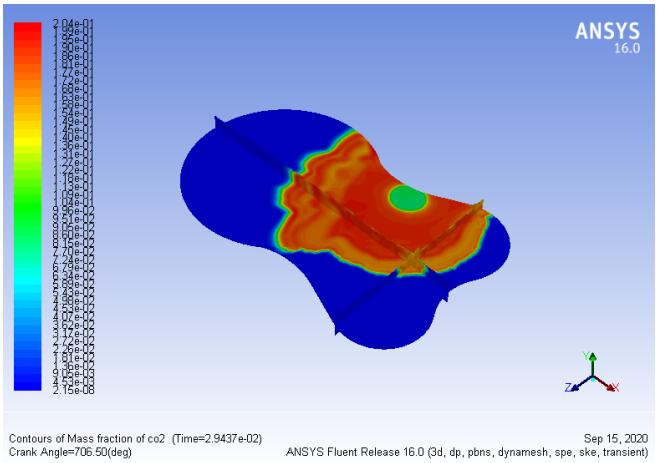

Figure 4.18: Carbon dioxide (CO_2) mass fraction at 706.5° crank angle and $4000RPM$.

4.0.3 Inlet Flow-Volumetric Efficiency

Mass flow through the intake valve into the cylinder as a function of the crankshaft angle is shown in Figure 4.19. Towards the end of the exhaust stroke, near TDC, the intake valves open, with the exhaust valves also open thus valve overlap occurs, which results in a momentary reverse flow of exhaust gas back into the cylinder due to pressure contrast. This, can also be seen at the end of intake before intake valve closes after BDC, due to the combined effect of piston movement, gas inertia and pressure drop in the admission ducts. Comparing Figure 4.19 with Figure D.5 in App.D.2 ,the simulated mass flow is not far from the literature. In addition, it can also be observed that the mass flow rate increases with the engine rotation speed and have similar curves.

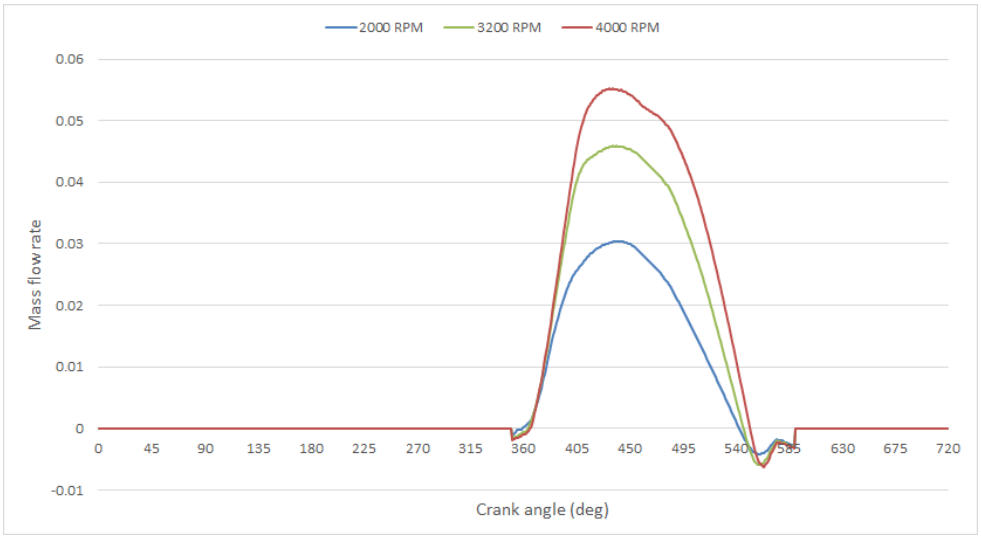

Figure 4.19: Mass flow rate through the admission valve.

During the cycle of an engine, air and fuel must be admitted, closed and exhausted from the cylinder, in order to have a decent combustion. Volumetric efficiency is one of the most important factors when discussing intake. It assesses the capacity of the cylinder to be filled with the actual capacity of the cylinder.

In order to calculate the volumetric efficiency for each engine speed in Table 4.1, Equation 4.1 was used and the total mass entering the cylinder was determined resorting to a program that runs in Matlab (see App.D.3) that calculates the area beneath the curve. As expected volumetric efficiency increases with engine speed [5].

$$\eta_v = \frac{m_a}{\rho V_d} \quad (4.1)$$

Where m_a is the total mass entering the cylinder, ρ is the fluid density at intake duct (considered to be 1.176 [12]) and V_d is the displaced volume, in this case $0,000286787m^3$[12].

Table 4.1: Inlet and exhaust mixture total mass and volumetric efficiency variation with engine speed.

	Exhaust mixture total mass (kg)	Inlet mixture total mass (kg)	Volumetric Efficiency (%)
2000 RPM	-2.769E-04	2.805E-04	83.16
3200 RPM	-2.871E-04	2.807E-04	83.21
4000 RPM	-2.955E-04	2.809E-04	83.29

4.0.4 Outlet Flow-Emissions

After combustion and expansion stroke, the burned gases used to transfer work to the crankshaft must be expelled from the cylinder to make room for the air-fuel charge of the next cycle. The exhaust stroke is responsible for this process and can be divided in two different moments: blow-down and exhaust [5]. When the exhaust valve opens near the end of the expansion stroke both pressure and temperature of gas within the cylinder are very high, whereas in the exhaust duct is practically at atmospheric pressure. This differential pressure causes an abrupt flow from the combustion chamber through the open exhaust valves, the blowdown process.

As the flow leaves the cylinder, it experiences a drop in pressure and temperature. When the pressure across the exhaust valve is finally equalized, the remaining gases are then pushed out of the cylinder by the piston as it travels from BDC to TDC during the exhaust stroke. Ideally, at the end of the exhaust stroke when the piston reaches TDC, all the exhaust gases should have been removed from the cylinder. However, due to valve overlap reverse flow of the exhaust gases into the intake system occurs, and therefore this flow is drawn back into the cylinder along with the air-fuel charge when the intake process starts.

Both phases blowdown and exhaust, can be observed in the simulated results for all the different engine speeds Figure 4.20. As expected blowdown occurs between $135°$ and $270°$ crank angle, and exhaust until the valves close. Reversed flow can also be noticed at the end of the exhaust stroke. In addition, similar to the intake flow, the mass flow increases with the rotation speed. Comparing Figure 4.20 with Figure D.6 in App.D.4 the simulated exhaust mass flow is also not far from the literature, with the exception of 2000RPM, where reversed flow through the exhaust system occurs.

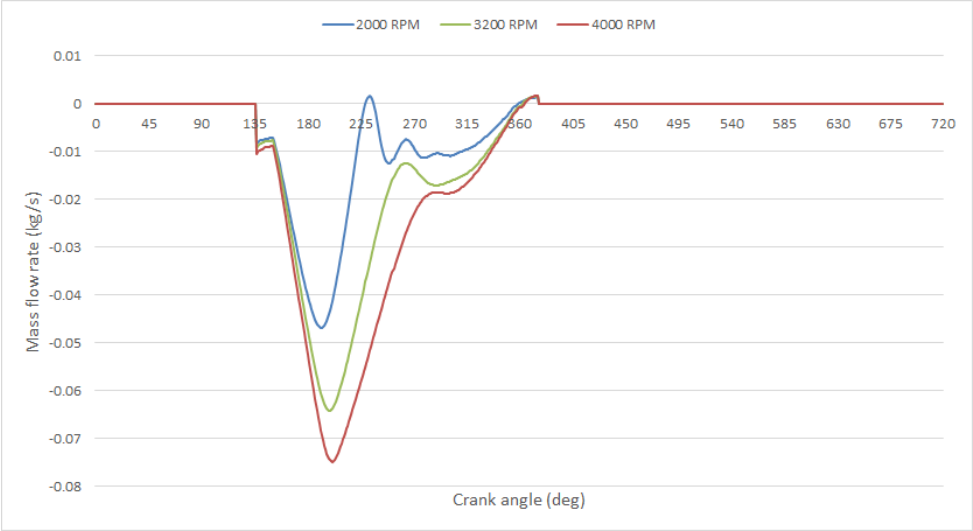

Figure 4.20: Mass flow rate through the exhaust valve.

One of the main goals of this study is to analyze the concentrations of the exhaust flow components in order to evaluate its impact when released in the environment. Table 4.2 shows the species that resulted from octane and air that crossed exhaust port during exhaust stroke. This table is divided for the three different engine speeds. The right side column of each sub table presents the total mass of the species that exited the cylinder, calculated using the Matlab program mentioned before. In the opposite side are the species mass fractions, determined by dividing each element total mass with the exhaust mixture total mass presented in Table 4.1.

Table 4.2: Total mass out and mass fraction of each mixture element, for the three engine RPM.

Species	$2000RPM$		$3200RPM$		$4000RPM$	
C_8H_{18}	$7.24E-14$	$-2.61E-10$	$6.32E-17$	$-2.20E-13$	$-1.57E-18$	$5.30E-15$
O_2	$-7.74E-07$	$2.80E-03$	$-1.25E-06$	$4.36E-03$	$-1.05E-06$	$3.57E-03$
H_2O	$-2.64E-05$	$9.52E-02$	$-2.56E-05$	$8.93E-02$	$-2.65E-05$	$8.98E-02$
CO_2	$-5.54E-05$	$2.00E-01$	$-5.26E-05$	$1.83E-01$	$-5.57E-05$	$1.88E-01$
CO	$-1.46E-06$	$5.27E-03$	$-2.47E-06$	$8.60E-03$	$-1.57E-06$	$5.33E-03$
NO_2	$-5.09E-10$	$1.84E-06$	$-8.67E-10$	$3.02E-06$	$-5.96E-10$	$2.02E-06$
NO	$-4.54E-07$	$1.64E-03$	$-7.68E-07$	$2.67E-03$	$-4.99E-07$	$1.69E-03$
N_2	$-1.92E-04$	$6.94E-01$	$-2.04E-04$	$7.09E-01$	$-2.10E-04$	$7.10E-01$
N	$-1.19E-10$	$4.29E-07$	$-2.00E-10$	$6.95E-07$	$-1.39E-10$	$4.72E-07$
H	$-6.22E-09$	$2.25E-05$	$-1.05E-08$	$3.65E-05$	$-6.46E-09$	$2.19E-05$
OH	$-3.17E-07$	$1.14E-03$	$-5.36E-07$	$1.87E-03$	$-3.41E-07$	$1.16E-03$
O	$-7.79E-08$	$2.81E-04$	$-1.31E-07$	$4.58E-04$	$-8.16E-08$	$2.76E-04$
Total	$-2.769E-04$	$1.00E+00$	$-2.871E-04$	$1.00E+00$	$-2.955E-04$	$1.00E+00$

Notice that C_8H_{18}, is positive, which means is entering the Combustion Chamber. Its mass fraction decreases with engine rotation as expected, which can be explained by valve overlap phenomena, i.e. at lower rotations there is more time for the admitted C_8H_{18} to flow through the exhaust valve.

Due to the importance of carbon monoxide and nitric oxides variables in IC engines emissions, this variables mass flow rate throughout the simulated cycle are presented in the figures below as well as their total mass that crossed exhaust port in percentage. It can be observed that the total mass of NO_2 that exited the cylinder as expected in SI engines is negligible, Section 2.7.

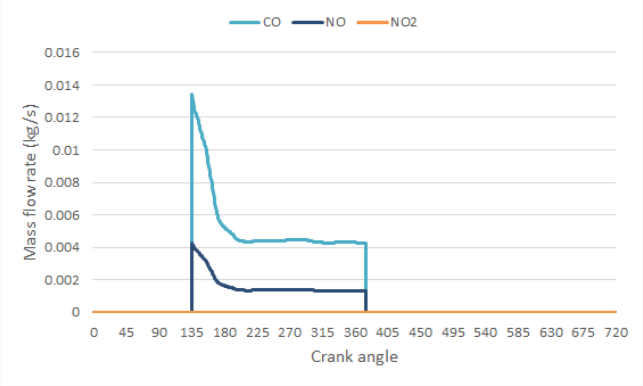

Figure 4.21: CO, NO and NO_2 mass flow rate through the exhaust valve, at 2000RPM.

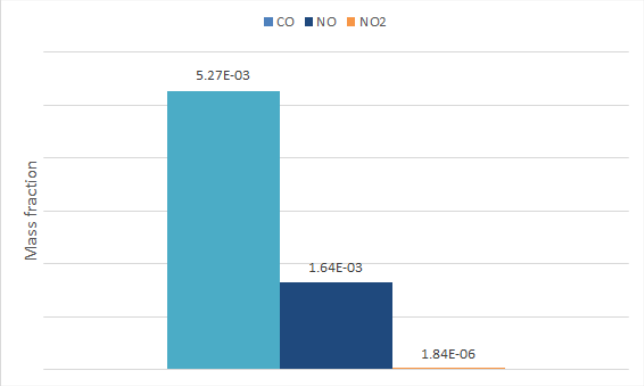

Figure 4.22: Total mass fraction out, CO, NO and NO_2, at 2000RPM.

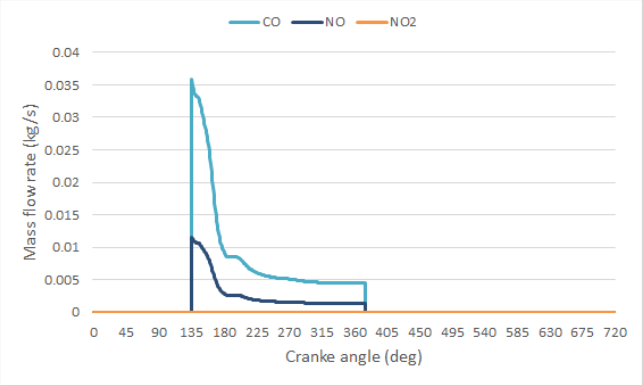

Figure 4.23: CO, NO and NO_2 mass flow rate through the exhaust valve, at 3200RPM.

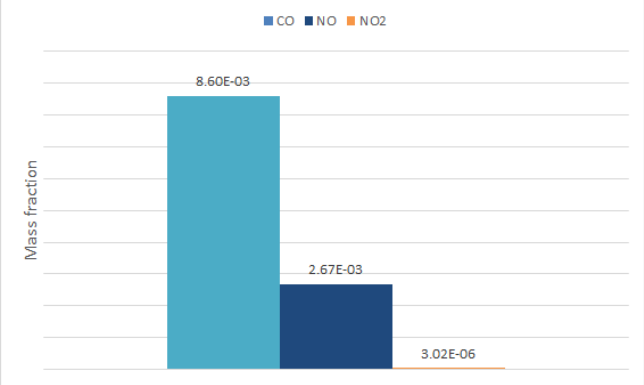

Figure 4.24: Total mass fraction out, of CO, NO and NO_2, at 3200RPM.

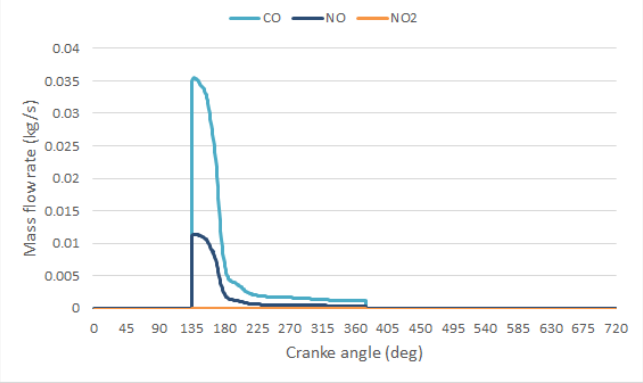

Figure 4.25: CO, NO and NO_2 mass flow rate through the exhaust valve, at 3200RPM.

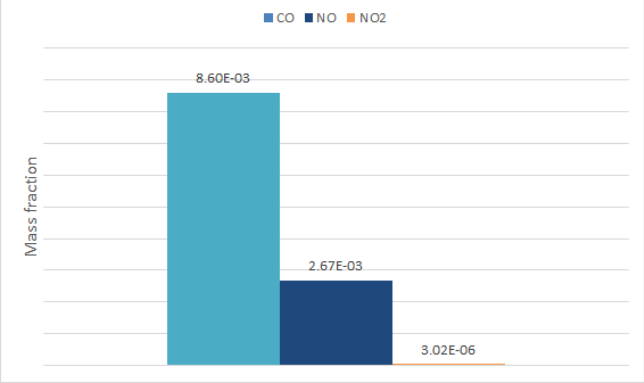

Figure 4.26: Total mass fraction out, of CO, NO and NO_2, at 3200RPM.

Chapter 5

Conclusion

This dissertation presents a numerical analysis of the combustion process in a four-stroke SI opposed piston engine. The geometry used was developed in Gregorios experimental and CFD cold flow simulation study [12]. Since he was not able to perform the combustion simulation this can be regarded as a continuity of part of its work. Thus, the aim of this study was to successfully simulate the combustion of octane-air mixture in the UBI/UDI-OPE-BGX286 based model and evaluate the relevant resulting emissions, in this case CO, NO and NO_2. When studying a complex CFD problem such as this, hundreds of different variables that can affect the outputs must be considered, and numerous setup parameters need to be defined. Just obtaining a combustion simulation that worked and results within the order of magnitude expected, is already a great achievement. Thus, and as expected, the simulations were very computational demanding and time consuming, several obstacles were encountered, costing sometimes months to overcome.

The simulation was run on the Fluent 16.0 software installed on a multi-Core high performance machine that belongs to Universidade da Beira Interior. The species transport model was chosen to model combustion from the available in Fluent. In order to gather enough data to be able to evaluate the overall engine operation and make some comparison with literature data three different engines speeds were simulated. After the simulation, the results were visualized, presented and analyzed.

Regarding the results obtained from the three CFD simulations, for each cycle the engine features such as temperature, pressure, flow behavior, species concentration and the volumetric efficiency were analyzed through the engine's four strokes: expansion, exhaust, intake and compression. The main unconformities detected were related to the very fast flame propagation, the maximum pressure occurred before expected (near TDC) and the maximum temperature registered in the three engine speeds simulation present values above what should be expected (around $3000K$). Due to the lack of experimental data a quantitative comparison and respective validation of the results was not possible. However, comparation was made with data from literature, and the obtained graphics revealed that the simulated results can be considered acceptable.

In one hand working in this study was very enlightening regarding IC engines operation and the theory behind CFD simulations. On the other hand, it was really challenging, a lot of resilience was necessary to carry this analysis. As a final note, it is the author's opinion that the development of a functional four-stroke SI OP engine should not be dismissed, despite its challenges.

5.1 Future Studies/Work

As mentioned in the beginning of this work, there are many possibilities in IC engine design as well as in modelling the engine and respective simulations. Thus, many important variables are involved in final engine parameters. Regarding this study many engine parameters and variables

were not considered once it would imply even more complexity in the study. Some contribute to better results and much closer to the reality. This work can evolve in the future, among other examples, by:

- Explore the use of more computationally expensive turbulence-chemistry interaction models such as the *Finit-rate/Eddy-Dissipation* and *Eddy-Dissipation Concept*, which would require improving the mesh quality.
- Import a CHEMKIN chemical mechanism, which will add more species and respective stoichiometric relations to the combustion model.
- Explore the *Partially Premixed Combustion* model and their influence on combustion efficiency and emissions.
- Reduce ignition advance angle so that the maximum pressure take place later in time.
- Adjust combustion model setup parameters in order to reduce the chemical reaction rate as wells as the flame propagation.
- Experimental studies would be of a great interest for this study. If pressure and temperature data were gathered, this would give a good starting point for future simulations.

Bibliography

[1] “Slide Player.” [Online]. Available: http://slideplayer.com/slide/7593517/ xi, 6

[2] “Thermopedia.” [Online]. Available: http://www.thermopedia.com/de/content/880/ xi, 12, 13

[3] B. Sendyka and M. Noga, “Combustion Process in the Spark-Ignition Engine with Dual-Injection System,” 2013. xi, 16

[4] B. Kegl, M. Kegl, and S. Pehan, Grenn Diesel Engines: Biodiesel Usege in Diesel Engines. Springer, 2013. xi, 16

[5] W. W. Pulkrabek, Engeneering Fundamentals of Internal Combustion Engines, 1st ed. New Jersey: Prentice Hall, 1997. xi, xii, 1, 5, 7, 8, 9, 10, 17, 19, 29, 31, 32, 36, 41, 42, 43, 44, 69, 92, 93

[6] V. Ganesan, Internal Combustion Engines, 2nd ed. Tata McGraw-Hill, 2006. xi, 15, 18

[7] R. Stone, Introduction to Internal Combustion Engines, 2nd ed. Macmillan Press Ltd., 1992. xi, 14, 18, 19, 36, 38

[8] R. V. Basshuysen and F. Schafer, Eds., Internal Combustion Engine Handbook: Basics, Components, Systems, and Perspectives. SAE International, 2004. xi, 7, 8, 16, 19, 20, 30, 36, 38

[9] J.-P. Pirault and M. L. S. Flint, Opposed Piston Engines: Evolution, Use, and Future Applications. Warrendale: SAE International, 2009. xi, 1, 21, 22, 23

[10] Y. A. Cengel and M. A. Boles, Thermodynamics: An Engineering Approach, 5th ed. McGraw-Hill, 2005. xi, 5, 29, 30, 31, 33, 34, 35

[11] E. Sher, Ed., Handbook of Air Pollution from Internal Combustion Engines: Pollutant Formation and Control. Academic Press, 1998. xi, 43, 44

[12] J. Gregório, “Desenvolvimento de um Motor Alternativo de Combustão Interna de Pistões Opostos,” Ph.D. dissertation, 2017. xi, xii, xiii, 51, 52, 54, 63, 69, 73, 79, 80, 81, 82, 83

[13] John D. Anderson, Computational Fluid Dynamics-The Basics with Applications. McGraw-Hill, Inc., 1995. xiii, 45, 46

[14] ANSYS 15.0, “Introduction to ANYS Meshing- Lecture 7: Mesh Quality and Advanced Topics.” [Online]. Available: https://www.academia.edu/16970000/MESH{_}QUALITY{_}AND{_}ADVENCED{_}TOPICS{_}ANSYS{_}WORKBENCH{_}16.0 xiii, 49, 55

[15] V. Ganesan, Internal Combustion Engines, 3rd ed. McGraw-Hill, 2007. 1

[16] J. B. Heywood, Internal Combustion Engines Fundamentals, int. ed. New York: McGraw-Hill, 1988. 1, 5, 6, 7, 8, 9, 10, 11, 13, 15, 18, 32, 33, 34, 35, 36, 38, 42, 44, 57

[17] D. Anderson, I. Graham, and B. Williams, Flight and Motion : The History and Science of Flying, 1st ed. Sharpe Reference, 2011. 2

[18] J. Schultz, Crafting Flight: Aircraft pioneers and the contributions of the men and women of NASA Langley Research Center, 1st ed., 2003. 2

[19] B. Andersson, R. Andersson, L. Hakansson, M. Mortensen, R. Sudiyo, and B. van Wachem, Computational Fluid Dynamics for Engineers, 2011. 2, 45

[20] E. Gregersen, Ed., The Complete History of Wheeled Transportation: From Cars and Trucks to Buses and Bikes. Britannica Educational Publishing, 2012. 5

[21] Colin R. Ferguson and Allan T. Kirkpatrick, Internal Combustion Engines: Applied Thermosciences, 2nd ed. New York: Jonh Wilwy and Sons, Inc., 2001. 5, 9, 13, 14, 20, 30

[22] International Energy Agency, "Key World Energy Statistics 2017," Tech. Rep., 2017. 15, 34

[23] ——, "Oil Information 2017," Tech. Rep., 2015. 15

[24] European Expert Group on Future Transport Fuels, "Future Transport Fuels," 2011. 15

[25] D. Johnson, M. Wahl, F. Redon, E. Dion, S. McIntyre, G. Regner, and R. Herold, "Opposed - Piston Two - Stroke Diesel Engine: A Renaissance," Symposium on International Automotive Technology, 2011. 21

[26] Richard G. Budynas and J. Keith Nisbett, Shigley´s Mechanical Engineering Design, 9th ed. McGraw-Hill, 2011. 21

[27] "Diesel air Limited," 2014. [Online]. Available: http://www.dair.co.uk/ 28

[28] M. GE□CA, Z. CZYŻ, and M. SUŁEK, "Diesel engine for aircraft propulsion system," 2017. 28

[29] "SUPERIOR AVIATION GROUP HAS ACQUIRED THE GEMINI DIESEL ENGINE," Tech. Rep., 2015. [Online]. Available: http://superiorairparts.com/files/2514/2966/5042/GEMINI{_}ANNOUNCEMENT{_}RELEASE-FINAL.pdf 28

[30] B. E. Milton, Thermodynamics, Combustion and Engines, 3rd ed., 2005. 29

[31] Anil W. Date, Analytic Combustion: With Thermodynamics, Chemical Kinetics and Mass Transfer, 1st ed. Cambridge University Press, 2011. 34, 39

[32] M. Liberman, Introduction to Physics and Chemistry of Combustion: Explosion, Flame, Detonation. Springer, 2008. 34, 42, 45, 46

[33] S. R. Turns, An Introduction to Combustion: Concepts and Applications, 3rd ed. McGraw-Hill, 2012. 35, 41

[34] C. K. Law, Combustion Physics. Cambridge University Press, 2006. 35

[35] Handbook of Combustion Vol.1: Fundamentals and Safety, Maximilian ed. Wiley-VCH, 2010. 35

[36] A. C. F.-P. Sara McAllister, Jyh-Yuan Chen, Fundamentals of Combsution Processes. Springer, 2011. 41, 50

[37] W. C. Gardiner, Combustion Chemistry, 1st ed., 1984. 41

[38] Encyclopaedia Britannica Editors, "Algorithm-Mathematics." [Online]. Available: https://www.britannica.com/science/algorithm 45

[39] J. BLAZEK, Computational Fluid Dynamics - Principles and Applications, 3rd ed., 2015. 45, 46

[40] H. K. Versteeg and W Malalasekera, An Introduction to Computational Fluid Dynamics, 2nd ed. Pearson Education, 2007. 46, 48, 56

[41] J. Tu, G.-H. Yeoh, and C. Liu, Computational Fluid Dynamics - A Practical Approach, 2nd ed. Elsevier, 2013. 46

[42] R. A. Knneth K. Huo, Fundamentals of Turbulent and Multiphase Combustion. John Wiley & Sons, Inc., 2012. 47, 48, 49, 50

[43] ANSYS Fluent Theory Guide, 2015. 47, 55, 56, 57, 60, 62, 63

[44] M. Chiodi, an Innovative 3D-CFD-Approache towards Virtual Development of Internal Combustion Engines, 1st ed. Vieweg+Teubner Research, 2011. 49

[45] T. Poinsot, Theoretical and Numerical Combustion, 2nd ed., 2005. 49

[46] Robert Gonçalves, "3D CFD Simulation of a Cold Flow Four-Stroke Opposed Piston Engine," Master, 2014. 52, 55, 59

[47] Sunil Moda, "Computational Modeling and Analyses of Heavy Fuel Feasibility in Direct Injection Spark Ignition Engine," Master, 2011. 55

Appendix A

Model Decomposition

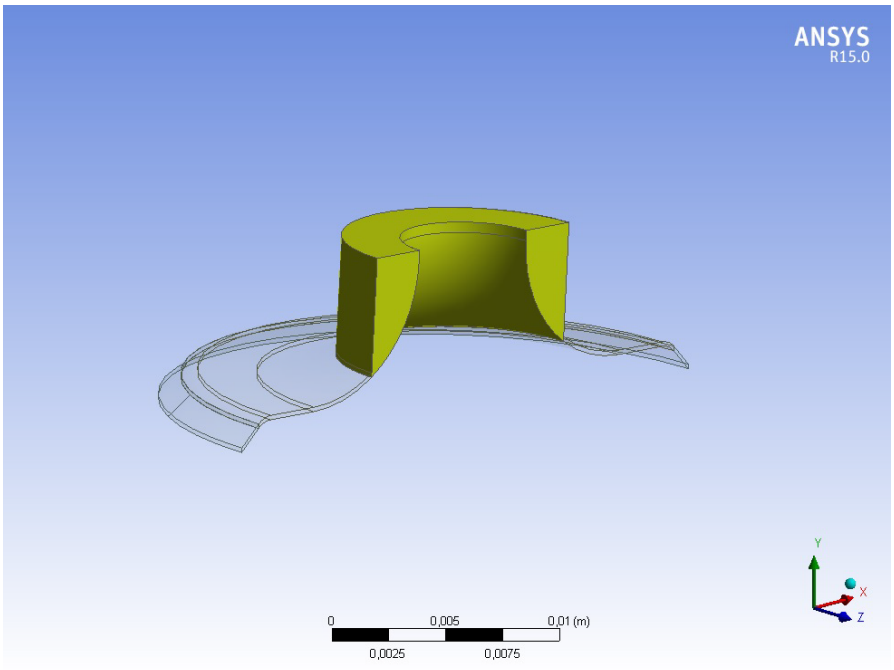

Figure A.1: Symmetrical view of the Inboard body (zone is shaded in yellow/green)[12].

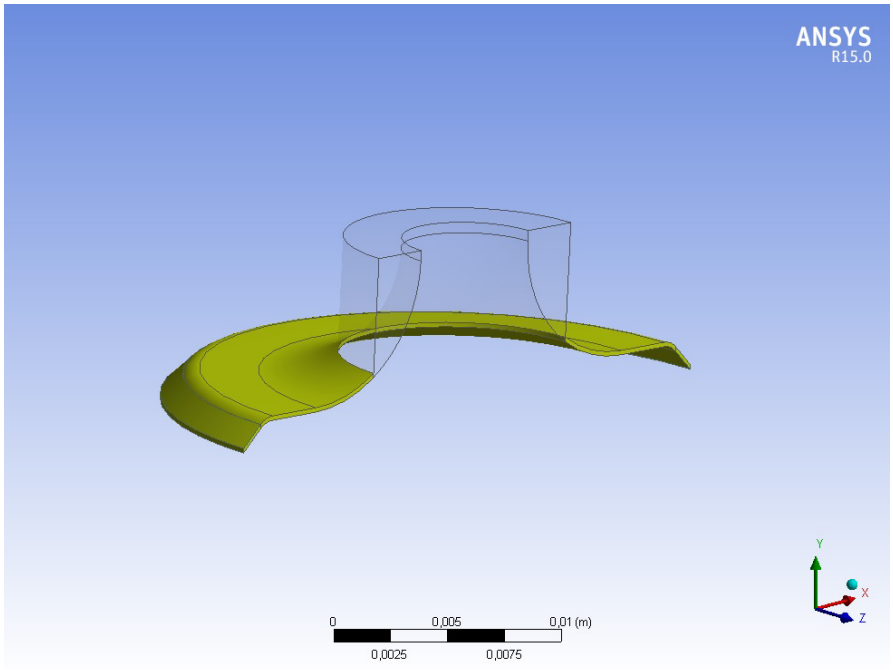

Figure A.2: Symmetrical view of the Vlayer body (zone is shaded in yellow/green)[12].

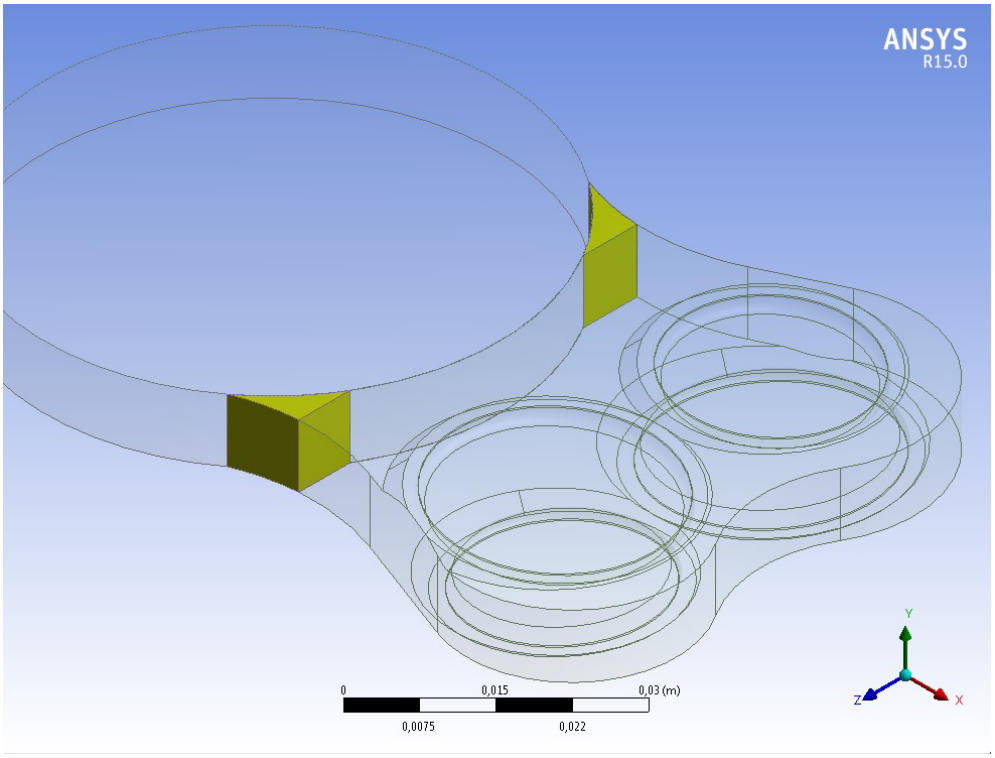

Figure A.3: View of the chamber where both corners (shaded in yellow/green) were cut off[12].

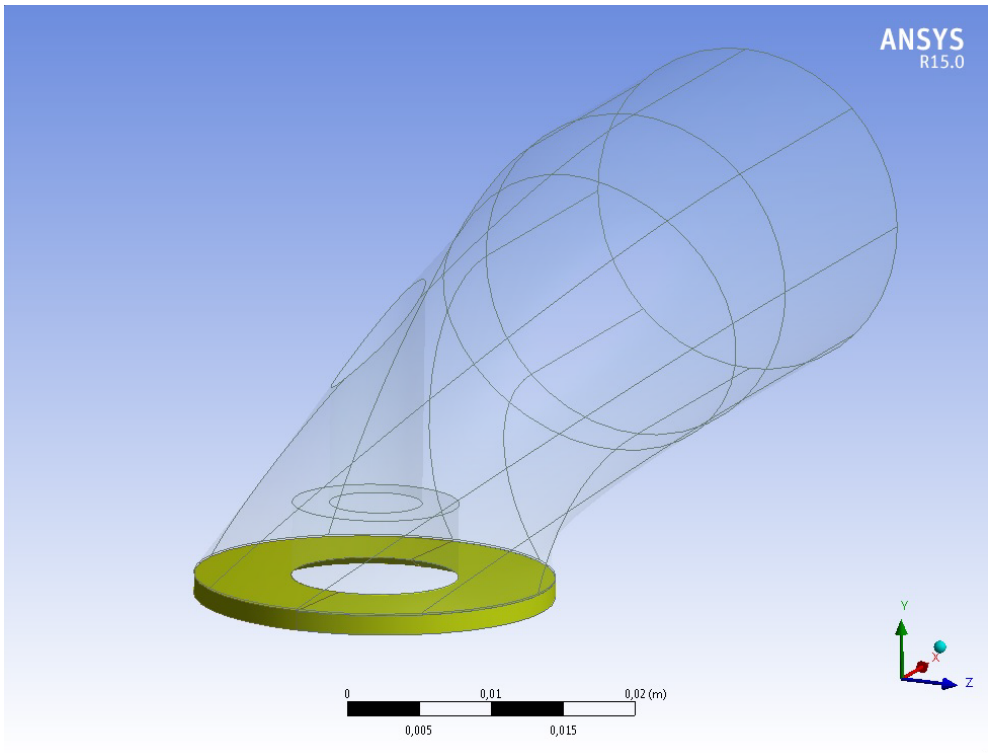

Figure A.4: View of one of the port decomposition. Bottom port is separated due to meshing issues (shaded in yellow/green)[12].

Appendix B

Mesh Details

Table B.1: Mesh Parameters [12].

Reference Size (RS)	$2\pi R_{ev}/100$	$0.00072\ m$
Minimum Mesh Size	$RS/3$	$0.00024\ m$
Maximum Mesh Size	$3 \times RS$	$0.00217\ m$
Vlayer Size	$2 \times RS/3$	$0.00048\ m$
Inboard Size	$RS/2$	$0.00036m$
Chamber-Vlayer Interface Size	$RS/2$	$0.00036\ m$
Cylinder and Chamber Size	RS	$0.00072\ m$
Edge Sizing (Top & Bottom Seat Edges)	$\frac{Larger\ Edge\ Lenght}{\frac{2 \times Vlayer\ Size}{3}}$	4
Edge Sizing (Top & Bottom *Vlayer* Edges)	$\frac{2 \times Vlayer\ Size}{3}$	$0.00032\ m$
Edge Sizing (Circular *Vlayer* Edges)	$\frac{\frac{100 \times Mesh\ Size}{Vlayer\ Size}}{2}$	75

Table B.2: Global Mesh Settings [12].

Defaults	Physics Preference	CFD
	Solver Preference	Fluent
	Relevance	0
Sizing	Use Advanced Size Function	On: Curvature
	Relevance Center	Fine
	Initial Size Seed	Active Assembly
	Smoothing	High
	Transition	Slow
	Span Angle Center	Fine
	Curvature Normal Angle	$18.0°$
	Minimum Size	$0.00024\ m$
	Maximum Face Size	$0.00217\ m$
	Maximum Size	$0.00217\ m$
	Growth Rate	1.20

Table B.3: Local Mesh Settings - Cylinder [12].

Sweep Method	Src/Trg Selection Free Face Mesh Type Sweep Bias Type Sweep Bias	Automatic All Quad - 1
Body Sizing	Elements Size Behavior Growth Rate	0.00072 m Soft 1.15

Table B.4: Local Mesh Settings - Chamber [12]

Body Sizing	Element Size Behavior Soft Growth Rate	0.00072 m Soft 1.15
Sweep Method (Chamber "Corners")($\times 2$)	Src/Trg Selection Free Face Mesh Type	Automatic All Tri
Face Sizing (intf-valve-ob-fluid-ch)($\times 4$)	Element Size Behavior	0.00036 m Soft
Body Sizing (Chamber "Corners")	Element Size Behavior	0.00017 m Soft

Table B.5: Local Mesh Settings - Ports [12].

Face Sizing (*Vlayer* & *Inboard* Faces)	Element Size Behavior Soft	0.00036 m Soft
Sweep Method (Bottom Port Zone)($\times 4$)	Src/Trg Selection Free Face Mesh Type Sweep Bias Type Sweep Bias	Manual Source (Symmetry Face) All Tri - 1
Face Sizing (Symmetry Port Face)	Element Size Behavior	0.00036 m Hard
Face Sizing (Bottom Large Exhaust Port Face)	Element Size Behavior	0.00036 m Soft

Table B.6: Local Mesh Settings - *Inboard* [12].

Sweep Method ($\times 4$)	Src/Trg Selection Free Face Mesh Type Sweep Bias Type Sweep Bias	Manual Source (Symmetry Face) All Quad - 1
Face Sizing (Symmetry Face)($\times 8$)	Element Size Behavior	0.00036 m Hard

Table B.7: Local Mesh Settings - *Vlayer* [12].

Edge Sizing (Top & Bottom Seat Edges)	Number of divisions Behavior	4 Hard
Edge Sizing (Top & Bottom *Vlayer* Edges)	Element Size Behavior	0.00032 m Hard
Edge Sizing (Vertical *Vlayer* Edges)	Number of divisions Behavior	4 Hard
Edge Sizing (Circular *Vlayer* Edges)	Number of divisions Behavior	75 Hard
Body Sizing	Element Size Behavior	0.00048 m Soft
Sweep Method ($\times 4$)	Src/Trg Selection Free Face Mesh Type Sweep Bias Type Sweep Bias	Manual Source (Bottom *Vlayer* Face) All Quad - 1

Appendix C

Problem Setup Details

C.1 Boundary Conditions

Table C.1: Wall temperatures.

Wall Name	Temperature (K)
Both admission port walls	300
cylinder-walls chamber-walls All admission valve walls invalve-seat	400
Both exhaust port walls	440
All exhaust valve walls exvalve-seat Both piston walls	450

C.2 Dynamic Mesh

Table C.2: Mesh interfaces.

Mesh Interfaces		
Mesh Interface	**Interface Zone 1**	**Interface Zone 2**
intf-ch-cyl	intf-chamber	intf-cylinder
intf-exvalve1-ib	intf-exvalve1-ib-fluid-ib	intf-exvalve1-ib-fluid-ob-port intf-exvalve1-ib-fluid-ob-vlayer
intf-exvalve1-ob	intf-exvalve1-ob-fluid-ch	intf-exvalve1-ob-fluid-vlayer
intf-int-exvalve1-ib	intf-int-exvalve1-ib-fluid-ib	intf-int-exvalve1-ib-fluid-port
intf-int-exvalve1-ob	intf-int-exvalve1-ob-fluid-port	intf-int-exvalve1-ob-fuid-vlayer
intf-exvalve1-port	intf-exvalve1-midport	intf-exvalve1-port
intf-exvalve2-ib	intf-exvalve2-ib-fluid-ib	intf-exvalve2-ib-fluid-ob-port intf-exvalve2-ib-fluid-ob-vlayer
intf-exvalve2-ob	intf-exvalve2-ob-fluid-ch	intf-exvalve2-ob-fluid-vlayer
intf-int-exvalve2-ib	intf-int-exvalve2-ib-fluid-ib	intf-int-exvalve2-ib-fluid-port
intf-int-exvalve2-ob	intf-int-exvalve2-ob-fluid-port	intf-int-exvalve2-ob-fluid-vlayer
intf-exvalve2-port	intf-exvalve2-midport	intf-exvalve2-port
intf-int-invalve1-ib	intf-int-invalve1-ib-fluid-ib	intf-int-invalve1-ib-fluid-port
intf-int-invalve1-ob	intf-int-invalve1-ob-fluid-port	intf-int-invalve1-ob-fluid-vlayer
intf-invalve1-ib	intf-invalve1-ib-fluid-ib	intf-invalve1-ib-fluid-ob-port intf-invalve1-ib-fluid-ob-vlayer
intf-invalve1-ob	intf-invalve1-ob-fluid-ch	intf-invalve1-ob-fluid-vlayer
intf-int-invalve2-ib	intf-int-invalve2-ib-fluid-ib	intf-int-invalve2-ib-fluid-port
intf-int-invalve2-ob	intf-int-invalve2-ob-fluid-port	intf-int-invalve2-ob-fluid-vlayer
intf-invalve2-ib	intf-invalve2-ib-fluid-ib	intf-invalve2-ib-fluid-ob-port intf-invalve2-ib-fluid-ob-vlayer
intf-invalve2-ob	intf-invalve2-ob-fluid-ch	intf-invalve2-ob-fluid-vlayer

Table C.3: Mesh method parameters.

Smoothing	Method	Spring/Laplace/Boundary Layer
	Spring Constant Factor	0.05
	Convergence Tolerance	0.001
	Number of Iterations	25
	Elements	Tet in Tet Zones
	Laplace Node Relaxation	1
Layering	Options	Ratio Based
	Split Factor	0.4
	Collapse Factor	0.05
Remeshing	Remeshing Methods	Local Cell & Region Face
	Minimum Length Scale	0.00024 m
	Maximum Length Scale	0.000841 m
	Maximum Cell Skewness	0.9
	Size Remeshing Interval	1

Table C.4: Dynamic mesh: Stationary zones

Stationary Zones	
Dynamic Mesh Zone	**Meshing Options**
	Cell Height
valve name-seat	$0.0002\ m$
intf-int-valve name-ib-fluid-ib	$0.0005\ m$
intf-int-valve name-ob-fluid-vlayer	$0.0002\ m$

Table C.5: Events defined for the dynamic mesh.

Events	
deactivate-exvalve-zone[1]	$0°$
deactivate-invalve-zone[2]	$0°$
reduce-urf-due-to-exvalve-opening [3]	$135°$
reduce-time-step-due-to-exvalve-opening [4]	$135°$
activate-exvalve-zone [5]	$135°$
increase-urf-due-to-exvalve-opening[6]	$140°$
increase-time-step-due-to-exvalve-opening[7]	$140v$
reduce-urf-due-to-invalve-opening	$350°$
reduce-time-step-due-to-invalve-opening	$350°$
activate-invalve-zone	$350°$
increase-urf-due-to-invalve-opening	$355°$
increase-time-step-due-to-invalve-opening	$355°$
reduce-urf-due-to-exvalve-closing	$370°$
reduce-time-step-due-to-exvalve-closing	$370°$
deactivate-exvalve-zone	$375°$
increase-urf-due-to-exvalve-closing	$375°$
increase-time-step-due-to-exvalve-closing	$375°$
reduce-urf-due-to-invalve-closing	$585°$
reduce-time-step-due-to-invalve-closing	$585°$
deactivate-invalve-zone	$590°$
increase-urf-due-to-exvalve-closing	$590°$
increase-time-step-due-to-exvalve-closing	$590°$

[1]All exhaust related domains are deactivated in order to decrease calculation time.
[2]All intake related domains are deactivated in order to decrease calculation time.
[3]URF values are decreased due to sudden variations caused by valve opening.
[4]Time-step is decreased due to sudden variations caused by valve opening.New time-step is 0.125.
[5]Due to valve opening, the respective zone is activated.
[6]URF values are increased to their previous values.
[7]Time-step is defined to its previous value - 0.25.

Table C.6: Dynamic mesh: Stationary zones

Rigid Bodies			
Dynamic Mesh Zone	**Motion Attributes**		**Meshing Options**
	Motion Profile	**Valve/Piston Axis**	**Cell Height**
exvalve1-ch	exvalve	X = 0.06104854 Y = 0.9981348	0 m
exvalve1-ib	exvalve	X = 0.06104854 Y = 0.9981348	0.0005 m
exvalve1-ob	exvalve	X = 0.06104854 Y = 0.9981348	0.0002 m
exvalve2-ch	exvalve	X = 0.06104854 Y = -0.9981348	0 m
exvalve2-ib	exvalve	X = 0.06104854 Y = -0.9981348	0.0005 m
exvalve2-ob	exvalve	X = 0.06104854 Y = -0.9981348	0.0002 m
fluid-exvalve1-ib	exvalve	X = 0.06104854 Y = 0.9981348	-
fluid-exvalve1-vlayer	exvalve	X = 0.06104854 Y = 0.9981348	-
fluid-exvalve2-ib	exvalve	X = 0.06104854 Y = -0.9981348	-
fluid-exvalve2-vlayer	exvalve	X = 0.06104854 Y = -0.9981348	-
fluid-invalve1-ib	invalve	X = 0.06104854 Y = 0.9981348	-
fluid-invalve1-vlayer	invalve	X = 0.06104854 Y = 0.9981348	-
fluid-invalve2-ib	invalve	X = 0.06104854 Y = -0.9981348	-
fluid-invalve2-vlayer	invalve	X = 0.06104854 Y = -0.9981348	-
invalve1-ch	invalve	X = 0.06104854 Y = 0.9981348	0 m
invalve1-ib	invalve	X = 0.06104854 Y = 0.9981348	0.0005 m
invalve1-ob	invalve	X = 0.06104854 Y = 0.9981348	0.0002 m
invalve2-ch	invalve	X = 0.06104854 Y = -0.9981348	0 m
invalve2-ib	invalve	X = 0.06104854 Y = -0.9981348	0.0005 m
invalve2-ob	invalve	X = 0.06104854 Y = -0.9981348	0.0002 m
lower-piston	**piston-full**	Y = 1	0.001 m
upper-piston	**piston-full**	Y = -1	0.001 m

Table C.7: Dynamic mesh: Deforming zones

Deforming Zones					
Dynamic Mesh Zone	**Geometry Denition**			**Meshing Options**	
	Cylinder Radius	**Cylinder Origin**	**Cylinder Axis**	**Zone Parameters**	
intf-exvalve1-ob-fluid-ch	$0.0115\ m$	X = $0.054\ m$ Z = $-0.015\ m$	X = 0.06104854 Y = 0.9981348	Min. Length Scale	$0.00010954\ m$
				Max. Length Scale	$0.00038339\ m$
				Max. Skewness	0.6
intf-exvalve2-ob-fluid-ch	$0.0115\ m$	X = $0.055\ m$ Z = $0.015\ m$	X = 0.06104854 Y = -0.9981348	Min. Length Scale	$0.00010954\ m$
				Max. Length Scale	$0.00038339\ m$
				Max. Skewness	0.6
intf-invalve1-ob-fluid-ch	$0.0135\ m$	X = $0.054\ m$ Z = $0.015\ m$	X = 0.06104854 Y = 0.9981348	Min. Length Scale	$0.00011098\ m$
				Max. Length Scale	$0.00038842\ m$
				Max. Skewness	0.6
intf-invalve2-ob-fluid-ch	$0.0135\ m$	X = $0.054\ m$ Z = $-0.015\ m$	X = 0.06104854 Y = -0.9981348	Min. Length Scale	$0.00011098\ m$
				Max. Length Scale	$0.00038842\ m$
				Max. Skewness	0.6

Table C.8: Solution Limits.

Solution Limits	
Minimum Absolute Pressure	$1000\ Pa$
Maximum Absolute Pressure	$5e+10\ Pa$
Minimum Static Temperature	$5\ K$
Maximum Static Temperature	$5000\ K$
Minimum Turb. Kinetic Energy	$1e+14\ m^2/s^2$
Minimum Turb. Dissipation Rate	$1e+20\ m^2/s^2$
Maximum Turb. Viscosity Ratio	1000000

Table C.9: Solution Initialization

Initial Values	
Gauge Pressure (Pa)	6000000
X-Velocity (m/s)	0
Y-Velocity (m/s)	0
Z-Velocity (m/s)	0
Turbulent Kinetic Energy (m^2/s^2)	1
Turbulent Dissipation Rate (m^2/s^3)	1
C_8H_{18} Mass Fraction	0.062
O_2 Mass Fraction	0.219
Other Species Mass Fraction	0
Tempertaure (K)	900

Appendix D

Results

D.1 Flame Propagation

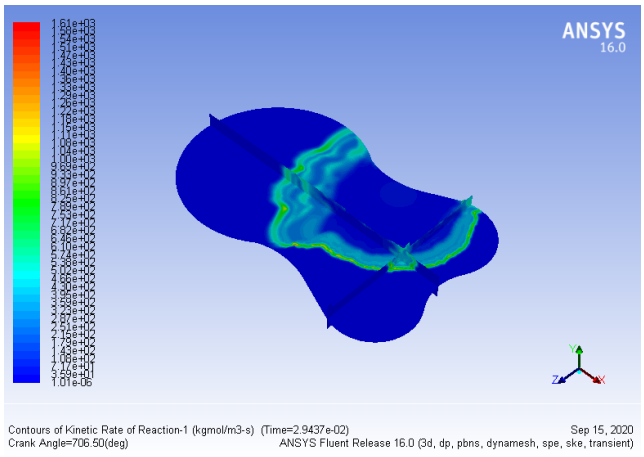

Figure D.1: Contours of kinetic rate of reaction-1 at $706.5°$ crank angle and $4000RPM$.

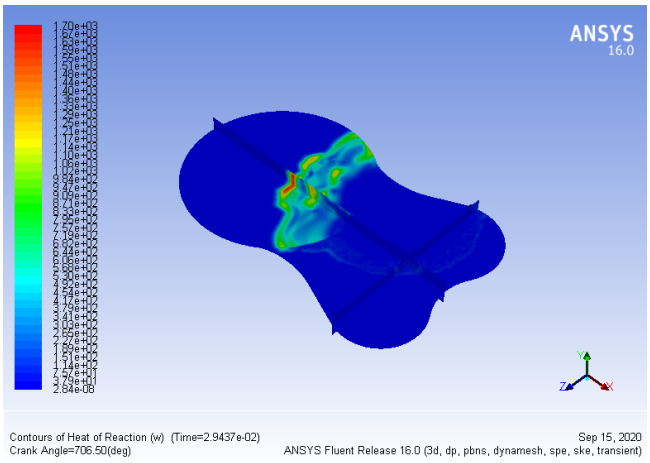

Figure D.2: Contours of heat of rection at $706.5°$ crank angle and $4000RPM$.

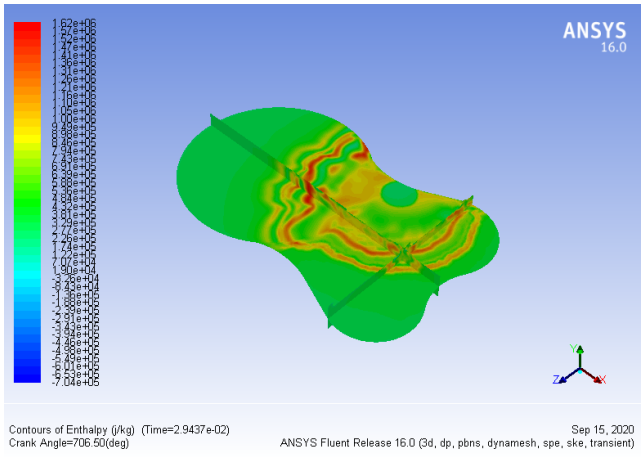

Figure D.3: Contours of enthalpy at $706.5°$ crank angle and $4000RPM$.

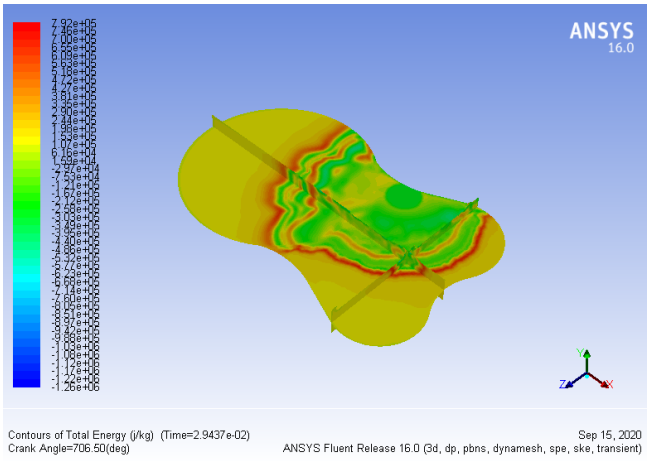

Figure D.4: Contours of total energy at $706.5°$ crank angle and $4000RPM$.

D.2 Inlet Flow

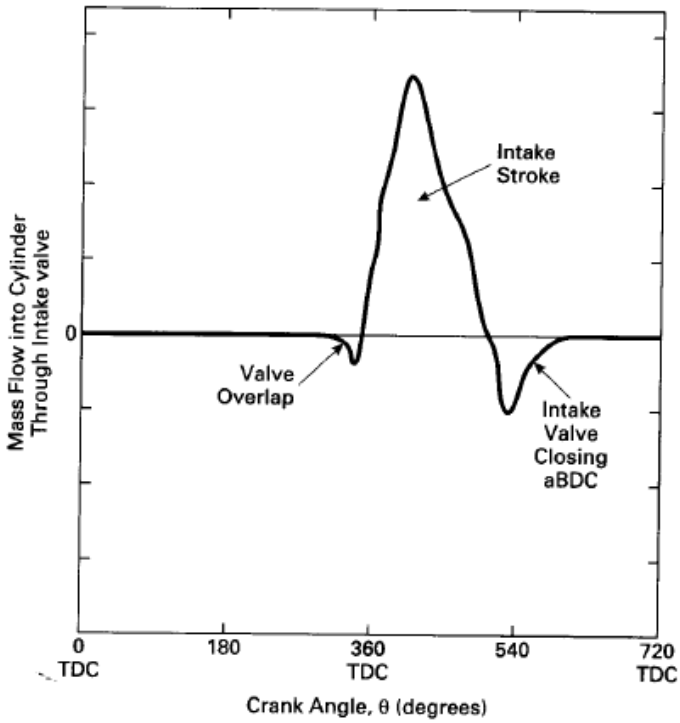

Figure D.5: Flow of air-fuel mixture through the intake valve(s) into an engine cylinder[5].

D.3 Matlab Code

```
function rate
clc
clear
format long
A = importdata('O.txt','%f');% Read mass flow rate values for admission or exhaust
I =trapz(A) % Trapz function is used to calculate the area underneath the plot in order to know the
total mass.
% Plot the result to confirm the area calculated
figure,
area(A);
end
```

D.4 Outlet Flow

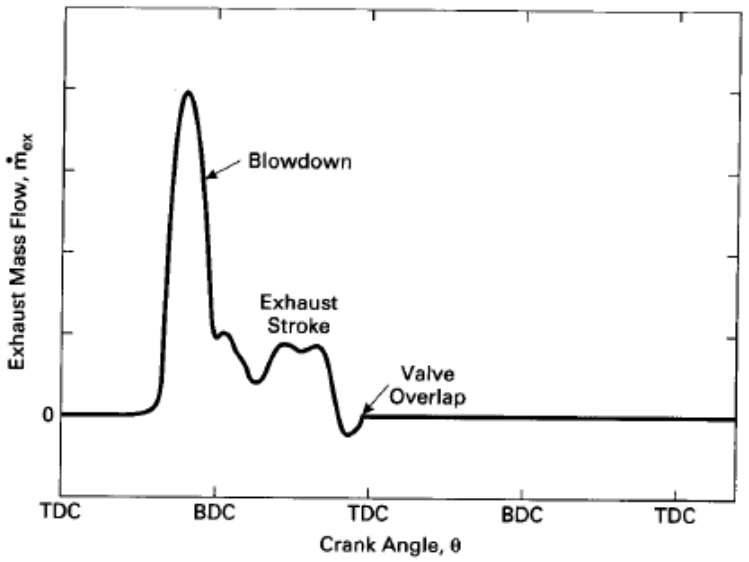

Figure D.6: Exhaust gas flow out of cylinder through the exhaust valves, showing blowdown and exhaust stroke [5].